NUREG/CR-3653
SAND83-7463
R1, RD, RG
Printed March 1984
CONTRACTOR REPORT

Final Report
Containment Analysis Techniques
A State-of-the-Art Summary

Lowell Greimann, Fouad Fanous, Delwyn Bluhm
Ames Laboratory
Ames, IA

Prepared by
Sandia National Laboratories
Albuquerque, New Mexico 87185 and Livermore, California 94550
for the United States Department of Energy
under Contract DE-AC04-76DP00789

Prepared for
U. S. NUCLEAR REGULATORY COMMISSION

Available from

GPO Sales Program
Division of Technical Information and Document Control
U.S. Nuclear Regulatory Commission
Washington, D.C. 20555

and

National Technical Information Service
Springfield, Virginia 22161

NUREG/CR-3653

SAND83-7463
R1, RD, RG

Final Report
Containment Analysis Techniques
A State-of-the-Art Summary

Lowell Greimann, Fouad Fanous and Delwyn Bluhm
Ames Laboratory
Ames, Iowa

Operated by Iowa State University
for the U.S. Department of Energy

March 1984

Sandia National Laboratories
Albuquerque, New Mexico 87185
Operated by
Sandia Corporation
for the
U. S. Department of Energy

Prepared for
Division of Risk Analysis
Office of Nuclear Regulatory Research
U. S. Nuclear Regulatory Commission
Washington, D C. 20555
Under Memorandum of Understanding DOE 40-55-75
NRC FIN No. A-1322

TABLE OF CONTENTS

1.0 INTRODUCTION

1.1 Brief Background

The purpose of the containment in a nuclear power plant is to prevent the release of radioactivity which may be present as the result of a severe accident. The containment has failed to perform its intended function when leakage of the radioactive material occurs.

The purpose of the work contained herein is to review the state-of-the-art for the analysis of LWR nuclear containments with uniform internal pressure. This includes:

(a) A review of calculated static failure pressures of various containments,

(b) A review of the different failure criteria used for predicting containment failure,

(c) Comments on possible uncertainties associated with analysis techniques, material and geometric models, and other analysis features.

This work is part of an ongoing program at Sandia National Laboratories entitled the Severe Accident Risk Reduction program (SARRP). The overall objective of the SARRP is to provide the Nuclear Regulatory Commission with a technical basis for deciding how to incorporate severe accidents into the regulatory and licensing process. To do this, two major efforts are involved: to rebaseline existing estimates of reactor risk and to evaluate the cost and benefits of a variety of potential safety improvements. The work reported herein is in support of the first effort in that the resistance of the containment is an integral part of the total risk assessments.

1.2 Failure Modes

Containments subjected to static, internal pressure can fail (leak) in one of a number of different modes. Even though the structure criteria for failure in each of these modes is not necessarily well-established, it is here appropriate to identify some of these modes. Failure in any of the following locations could permit leakage.

- Cylindrical vessel (steel shell/stiffener system or concrete/reinforcement system)
- Doubly curved head
- Basemat
- Penetrations and reinforced openings
- Liner (concrete containments)

- Anchorage system or basemat/cylinder junction
- Equipment Hatch Assembly
- Personnel Lock Assembly
- Valves
- Expansion joints, bellows
- Attached piping
- Seals

The review will be addressed to the structural aspects of these modes. Hence, for example, leakage associated with the last four locations will not be reviewed per se, but only insofar as it is related to the structural behavior of the surrounding structural system.

2.0 SUMMARY OF CONTAINMENT ANALYSIS RESULTS

Table 2.1 represents a summary of the results of various containment analyses by several investigators. The containment name, investigator, and predicted internal static pressure at failure are listed. The analysis technique, the failure criteria, and the failure location are briefly identified. A more detailed review at each of these items is presented in Section 3.

A not-too-close examination of Table 2.1 may be disturbing to a person being first exposed to containment structural analysis. There is a noticeably wide range in the predicted ultimate strengths for containments within a given type. For example, the predicted failure pressures for PWR ice condensor containments differ by a factor of almost 2.5. However, this difference is easily explained by the difference in the actual containment configuration, i.e., the cylindrical shell of one containment is 3 times as thick. Material properties and stiffener geometries also differ from containment to containment.

More interesting, however, is the difference in the predicted pressure resistance of the same containment by two investigators. Again, closer examination of the two investigations easily explains the discrepancies. Almost always, the primary difference is in the definition of the failure mode. All agree that leakage represents failure but few agree what structural definition of leakage is appropriate. Smaller differences can be attributed to differences in material properties (estimated versus actual) and analysis technique (finite element versus hand calculations). Each of these differences is more fully discussed in the following section. (It is quite possible that the variance in experimental leakage pressures from "identical" containments fabricated by independent fabricators will be larger than analytical leakage pressures predicted by independent analysts.)

Table 2.1 Ultimate pressure strength of various containments.

Containment, Unit Number	Predicted Ultimate Pressure (psig)	Analysis Method	Analysis Source	Failure Criteria	Failure Location
PWR - ice condenser containments					
Sequoyah, 1	60	FE (GN, MN) & HC	AL	deformation twice yield	cylinder
Sequoyah, 1	57	FE (GN, MN) & HC	OPS	beyond yield	cylinder
McGuire, 1	84	FE (GN, MN) & HC	AL	deformation twice yield	cylinder
McGuire, 1	__*	FE (GN, MN)	OPS	beyond yield	cylinder
Watts Bar, 1	98	FD (GN, MN) & HC	AL	membrane hoop strain twice yield	sphere
Watts Bar, 1	120 (LB) 140 (UB)	FE (GN, LS)	SNL	general yielding/ equipment hatch buckling	cylinder equipment hatch
PWR - dry containments					
St. Lucie, 1	95	FE (GN, MN) & HC	AL	membrane hoop strain twice yield	hemispherical dome
Cherokee, 1	116	FE (GN, MN) & HC	AL	membrane hoop strain twice yield	sphere

*Pressure-displacement relationship is given.

Table 2.1 Continued.

Containment, Unit Number	Predicted Ultimate Pressure (psig)	Analysis Method	Analysis Source	Failure Criteria	Failure Location
Indian Point, 2, 3	110	FE (GN, MN) & HC	SNL	yielding of rebars and liner	cylinder
Indian Point, 3	118	FE (GN, MN)	LA	numerical nonconvergence	side wall/base-mat junction
Indian Point, 2, 3	126	HC	UE&C	yielding of rebars	cylinder near springline
Main Yankee	96 (LB) 118 (UB)	FE (GN, MN)	SNL	yielding of hoop steel/numerical instability	cylinder/base cylinder
Zion, 2	120 w/o L 134 WL	FE (GN, MN)	S&L	hoop tendons strain reaches 1%	cylinder
Zion, 2	125	FE (GN, MN)	LA	numerical nonconvergence	cylinder/base mat junction
Bellefonte	130 (LB) 139 (UB)	FE (GN + MN) & HC	SNL	general yielding	dome tendons cylinder tendons
Oconee, 1	151	HC	SNL	general yielding	cylinder
Calvert Cliffs, 1	123	HC	SNL	general yielding	cylinder

Table 2.1 Continued.

Containment, Unit Number	Predicted Ultimate Pressure (Psig)	Analysis Method	Analysis Source	Failure Criteria	Failure Location
Mark III containments					
Perry, 1	100	FE (GN + MN) & HC	AL	membrane hoop strain twice yield or or buckling	buckling at the head knuckle
Grand Gulf, 1	55	FE (GN + MN)	BNL	allowable strain in liner and yielding of rebars	cylinder
Mark III "standard"	80	FE (LD + PL)	S&L	general yielding	personnel airlock
Mark III "standard"	59	FE & HC	GE	ASME, level C	knuckle
Mark III	67	FE (GN, MN)	B	general yielding	cylinder
Mark II containments					
WPPSS, 2	133	FE (GN, MN) & HC	AL	membrane hoop strain twice yield	cylinder
Limerick	140	FE & HC	GE/SA	general yielding	cylinder
Mark II "standard"	150	FE (GN + MN)	S&L	general yielding	personnel airlock

Table 2.1 Continued.

Containment, Unit Number	Predicted Ultimate Pressure (psig)	Analysis Method	Analysis Source	Failure Criteria	Failure Location
Mark I containments					
Browns Ferry, 1	117	FE (GN + MN) & HC	AL	membrane hoop strain twice yield	cylinder/sphere intersection
Peach Bottom, 1	123	HC	SNL	general yielding	neck area and suppression pool
Peach Bottom, 1	175	FE (GN) & HC	BCL	halfway between yield and ultimate	torodial suppression pool

Abbreviations

LB = lower bound;
UB = upper bound;
FE = finite element;
GN = geometric nonlinearity;
MN = material nonlinearity;
LS = large strains;
HC = hand calculations;

AL = Ames Laboratory;
SNL = Sandia National Laboratories;
OPS = Offshore Power System;
LA = Los Alamos National Laboratory;
UE&C = United Engineer and Construction, Inc.;
S&L = Sargent and Lundy Engineers;
BCL = Battelle's Columbus Laboratory;
B = Bechtel Power Company;
w/o L = Without liner plate;
WL = with liner plate

3.0 DISCUSSION OF ANALYSIS METHODS

A summary of the analysis methods for containments and the associated uncertainties is presented in this section. The information presented here is, in many cases, the result of the authors' opinion which is based upon their mutual experience and a review of the literature in this field. A summary of the individual studies conducted in this area can be found in Appendix I and Appendix II. A list of references follows.

3.1 Geometric Containment Model

Almost all containment analyses, to date, have been based upon an axisymmetric structural model of the containment shell. For this model many nonsymmetric features must be neglected or accounted for in an approximate way. All of these approximations introduce a degree of uncertainty.

- Longitudinal stringers are typically smeared in the circumferential direction to obtain an "average" equivalently stiff axisymmetric shell. This is acceptable for certain ranges in stiffener configurations, but cannot be generalized to all cases. [I.1.1-1, I.1.7-1, I.3.1-1, I.4.1-1, II.1.2-1, II.1.5-1]*

- Circumferential variations in thicknesses, ring and stringer sizes, amount of reinforcing steel and shell imperfections cannot be incorporated into an axisymmetric model. The usual, and probably conservative, approach is to select the worst case, i.e., smallest size or largest imperfection, and assume this case is constant around the circumference. [I.1.1-1, I.3.1-1, I.4.1-1]

- Penetrations and other reinforced openings introduce nonsymmetric features into the containment which must be ignored in axisymmetric models. Typically, the argument is made that these "local" features are sufficiently small and appropriately reinforced, e.g., thickened steel plates (ASME area replacement rule) or extra concrete reinforcement, so that the strength of the penetrated shell is greater than or equal to that of the unpenetrated shell. Several investigators have looked at isolated penetrations to verify this assumption and found that, in the case of uniform internal pressure, i.e., without buckling, this approximation is acceptable. The reinforcement and welds in the vicinity must be sufficiently ductile to allow redistribution of forces as the limit strength of the shell system is approached. [I.1.1-1, I.3.1-1, I.3.2-1, I.4.1-1, I.6.1-1, I.6.2-1, I.6.3-1, I.7.1-1, I.8.1-1, I.8.2-1, I.9.1-1, I.13.1-1, I.15.1-1, II.1.1-1]

---

* Number in brackets indicates reference number.

- Prestressed concrete containments have additional features - prestressing tendons and anchorage buttresses - which are not axisymmetric and must be "smoothed" into an axisymmetric model. Prestressing of both the cylindrical and doubly curved portions of the containment present such problems. The effect of these nonsymmetries are generally neglected based upon some heuristic argument. The discrete nature of the tendons is not seldom included, but the effects are usually smeared. [I.8.1-1, I.8.2-1, I.9.1-1, II.2.1-1] One investigator [II.1.11-1] has studied the discrete nature of the reinforcing and post-tensioning steel with a three-dimensional analysis. The prestressing ring for the dome was included but cylindrical prestressing buttresses were not. The study suggests that the unsymmetrical anchorage effects cannot be represented by an axisymmetric model.

- Several pieces of equipment or other structures are often attached to the containment, e.g., ice storage areas, walkways, floor systems, cranes, plumbing, and seismic anchors. The effect of these "smaller" nonsymmetries has not been studied.

- A limited number of three dimensional analyses have been performed on isolated features, e.g., equipment and personnel assemblies. These analyses are usually performed as if the feature were isolated from all other features. [I.1.1-1, I.8.1-1, I.8.2-1] Neither interaction between nonsymmetrical parts nor the effect of their behavior on the remote "smooth" shell have been studied.

- Interference with adjacent equipment or buildings is usually not considered. Thus, interaction with a shield building is often mentioned, e.g., by limiting displacements, but not included in the model. [I.1.1-1, I.3.2-1, I.4.1-1] The restraint of attached equipment which is anchored inside or outside containment is not included in the structural model.

- Base boundary conditions are often highly idealized. For steel containments, the base is usually assumed to be fixed where it intersects the thick basemat. [I.1.1-1, I.3.1-1, I.3.2-1, I.4.1-1] The base is frequently included in the model of concrete containments. Sometimes the base is not allowed to move vertically (no uplift); sometimes uplift is permitted. If the base is included, it and the supporting soil are assumed to be axisymmetric and flat. [I.6.1-1, I.6.2-1, I.6.3-1, I.7.1-1, I.8.1-1, I.8.2-1]

- Geometric imperfections are not modeled directly.

- The liner in concrete containments is taken to be intimately attached to the shell wall. Local buckling of the liner due to temperature rises is mentioned by several, but analyzed by few. The structural effectiveness of the liner is debatable - some

investigators publish two results: one with and one without the liner participation. [I.6.1-1, I.6.2-1, I.6.3-1, I.7.1-1, I.8.1-1, I.8.2-1, I.9.1-1, I.13.1-1, II.1.4-1, II.1.6-1, II.1.11-1]

3.2 Material Model

3.2.1 Steel

The ductility of steel is used in almost all analyses - very few have restricted maximum stresses to the proportional limit.

- The uniaxial stress-strain curve is usually approximated by a piece wise linear curve, often elastic-perfectly plastic. [I.1.1-1, I.1.2-1, I.3.1-1, I.4.1-1, II.1.1-1] The effect of residual stresses and a reduced proportional limit are not included. Their effect is unknown, but probably small in this application.

- The Prandtl-Reuss flow rule and the von Mises yield surface are always used in the nonlinear material description. This has long been accepted as an adequate description for metal behavior, though questions still arise with regard to deformation versus incremental plasticity theory for buckling applications. [I.1.1-1, I.2.1-1, I.3.1-1, I.3.2-1, I.4.1-1, I.13.1-1, II.1.1-1, II.7.1-1]

- The effect of temperature on steel properties is neglected on the premise that accident temperatures are sufficiently low

- Actual material properties are used if they are available These properties are usually averages of mill test reports taken from each component plate. Uncertainty often exists in these data due to strain rate differences, specimen location and orientation within the plate, limited sample size, and censoring of test data. Material properties vary from plate to plate and, even, from point to point. Thickness also affects yield strength and ductility.

- Weld and heat-affected-zone properties are taken to be the same as the base metal. Good weld quality is assumed. [I.8.1-1]

3.2.2 Reinforced Concrete

A "standard" model for concrete under biaxial stress is still evolving. The uncertainty associated with an analytical description of a reinforced concrete segment under biaxial stress is one of the larger uncertainties in the analysis of concrete containments.

- The uniaxial compression behavior of concrete is the best described aspect. Actual compressive properties are used, if available. However, the same uncertainties are associated with

the collection of this information as are mentioned in the steel description, e.g., testing techniques, specimen representativeness, and sample size.

- The uniaxial tensile strength of concrete has wide variations. Some use $6\sqrt{f'_c}$, some use the split cylinder strength. A representative test specimen has not been agreed upon. [I.8.1-1, II.2.1-3, II.3.1-1]

- The introduction of reinforcement into the concrete significantly complicates its description. Aspects at the steel/concrete interface, i.e., bond, anchorage, are difficult to describe analytically, let alone incorporate into a complete analytical model of the containment. The cracking (crushing)/bar yielding/bond/aggregate interlock problem is still with us.

- The biaxial stress-strain behavior is even less universally agreed upon. Various investigators have used the Chen and Chen, von Mises, Tresca and/or Drucker-Prager model. A good description of the tension cracking and post-cracking behavior is particularly missing. Arbitrary cracking criteria and reductions in shear and tension stiffness (50 and 0.01 percent, respectively) are usually used. Crack pattern (size, spacing, orientation and location) predictions are unreliable and semi-empirical at best. [I.6.1-1, I.6.2-1, I.7.1-1, I.8.2-1, I.9.1-1, I.13.1-1, I.15.1-1, II.1.9-1, II.1.11-1, II.2.1-3, II.3.2-1, II.5.1-1, II.7.1-1]

- The effect of cracks on other properties is not usually incorporated into the analysis. Hence, radial shear strength and reinforcement bond are apparently related to the biaxial stress state and the extent of cracking, but the effect is not well-described analytically. In other words, a description of the behavior of reinforced concrete under all pertinent stress states up through complete cracking and/or crushing needs work. [I.6.2-1, I.8.2-1, I.13.1-1, I.15.1-1, II.1.9-1, II.1.11-1, II.3.2-1, II.3.3-1, II.7.1-1]

- Perfect concrete quality is assumed. Possible imperfections, e.g., concrete placement in areas of congested reinforcement, are not considered. Variation in concrete strength with location and time are not included. [II.1.6-1]

- Temperature effects on concrete strength are usually rationalized away because of the "low" accident temperatures. [I.15.1-1, II.1.6-1, II.3.1-1, II.3.2-1]

3.2.3 Soil

If the soil is included with the base model, it is usually approximated as an axisymmetric Winkler foundation with compression - only

springs. Analytical modeling of soil behavior has its own set of uncertainties, princpally having to do with the flow rule, yield surface and material constants. Most likely, this is not a major uncertainty for this application, although it becomes a predominate problem if seismic effects are important. [I.6.1-1, I.6.2-1, I.6.3-1, I.7.1-1, I.8.1-1, I.8.2-1]

3.3 Load Model

For this review, the load has been restricted to uniform internal pressure.

- There is little uncertainty involved in the description of a uniform, static internal pressure for structural analysis purposes. (Whether the pressure is actually uniform and static is not addressed here. Dynamic effects become significant if the pressure changes rapidly, relative to the containment response time. Locally high pressures cause locally high stresses.)

- Temperature effects are often mentioned, but seldom included. Since temperature stresses are self-limiting, the argument goes, they have little effect on the ultimate strength of the containment. [I.8.1-1]

- Pre-existing stresses, e.g., concrete shrinkage, steel residual stresses, erection stresses, settlement stresses are not included. These are also self-limiting. [II.3.2-1]

- Weight forces are often combined with the pressure forces. Some account is usually taken of attached pieces, but the effect is usually distributed axisymmetrically. [I.6.1-1, I.6.2-1, I.7.1-1, I.8.1-1, I.8.2-1, I.9.1-1, I.13.1-1, II.7.1-1]

- Prestressing forces are included in at least two different ways ways -- external forces (pressures) are applied which are equivalent to the prestress force, or equivalent temperature changes are introduced into the prestress tendons to produce a prestress condition. Sometimes concrete creep is included to account for some of the prestress loss. Other prestress losses may or may not be important. [I.8.2-1, I.9.1-1, II.1.11-1, II.5.1-1, II.7.1-1]

3.4 Analysis Methods

3.4.1 Hand Calculations

Hand calculation methods are based on equilibrium of an assumed limit mechanism. Limit mechanism solutions are available for uniform reinforced concrete cylinders and spheres, stiffened and unstiffened steel cylinders and cones, collapse and buckling of ellipsoidal and torispherical heads, anchorage bolts, cylinder/cylinder penetrations and cylinder/sphere penetrations. (A less sophistocated hand

calculation is to multiply the containment design pressure by the design factor of safety to arrive at the ultimate strength. Fortunately, this approach isn't used much anymore.)

- A very basic assumption in limit analysis is that the materials have the ductility to permit the formation of a limit mechanism. If the materials are brittle and/or locally high strains exist, local failure may occur before the complete mechanism forms. [I.1.1-1, I.4.1-1, I.6.1-1, I.8.1-1, II.1.6-1]

- Sometimes, e.g., penetrations, the critical mechanism is not clear and several must be examined. Whether the least upper bound mechanism has been found can be uncertain. [I.1.1-2, I.1.1-3, I.1.6-1]

- By their nature, limit analyses can be applied to quite a specialized and small number of cases. Interaction of adjacent mechanisms and complex geometries, e.g., curved knuckles, changing thicknesses, are not easily analyzed. Local details are usually not included. [I.4.1-1]

- Large displacement effects are typically omitted. The (usually) strengthening effect of membrane tension is often neglected.

- Many of the limit analysis techniques have not been extensively calibrated with experiment. For example, the limit mechanism for a concrete cylinder under internal pressure is reasonably simple, but several questions can be raised regarding the crack size, radial shear strength, bond characteristics, reinforcement participation and the linear behavior over the cracks at the strains associated with the mechanism.

3.4.2 Finite Element or Finite Difference Solutions

Finite element or finite difference solutions are relatively powerful in that local geometric and material details can be incorporated into the model. Complete descriptions of the stress-strain state throughout the model are obtained. Complex nonlinear material constitutive relationships and geometric nonlinearities are usually included. However, such an analysis has its own uncertainties.

- Characteristics of the basic finite element vary from case to case. Solid elements and shell type elements incorporate different features. First and second order elements require different discretizations. Accuracy is affected by element size, aspect ratio, orientation and gradation, in addition to the assumptions involved in the element formulation. [I.1.1-1, I.3.1-1, I.4.1-1, II.1.1-1]

- Nonlinear problems always involve some sort of iterative procedure, e.g., Newton-Raphson, modified Newton-Raphson. The

convergence properties of the procedure significantly affect the accuracy (and cost) of the solution. Convergence tolerance tightness and convergence criteria, e.g., plastic strains, displacements, must be carefully understood and specified. Numerical stability problems have almost always been encountered in the analysis of concrete containments. This problem is usually associated with the tension cracking and post-cracking behavior of the concrete material model. Large changes in stiffness occur when cracks occur and this causes numerical problems. Often this is also the physical situation, i.e., cracking causes big "jumps" in the physical structure. Whether the numerical instabilities encountered in containment analyses represent corresponding physical instabilities is uncertain. [I.1.1-1, I.3.1-1, I.3.2-1, I.4.1-1, I.7.1-1, II.1.11-1]

- Several aspects of finite element modeling are unclear. A common model of bar cutoffs (the bond/anchorage problem) is not available. Some investigators taper the bar areas to represent the development of the bars. [II.2.1-3] Rings/stringer/shell attachments are often modeled by rigid constraints, though this represents an approximation. [I.7.1-1]

- Reinforcing layers are often represented with orthotropic elements which effectively "smear" the discrete nature of the reinforcing. [I.6.1-1, I.6.2-1, I.7.1-1, I.8.1-1, I.9.1-1, I.13.1-1]

- Bond is assumed to be perfect. (See uncertainties associated with this assumption in Section 3.2.2.) [I.6.1-1, I.6.2-1, I.7.1-1, I.8.1-1, I.9.1-1, I.13.1-1, II.1.11-1]

- The liner is usually modeled by a shell type element, rigidly attached to the inner concrete surface. [I.6.1-1, I.6.2-1, I.7.1-1, I.8.1-1, I.9.1-1, I.13.1-1, II.1.4-1, II.1.11-1]

- Three-dimensional analyses of, for example, penetrations, have been done in a few cases. Typically, a portion of the structure is isolated from the remaining containment (for practical reasons) and analyzed by, say, two-dimensional shell type elements. Force and displacement boundary conditions at the limit of this isolated region are obtained from an analysis of a larger portion. Uncertainty is associated with this process. Often, the reinforcement detail in the vicinity of a penetration is geometrically complex and is difficult to represent accurately, even with finite element methods. [I.1.1-1, I.8.1-1, I.8.2-1]

- As with all analysis methods, theoretical and experimental results never exactly agree - even if all the above uncertainties do not exist. Hence, there will always exist some aspects of the physical model which cannot be incorporated into the

analytical model. The scatter in this difference can be reduced, but must always remain a random variable. [I.1.1-1, I.3.1-1, I.4.1-1, I.6.1-1, I.6.2-1]

3.5 Failure Criteria

Failure criteria are one of the two or three major unresolved problems in containment ultimate strength analysis. Most investigators agree that the containments should be considered to have failed when leakage occurs, since it can no longer perform its intended function. However, few would agree as to what this means as related to the current state of structural knowledge, or how to define leakage in structural terms.

- The formation of a limit mechanism is often taken to coincide with failure - especially in hand calculation analyses. In many cases, it is not clear that sufficient ductility exists for a formation of a mechanism - Section 3.4.1. On the other hand, the structure may be very ductile and the pressures may increase beyond a limit pressure because of strain-hardening and tension-membrane effects. [I.1.1-1, I.4.1-1, I.6.3-1, I.10.1-1, I.11.1-1, I.15.1-1, I.17.1-1]

- Some (few, fortunately) find the ultimate pressure to be that associated with the ultimate tensile strength of the steel (from a smooth tensile specimen). There is little reason to expect that the as-built containment will have the ductility to reach this state. Welds, imperfections, heat-affected zones, local strain concentrations (penetrations, attachments, holes, etc.) will not permit this. Recognizing this, some investigators have used the average of the yield and ultimate tensile strengths. There is little reason for this except that it is not as unconservative as the former approach. [I.17.2-1, II.1.6-1, II.1.7-1]

- Several investigators have used a strain criteria to predict leakage - the idea being that the material strain is one of the better indicators of material distress and potential separation. This criteria is often applied to the membrane component of the shell strain or the reinforcement strain. Strain concentrations (penetrations and other nonsymmetric geometric discontinuities) are not directly included, but may be considered when the strain limits are set. Hence, strain limits for failure have been defined, by different investigators, between two and fifteen times the yield strain. Some have analyzed containments up to 15 percent strain. [I.3.1-1, I.3.2-1, I.4.1-1, I.5.1-1, I.8.1-1, I.12.1-1, I.13.1-1, I.14.1-1, I.16.1-1]

- Deformation limits have been established in some cases to define failure. This criteria makes sense if it is recognized that more than just the containment shell is involved here.

Attached piping, penetrations, etc. will themselves begin to leak if they are forced to deform too much. Seals and gaskets and sealed electrical penetration assemblies cannot withstand indefinite deformation of the surrounding material. The values for the deformation limits are uncertain at this time. Some have selected strain limits for tendons of one percent based on deformation considerations. [I.1.1-1, I.1.2-1, I.2.1-1, I.2.2-1, I.3.2-1, I.6.1-1, I.7.1-1, I.8.1-1, I.13.1-1, II.1.1-1, II.1.10-1, II.7.1-1]

- Buckling may be used as a failure criteria, even though the instantaneous bifurcation buckling itself, most likely, does not induce leakage. Only if the post-buckling strains (or displacements) become sufficiently large - as discussed above - is it reasonable to expect failure. This applies, in this situation, particularly to ellipsoidal and torispherical heads. On the other hand, buckling of an equipment hatch may induce deformations which could cause the seal to leak. (See paragraph above.) [I.3.1-1, I.3.2-1, I.4.1-1, I.12.1-1, II.1.1-1, II.1.5-1, II.1.7-1, II.1.8-1]

- In some cases, numerical instabilty has been interpreted as structural failure. As discussed in Section 3.4.2, this may or may not be true. [I.6.2-1, I.7.1-1, I.8.2-2, II.1.11-1]

- In concrete containments, failure is defined by limiting reinforcement, liner and/or concrete compression strain. [I.6.1-1, I.7.1-1, I.8.1-1, I.9.1-1, I.13.1-1, II.1.4-1, II.1.6-1, II.1.9-1, II.3.2-1, II.5.1-1]

- Usually concrete tensile cracking is not considered as a failure condition but only as an intermediate stage on the way to ultimate. However, some have predicted that the liner will tear when the concrete cracks become too large. Failure prediction then amounts to selecting the crack size which the liner can tolerate and predicting when this limiting crack size is attained. [I.13.1-1, II.1.6-1, II.2.2-1, II.5.1-1] Another has predicted that the tendon anchorages will fail because of excessive concrete cracking [II.1.11-1].

- Radial shear stress is often used as the failure criteria to check peripheral shear around penetrations and the basemat/cylinder junction for concrete containments. Work on this idea has some way to go and significant uncertainty still exists. For example, the influences of extensive local cracking around the penetration or of the amount of hoop reinforcement adjacent to the basemat are still being investigated. [I.6.2-1, I.7.1-1, I.8.1-1, I.8.2-1, II.1.3-1, II.1.6-1, II.3.2-1, II.3.3-1]

- If failure criteria are uncertain, failure size is a wild guess. Few investigators have gone beyond predicting that the failure will be small (local) or large (global). These

predictions typically rest upon the judgment and experience of the engineers making them. The more experienced engineer may not make this guess.

3.6 Additional Uncertainties

One uncertainty that continues to come to mind during a containment analysis is: How close is the actual in-place containment to the fabrication drawings and specifications? Hence, answers to questions about, for example, concrete placement in critical areas, weld quality, tolerance acceptance, and mill test or concrete cylinder representativeness always have an associated uncertainty.

Finally, uncertainty exists in the uncertainty. That is, we are often uncertain whether we have considered all the uncertainties. For example, failure could occur in a location and by a mode the analyst has not thought to investigate.

3.7 Uncertainty Assessments

A relatively small number of investigators have attempted to quantify some of the above uncertainties into a reliability analysis of specific containments. [I.1-1, I.3.1-1, I.4.1-1, I.8.1-1, II.1.6-1, II.1.7.1] Their results are often presented in the form of fragility curves or probability of failure distributions conditional on a prescribed static pressure level. The material properties and geometric configuration are taken to be random quantities which are described by a mean, standard deviation and distribution type. Analysis uncertainties are quantified by comparing experimental and analytical results. More subjective uncertainties, such as the definition of the failure criteria, actual in-place containment versus the containment described in drawings and other errors, have not yet been introduced into uncertainty assessments.

It is not the purpose of this work to review the state-of-the art in the reliability analysis of structures. Briefly, the uncertainty assessments to-date must be considered preliminary and the results interpreted only as notional probabilities. The results can become meaningful only after these methods have been calibrated with real-world failure experience. However, reliability assessments are very useful tools to focus attention on important uncertain quantities. Thus, for example, sensitivity studies point to the basic structural parameters which are significantly random. More study and data collection should be devoted to these quantities (see the following section).

3.8 Summary

The analysis of steel and concrete containments involves many uncertainties in the containment geometry, the containment material, the containment loads, the analysis techniques, and the failure criteria. All of these have been summarized above in Section 3. Each

uncertainty represents a potential difference of opinion between two investigators. Hence, as discussed in Section 2, two independent investigators will often predict noticeably different results for the same containment. Of the uncertainties presented above, the following uncertainties are, in the opinion of the authors, most often the cause for discrepancies in results.

- In-place versus as-designed containment: How close is the actual containment to the containment specified in the engineering drawings, e.g., welds, reinforcement details, geometric tolerances, material properties?

- Behavior of reinforced concrete under biaxial stress condition: What are appropriate constitutive equations for a steel/concrete system, particularly at and beyond cracking and/or crushing?

- Failure criteria: What is an appropriate structural definition for failure (leakage)?

- Failure modes: Have all realistically possible failure modes been analyzed, e.g., does an axisymmetric model miss important effects?

Uncertainty can be decreased only if these problems are addressed by further study.

3.9 Conclusion

A state-of-the-art containment analysis is a finite element solution of an axisymmetric model. Material and geometric nonlinearities are included. Nonsymmetric features may be analyzed on an individual basis but are omitted in the axisymmetric model. State-of-the-art models of the material constitutive relationships are used. Deformation predictions are generally regarded as reliable, assuming the containment configuration is accurately described, e.g., known geometry, material and loads. Predictions of leakage are much more uncertain. There is no general agreement on when and where leakage will occur. In this regard, the results presented in Table 2.1 should be interpreted as predictions of containment deformation states rather than leakage indicators.

4.0 ACKNOWLEDGMENT

The authors would like to express their appreciation for Mr. Joseph Jung from the Sandia National Laboratories for providing some of the information needed to complete this work. We also wish to acknowledge the able assistance of the Project Secretary, Connie Bates, for the word processor operations and the secretarial services associated with this work.

APPENDIX I - SPECIFIC CONTAINMENTS

PWR - ICE CONDENSER CONTAINMENT

1.1 Sequoyah (by Ames Laboratory) [1.1-1]*

Objective

Uncertainty assessment of ultimate internal pressure resistance.

Containment Description

Ice condenser, steel (Fig. 1.1-1)**

Uncertainty Assessment

<Beyond the scope of this review.>

Material Properties

Actual values from mill test results

Failure Criteria

- Leakage of containment shell - controlled by fracture (elastic-plastic fracture mechanics). Probability of failure by this mode is shown to be low relative to the following mode.
- Leakage of attached piping and equipment - controlled by large deformation of containment (limit mechanism or deformations beyond twice yield). (Fig. 1.1-2)

Simplified Analysis

Limit pressures for stiffened cylinders and spheres, based on limit mechanisms. Minimum mean limit pressure = 59 psig, controlled by hoop forces near springline.

Penetration analysis with limit pressures derived by others:

- Cylinder/Cylinder Intersection [1.1-2];

$$P_{ot} = \left\{ \frac{\left[162\left(\frac{t}{T}\right)^2 + 228\left(\frac{t}{T}\right)\left(\frac{d}{D}\right) + 210\right] K + 155}{108K^2 + \left[228\left(\frac{d}{D}\right)^2 + 228\right] K + 152} \right\} P_{co}$$

---

* Number in brackets indicates reference number.

** Number in parentheses indicates figure number.

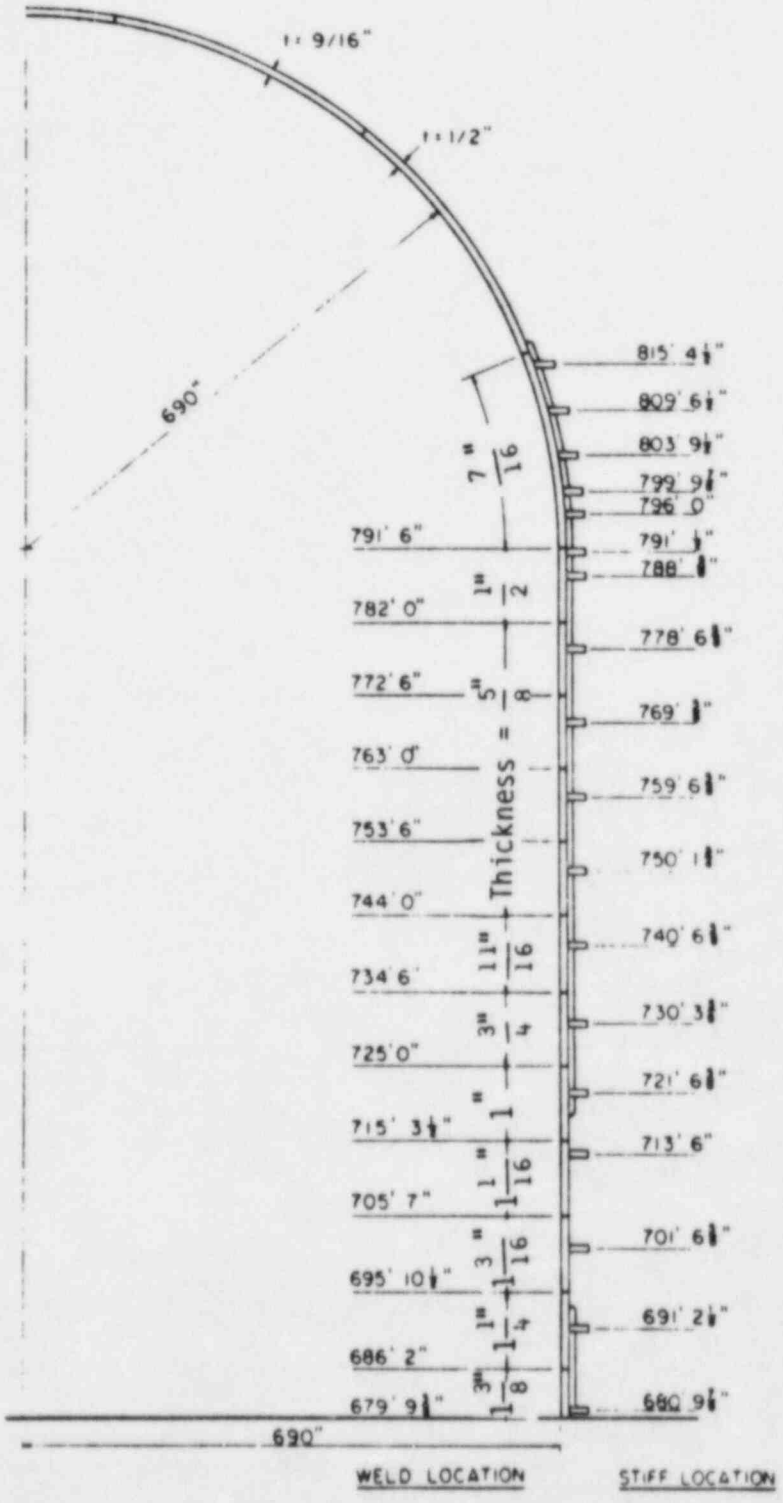

Figure 1.1-1 Sequoyah Containment Vessel Geometry

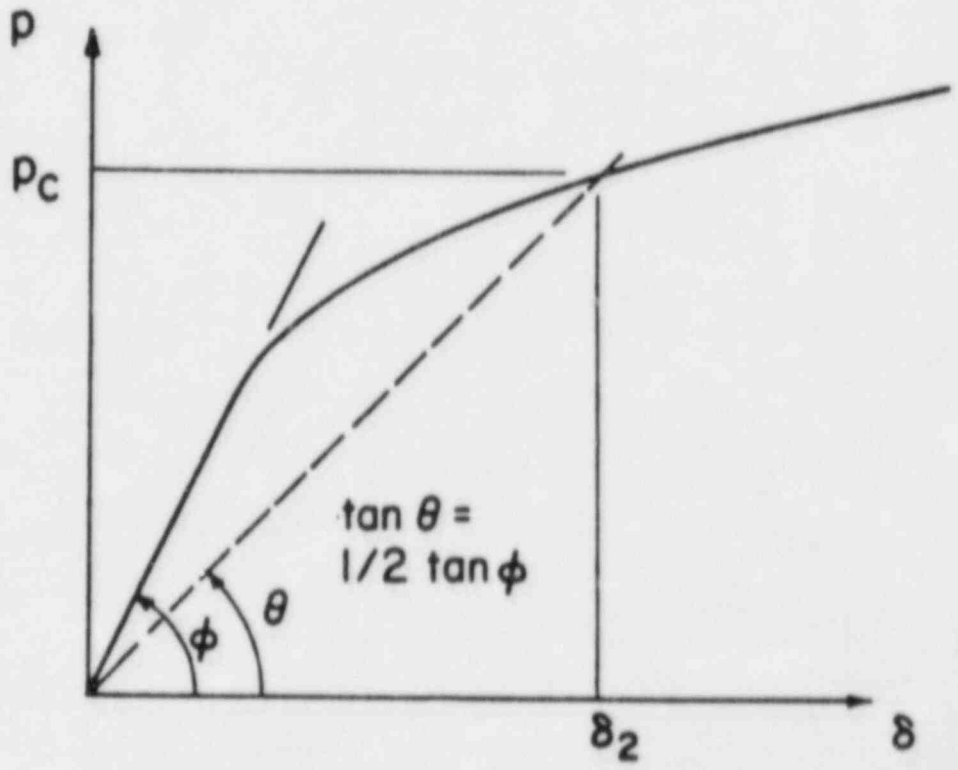

Figure 1.1-2 Definition of Half-Elastic Slope Plastic Pressure

- Cylinder-Sphere Intersection [1.1-3];

$$P_{ot} = p_s P_{so}$$

in which p_s is found from

$$\sqrt{\frac{T}{D}\left\{\left[1+\left(\frac{t}{T}\right)^2\right](1-p_s)\right\}} = p_s \frac{d}{D}\sqrt{\left[1-\left(\frac{d}{D}\right)^2\right]} - \frac{d}{D}\frac{t}{T}\sqrt{\left[\frac{2t}{d}\left(1-\frac{2T}{D}\frac{d}{t}p_s\right)\right]}$$

and where

t = penetration wall thickness

T = vessel wall thickness

d = penetration diameter

D = vessel diameter

$K = d/D\sqrt{D/T}$

$P_{co} = 2F_yT/D$

$P_{so} = 4F_yT/D$

Experimental/theoretical result, penetration limit pressure.

	Mean	Standard Deviation
Cylinder/cylinder (12 specimens)	0.99	0.15
Cylinder/sphere (12 specimens)	1.23	0.23

Minimum mean limit pressure from penetration analysis is 67 psig (193 penetrations).

Finite Element Analysis

ANSYS - general purpose finite element program with nonlinear capability.

Axisymmetric finite element model:

- Shell and rings-isoparametric, axisymmetric solid element with mid-side nodes, maximum length = $\sqrt{rt}/2$;

- Stringers - beam element with constraint equation;
- Nonlinear material (elastic-plastic) and geometric behavior.

Experimental/theoretical result, finite element analysis - six smooth finite length cylinders with internal pressure: mean = 1.13, standard deviation = 0.07.

Failure pressure equals 60 psig, controlled by radial displacement near springline.

Penetration finite element model (Fig. 1.1-3):

- Triangular flat shell element, maximum size = $\sqrt{rt}/4$ near discontinuities;
- Nonlinear materia' and geometric behavior.

Experimental/theoretical result greater than one (1 specimen).

Failure pressure for controlling penetration is greater than 65 psig.

Conclusion

Mean predicted failure pressure is 60 psig (approximately lognormal distribution with standard deviation of 8 psi).

1.2 Sequoyah (by Offshore Power System) [1.2-1, 1.2-2]

Objective

Investigation of the vessel capacity under internal pressure.

Containment Description

Stiffened steel cylindrical shell covered with hemispherical cap, Fig. 1.1-1.

Analysis

Finite element analysis using ANSYS.

Typical panel - shell skin framed by the stringer and ring stiffeners, Fig. 1.2-1.

Plastic triangular shell element.

Analysis was carried up to and beyond yield stress of 45 ksi.

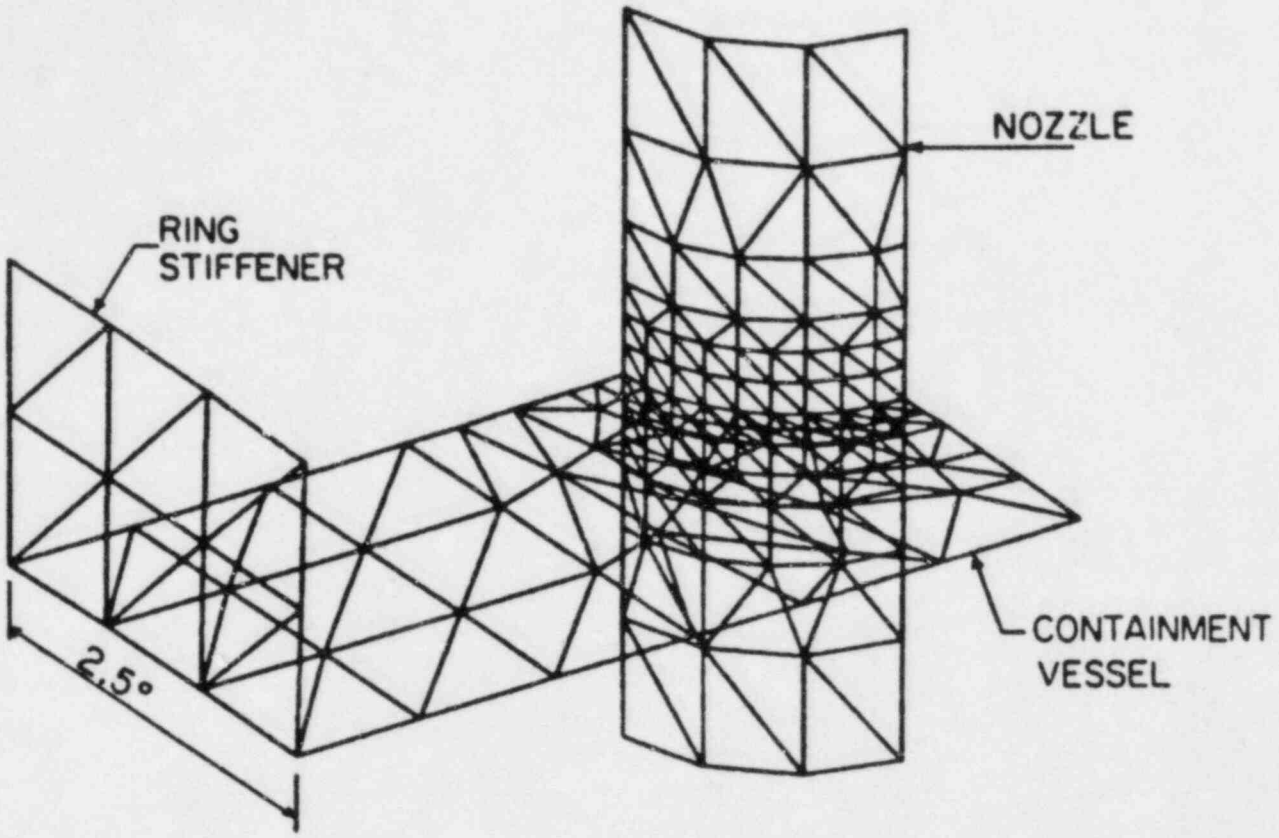

Figure 1.1-3 Ring Stiffener, Penetration and Containment Vessel Mesh Layout (Sequoyah vessel)

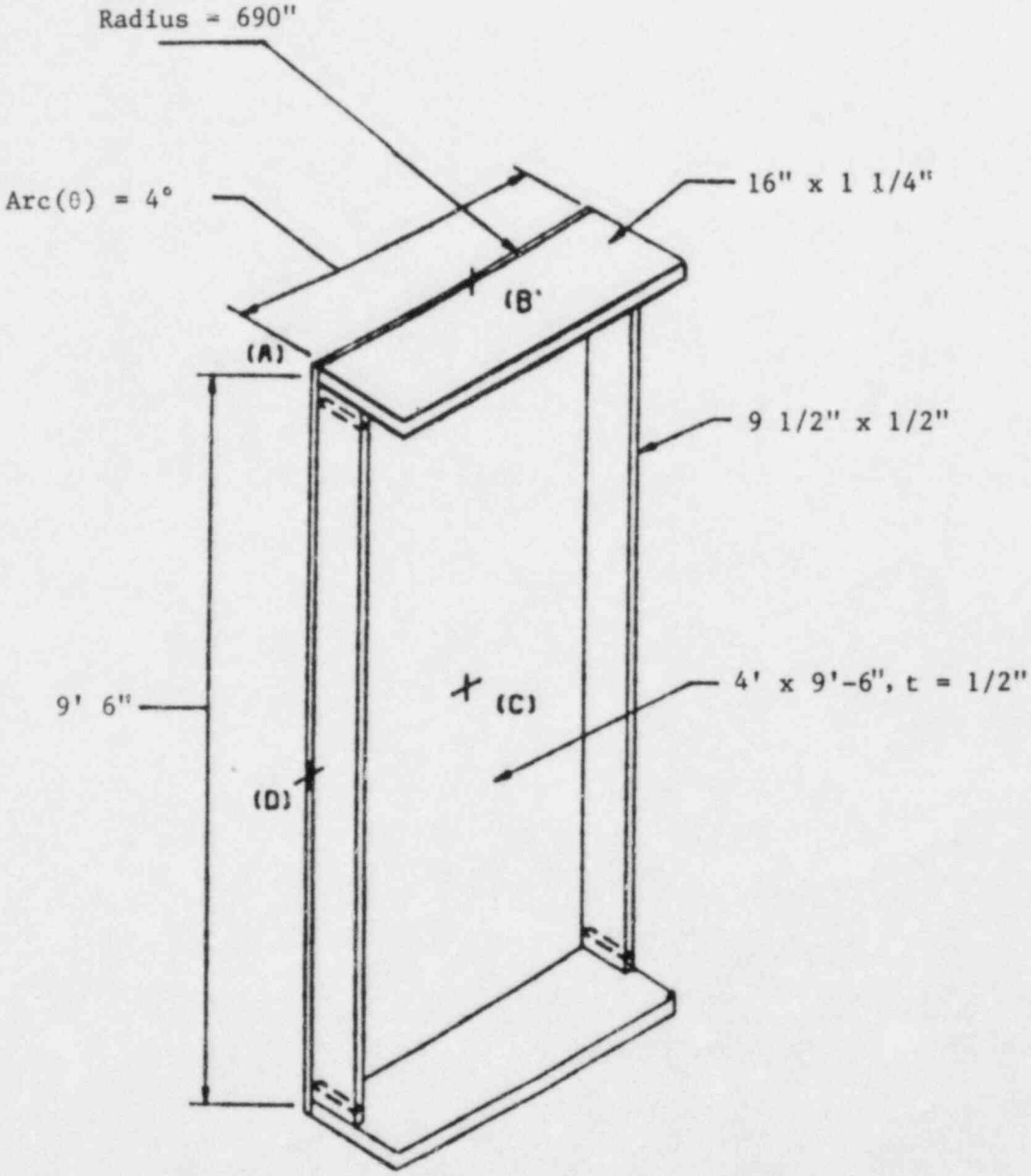

Figure 1.2-1 Idealized Panel - Sequoyah

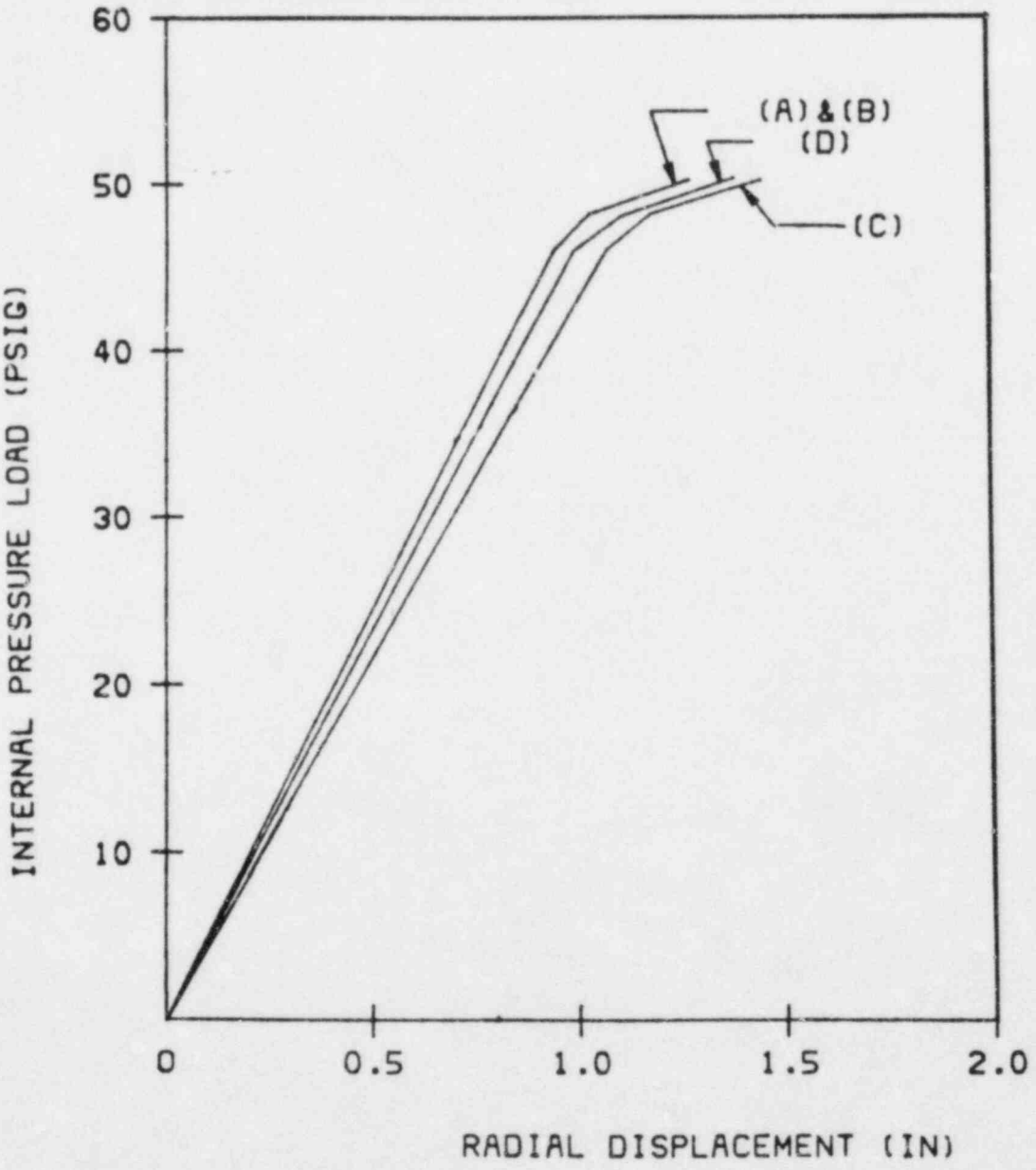

Figure 1.2-2 Pressure-Displacement Curve for Sequoyah Containment

Results

Pressure - radial displacement, Fig. 1.2-2.

Yield pressure, hand calculation [1.2-2] = 57 psig.

1.3 Sequoyah Preliminary Calculation (by Ames Lab) [1.3-1]

Objective

Preliminary calculation of vessel ultimate strength.

Assumptions

Stresses in ring/stringer stiffened shell are approximately equal to stresses in equivalent shell with smeared stiffeners.

von Mises failure criteria.

Limit pressure occurred when stresses reach the specified material yield strength, conservative assumption.

Burst pressure was calculated when stresses reach material ultimate strength.

Penetrations do not control - reinforced according ASME rules.

Minimum specified material properties used.

Calculated limit pressure is 36 psig as controlled by yielding of the rings near 1/2" plate.

1.4 Sequoyah Containment Analysis (by Hubbard, H.W.; R&D Associates) [1.4-1]

Objective

Analysis of Sequoyah vessel ultimate strength.

The Analysis of a Shell with Ring and Stringer Stiffeners

Linear elastic analysis with strain compatability between shell skin and stringers.

Stringer Effectiveness

Stringers are about 40% effective in linear elastic range.

Ring Effectiveness

Rings have to be much closer than 80 inches to have any appreciable reduction on the membrane hoop stresses. Rings therefore are completely ineffective.

Critical region is between two rings with thicknesses of 1/2 inch.

For F_y = 32 ksi, the critical internal pressure is 27 psi using the von Mises yield criteria.

Alternative Panel Analysis

Rectangular panel framed by stringer and ring. Flat elastic plate analysis gives pressure of 13.1 psig which causes yielding in extreme fiber of plate.

Large deflection plate analysis - local yielding would occur at 7.8 psig while full plastic hinge would occur at 11.7 psig.

Hold Down Bolt Stresses

Bolts are prestressed to a level of 25 ksi.

Bolts yields at 64.5 psig internal pressure.

Conclusions

Limit pressure is about 27 psig, controlled by 1/2 in. plate.

1.5 Sequoyah Containment Analysis (by TVA) [1.5-1]

Objective

Prediction of the vessel strength.

Determination of Critical Sections <No details printed.>

Anchorage.

Penetrations, bellows and valves.

Personnel locks and equipment hatch.

Seals.

Shell plate.

Material Properties

Mean value of yield strength equals 47.2 ksi. Lowest test valve of 45.7 ksi used in the analysis.

Method of the Analysis <No details printed.>

Finite element shell model.

Panel.

Membrane.

Failure criteria - maximum shear strss and von Mises.

Containment ultimate pressure is 38.2 psig, controlled by hoop forces near springline (1/2 in. plate).

1.6 Sequoyah Containment Analysis (by NRC Research) [1.6-1]

Objective

Analysis of Sequoyah containment capacity.

Assumptions

Ignore local bending effects.

Applied pressure is resisted by circumferential tension in the shell plus bending of the stringer.

Deformation are symmetric circumferentially.

Local shell bending effects are ignored.

Analysis of Internal Pressure Loading

Equilibrium of a segment of the cylindrical shell with internal pressure and stringer as a beam spanning between rings.

Mechanism occurs when shell yields in hoop direction and plastic hinge forms in stringer.

Minimum specified yield strength used (37 ksi).

Conclusions

Containment capacity at yield is 34 psig.

1.7 Sequoyah Containment Analysis (by Franklin Research Center) [1.7-1]

Objective

Analysis of Sequoyah containment strength.

Material Properties

Minimum specified yield and ultimate strength.

Analyses Methods

Four different analyses were performed:

Analysis	Notes	Pressure (psig)
1	Ring stiffeners only and ignoring stringers (axisymmetric analysis).	28 (membrane yield)
2	Axisymmetric ring stiffened shell with smeared stringers.	36 - 38 (total cross section plasticity)
3	Finite element analysis of stiffened panel bounded by rings and stringers. Confirmed smeared assumption of Analysis 2.	34.3 - 38.6 (gross shell yield)
4	Axisymmetric ring stiffened shell with smeared stringer.	34.7 (total cross section plasticity)

Analyses 1, 2 and 3 for 5/8" thick shell. Analysis 4 is for the 1/2" thick shell.

All analysis are linearly elastic. Full plasticity predicted by extrapolated linear results.

2.1 McGuire (by Ames Laboratory) [2.1-1]

Objective

Uncertainity assessment of ultimate internal pressure resistance.

Containment Description

Ice condenser, steel (Fig. 2.1-1).

Uncertainty Assessment, Material Properties, Failure Criteria

See Sequoyah (Ames Laboratory).

Simplified Analysis

See Sequoyah (Ames Laboratory).

Limit pressure for stiffened cylinder = 78 psig, controlled by hoop forces near mid-height of cylinder.

Minimum mean limit pressure for penetration analyses is 79 psig (258 penetrations).

Finite Element Analysis

See Sequoyah (Ames Laboratory).

Axisymmetric shell failure mode near cylinder mid-height at 84 psig.

Failure pressure for controlling penetration is greater than 88 psig.

Conclusion

Mean predicted failure pressure is 84 psig (approximately lognormal distribution with standard deviation of 12 psi).

2.2 McGuire (by Offshore Power System) [2.2-1]

Objective

Investigation of the vessel capacity under internal pressure.

Containment Description

Stiffened steel cylindrical shell covered with hemispherical head, (Fig. 2.1-1).

Analysis

Finite element analysis using ANSYS.

Typical panel, see Fig. 2.2-1.

Plastic triangular shell element.

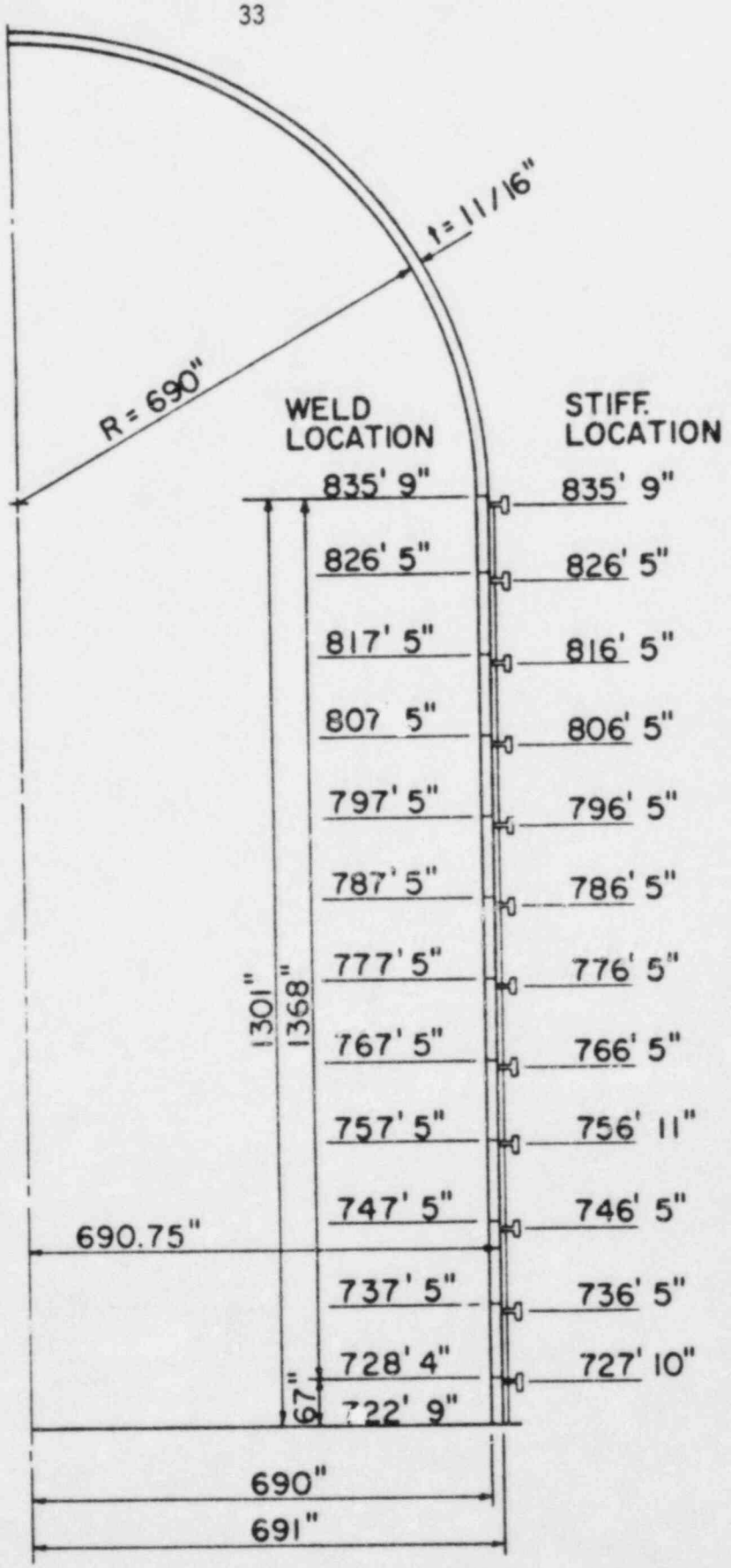

Figure 2.1-1 McGuire Containment Vessel Geometry

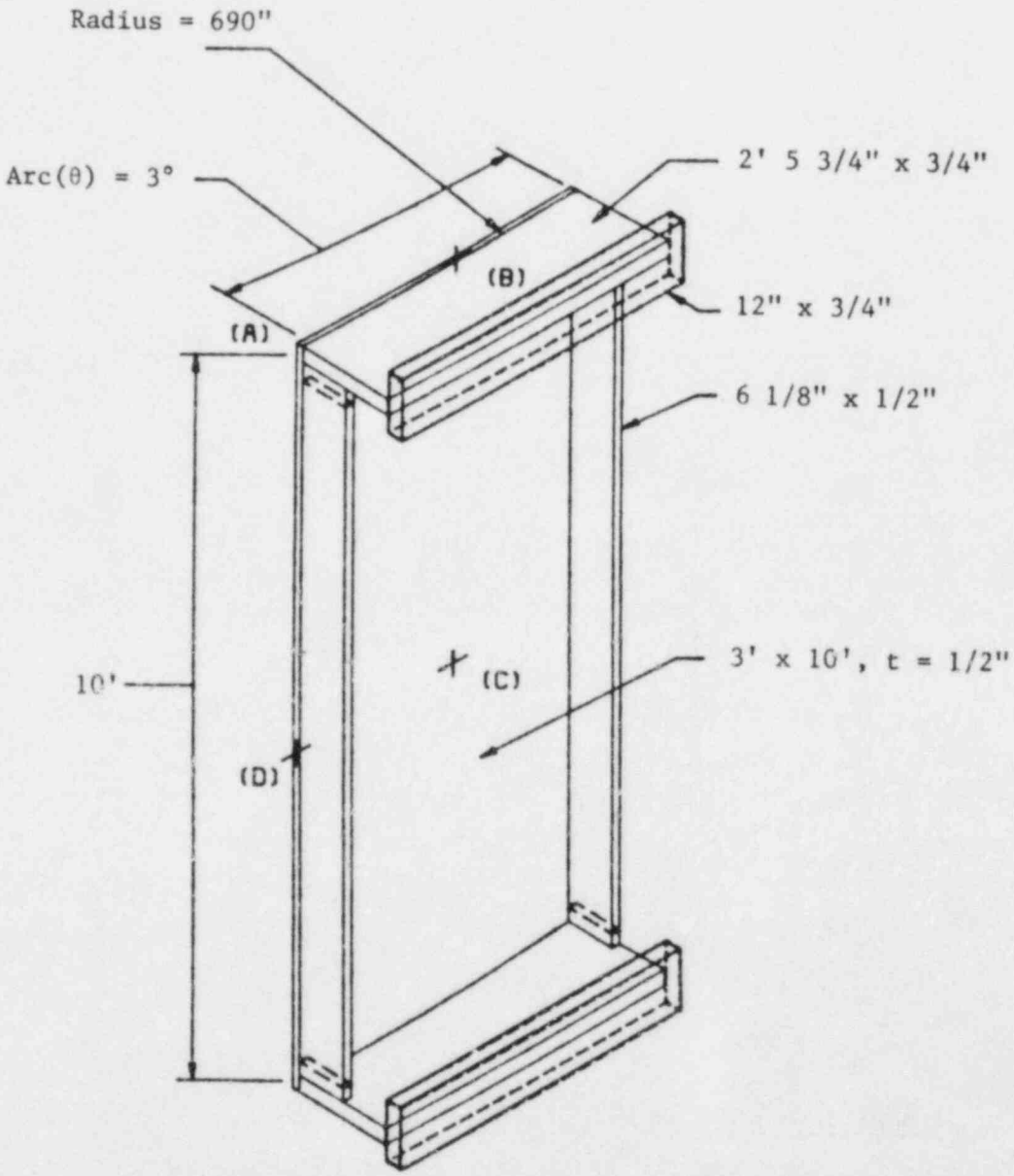

Figure 2.2-1 Idealized Panel - McGuire

Analysis was carried out up to and beyond yield stress of 42.1 ksi.

Results

Pressure - displacement, (Fig. 2.2-2).

3.1 Watts Bar (by Ames Laboratory) [3.1-1]

Objective

Uncertainty assessment of ultimate internal pressure resistance.

Containment Description

Ice condenser, steel (Fig. 3.1-1).

Containment Uncertainty Assessment, Random Vibration Analysis

<Beyond scope of this review.>

Failure Criteria

Maximum shell membrane strain equals twice the yield strain.

Penetration assumed not to control because of ASME area replacement rule.

Shell Buckling with BOSOR

BOSOR5 - finite difference program for axisymmetric shells with axisymmetric loads, nonlinear material and geometric capabilities.

Modeling guidelines:

- Maximum element length = $\sqrt{rt}/2$;
- Rings idealized as shell segments;
- Deformation theory of plasticity.

Application to Containments

Estimated material properties (actual not furnished).

Simplified method (see St. Lucie, Section 4.1 (Ames Laboratory)) - minimum mean pressure resistance is 98 psig, controlled by thin portion of dome.

Finite element analysis (BOSOR5) - failure pressure is 100 psig, controlled by membrane strain in the thin portion of the dome.

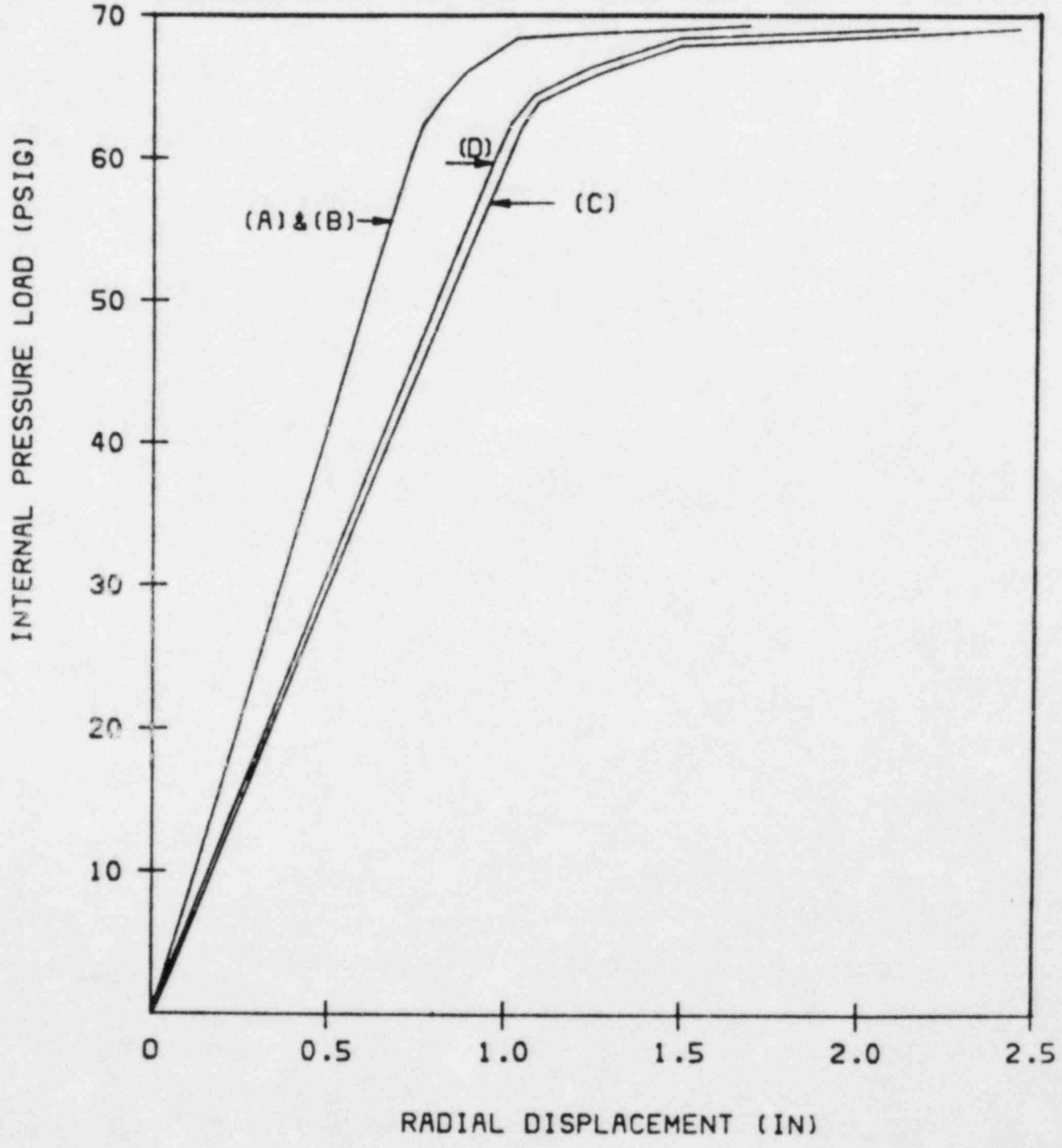

Figure 2.2-2 Pressure - Displacement Curve for McGuire Containment

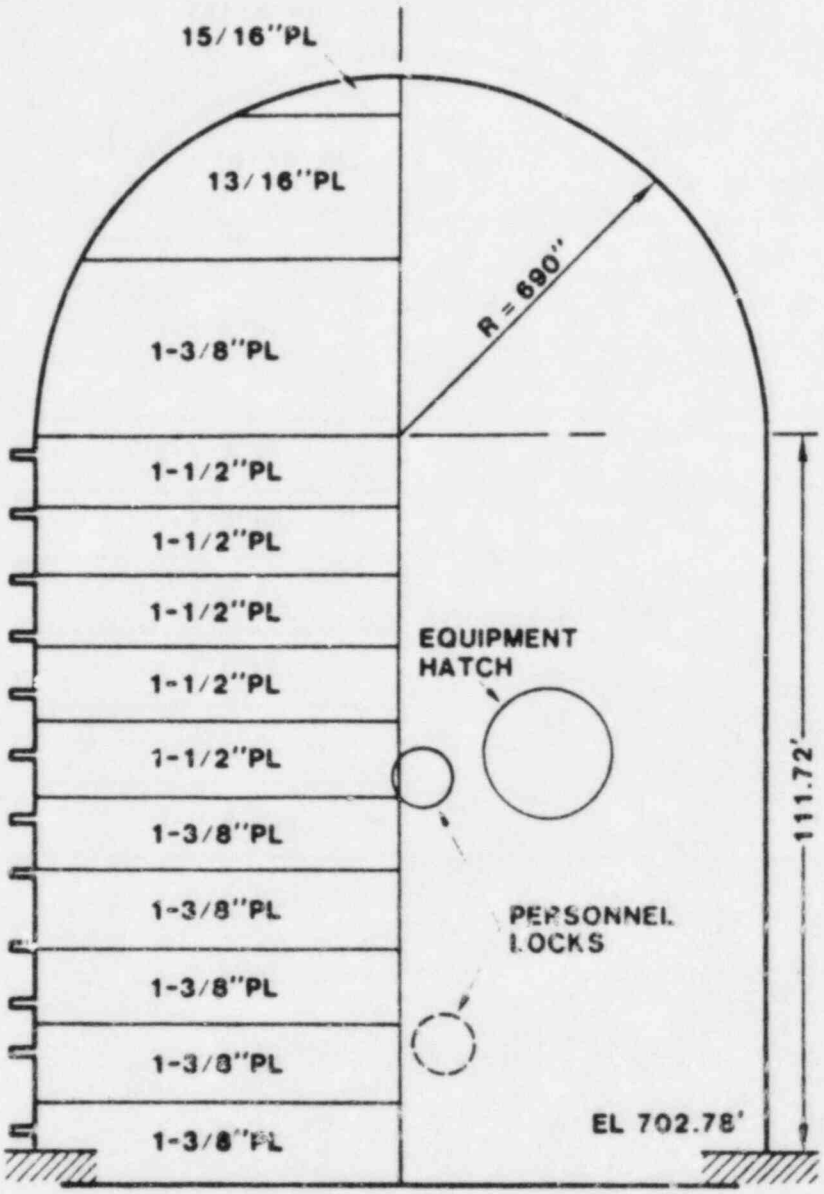

Figure 3.1-1 Watts Bar Steel Containment Vessel

Seismic resistance - <beyond scope of this review>.

Conclusion

Mean failure pressure is 98 psig (approximately lognormal distribution with a coefficient of variation of 0.16).

3.2 Watts Bar Containment (by Sandia National Laboratory) [3.2-1]

Objective

Realistic prediction of the vessel ultimate static pressure capability.

Containment Description

Ice condenser, steel (Fig. 3.1-1).

Containment Analysis

Structural analysis of:

- Containment shell without penetration;
- Equipment hatch;
- Containment anchorage system;
- Personnel airlock.

Finite element using:

- MARC computer code - large strain capability;
- ABAQUS computer code - large strain and automatic adjustment of load step size capabilities.

Actual containment material properties based upon provided mill test data by TVA.

Containment Shell Analysis

Description of the containment structure, (Fig. 3.1-1).

Finite element model - MARC computer code:

- Axisymmetric model;
- Containment base considered as fixed support;
- Large displacement and finite strain plasticity;

- Shell failure was based on the maximum Von Mises equivalent stress criteria;
- No restraining element to limit the containment deformation.

Results

Pressure (psig)	Radial Displacement of Cylinder - Midheight (in.)	Notes
90	≈ 0.75	First yield occurred at the containment base.
120	1.00	Cylinder wall at midheight and dome materials yielded.
175	40	Unrealistic - containment piping and penetration system could be damaged.

Lower bound value for Watts Bar pressure capacity (shell failure only) is 120 psig.

Equipment Hatch Analysis

Buckling analysis utilizing ABAQUS computer code.

Large deformation and elastic-plastic material behavior.

Equipment hatch boundary conditions idealization:

- Roller (radial displacement but no rotation allowed);
- Other boundary conditions such as inclusion of the shell insert of the containment wall were considered. This was rejected because of the incapability of the bolts around the hatch to maintain continuity between the sleeve and the hatch of high pressure loads.

Axisymmetric model with no imperfection.

Results

Yielding of the equipment hatch ring and door adjacent to the ring occurred before buckling occurs at 140 psig.

Hatch displaced shape at 140 psig pressure (Fig. 3.2-1).

Inclusion of imperfection should lower the predicted buckling load.

Containment Anchorage System and Personnel Lock Analysis

The analysis <no details given> showed that the pressure at which yielding of the tie down bolts occur is 172 psig and the personnel lock has a strength greater than 150 psig.

Conclusion

Containment ultimate capacity based upon containment shell yielding and equipment hatch door buckling is 120 psig and 140 psig, respectively.

PWR - DRY CONTAINMENTS - CYLINDRICAL

4.1 St. Lucie (by Ames Laboratory) [4.1-1]

Objective

Uncertainty assessment of ultimate internal pressure resistance.

Containment Description

PWR, cylinder, steel (Fig. 4.1-1).

Uncertainty Analysis

<Beyond scope of this review.>

Failure Criteria

Maximum shell membrane strain equals twice the yield strain.

Penetrations assumed not to control because of ASME area replacement rule.

Finite Element Software and Calibration

Survey of applicable programs.

ANSYS, modeling guidelines and static calibration - see Sequoyah (by Ames Laboratory).

Experimental/theoretical result greater than one for two torispherical heads under internal pressure.

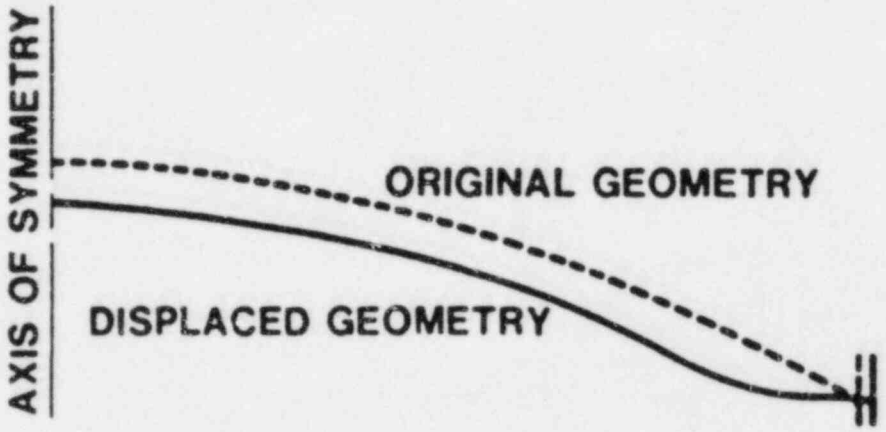

Figure 3.2-1 Displaced Shape of the Watts Bar Equipment Hatch at 140 psig (Displacement Magnification of 10%)

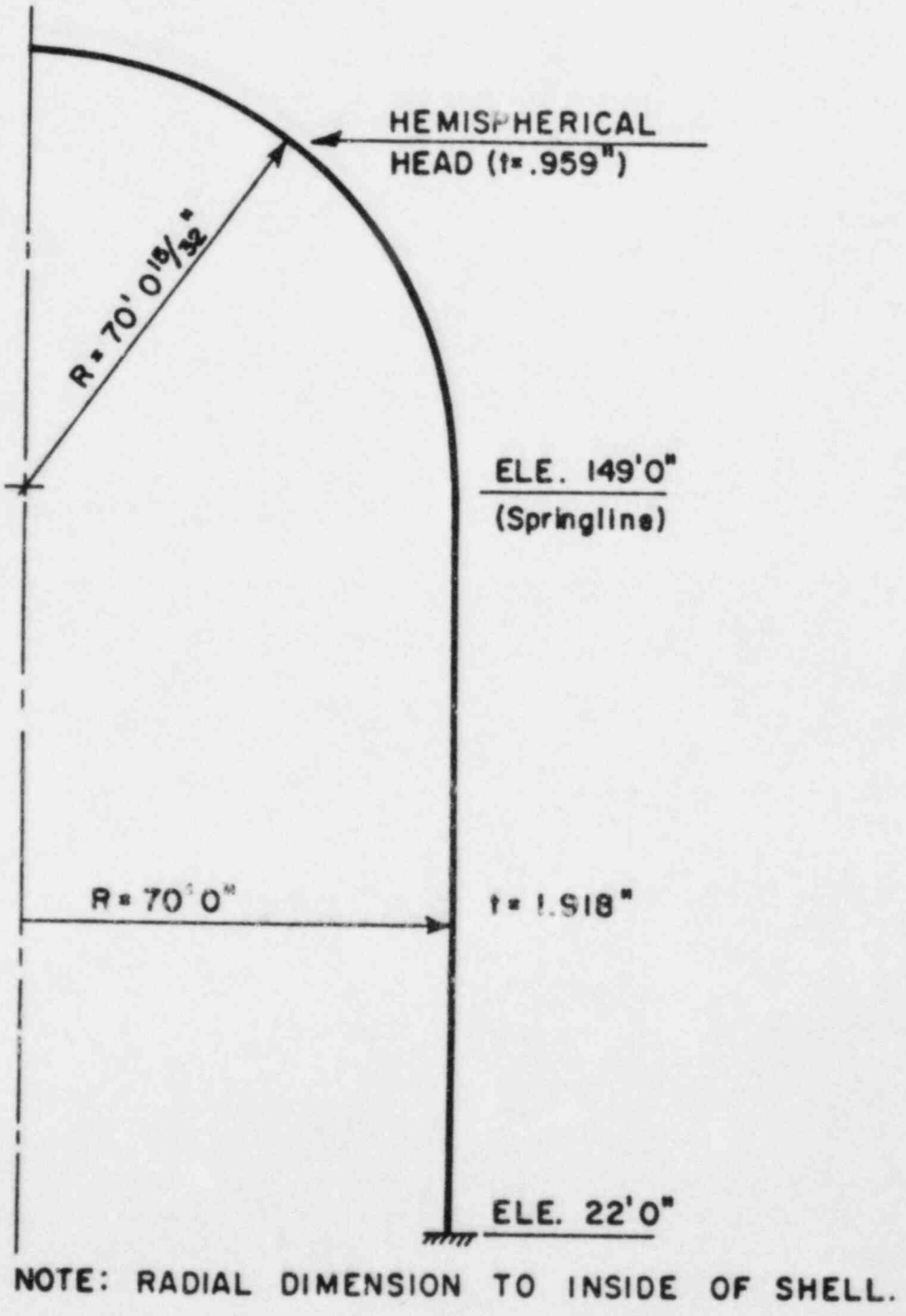

Figure 4.1-1 St. Lucie Containment Vessel Geometry

Simplified Analysis Methods [4.1-2]

Cylindrical panel bonded by stringer and ring (Fig. 4.1-2) analyzed by finite element. Three failure modes - general (includes ring), inter-ring (between rings) and panel (between rings and stringers). Panel mechanism eliminated for usual containment stiffening patterns.

Guided by finite element analysis, developed simplified methods for determining limit pressures for large displacements and maximum membrane strain at twice yield. (The experimental/theoretical results listed below are based on both experimental evidence and subjective input)

- General mode, stiffened cylinder;

$$p_o = \frac{t\,F_y}{r}\left(\frac{2}{\sqrt{3}} + \frac{A_1}{s_1 t}\right)$$

where A_1, s_1 = ring area and spacing, respectively.

(experimental/theoretical result mean = 0.99, COV = 0.12)

- Inter-ring mode, stiffened cylinder;

$$p_o = \frac{F_y\,t/r}{\left(1 - \frac{8\,\varepsilon_y r^2}{s_1^2}\right)}\left\{\frac{2}{\sqrt{3}} + \frac{12\,Zr}{s_1^2\,t}\right\}$$

where Z is the plastic section modulus of the shell and stringer per unit circumference.

(Experimental/theoretical result mean = 0.96, COV = 0.11)

- General mode, stiffened cone;

$$p_o = \frac{F_y\,t/r}{\left(1 + \frac{\rho_1}{12}\right)^2}\left(\frac{2}{\sqrt{3}} + \frac{A_1\,r_r}{s_1\,t\,r}\right) \quad ; r = \frac{r_1 + r_2}{2\sin\phi} \; ; \; \rho_1 = \frac{r_2 - r_1}{r\sin\phi}$$

in which r_1 and r_2 are the upper and lower radii of the cone segment, respectively, r_r is the ring radius and ϕ is the slope of the shell meridian line.

- Inter-ring mode, stiffened cone;

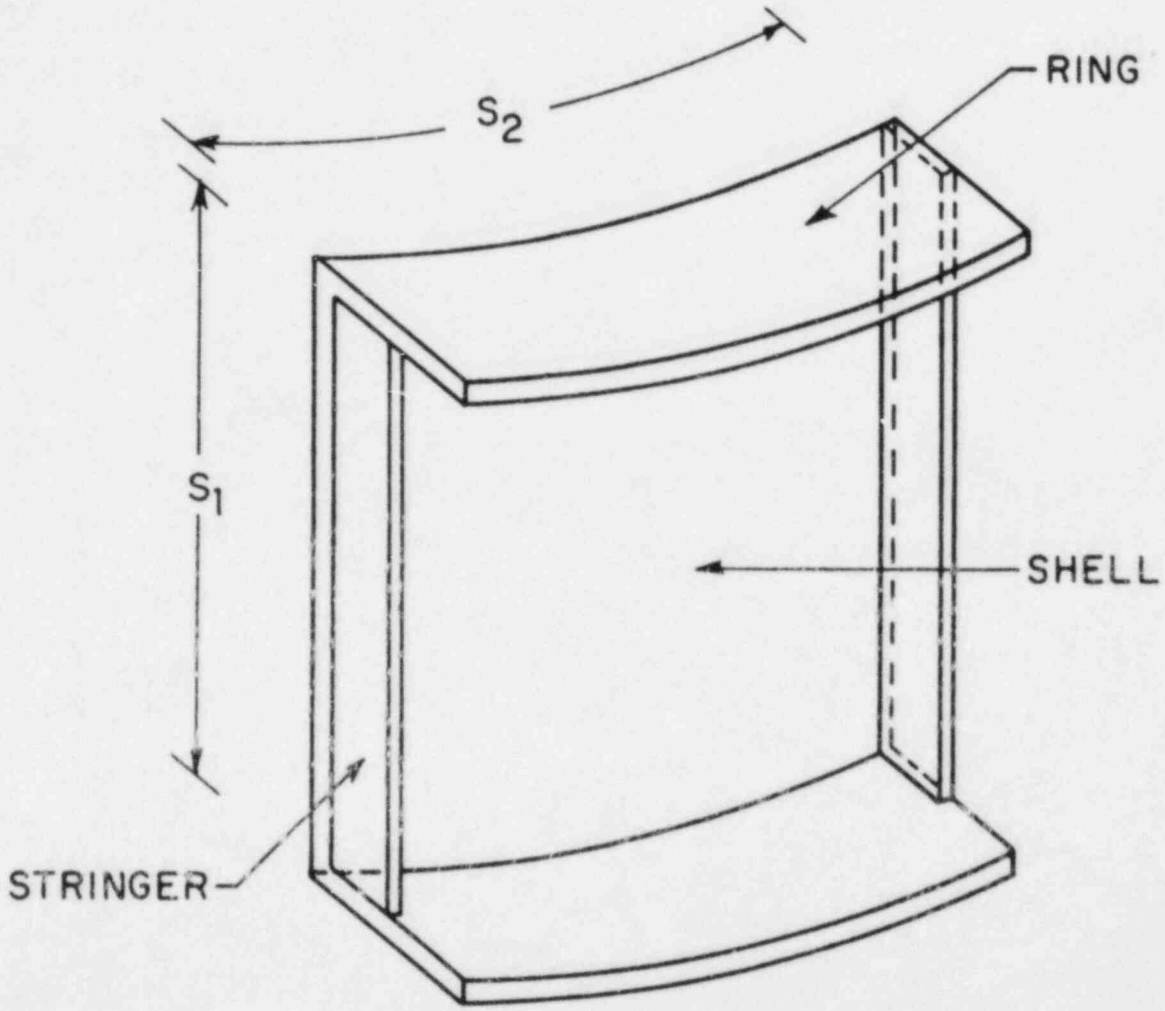

Figure 4.1-2 Typical Stiffened Shell Panel

$$p_o = \frac{F_y \, t/r \, \left(\frac{2}{\sqrt{3}} + \frac{12 \, \bar{Z} \, r}{t \, L^2} \right)}{1 + 0.05 \, \rho_1^2 - 8\varepsilon_y \, \rho_2^2 (1 + 0.15 \, \rho_1^2 + 0.375 \, \rho_3^2)}$$

where

$$\rho_2 = \frac{(r_1^2 + r_2^2)}{s_1} \; ; \quad \rho_3 = \frac{2(r_2 - r_1)}{(r_1^2 + r_2^2)} \; ; \quad \bar{Z} = \frac{Z_1 r_2^2 + Z_2 r_1^2}{(r_1 + r_2)^2}$$

in which L is the ring spacing measured in the meridional direction. The plastic section moduli per unit circumferential length at the top and bottom boundaries are Z_1 and Z_2, respectively.

- Hemispherical head

$$p_o = \frac{2t \, F_y}{r}$$

- Ellipsoidal head, asymmetric buckling

$$p_{cr} = 10.4 \, F_y \left(\frac{t}{2r}\right)^{1.25}$$

(experimental/theoretical result mean = 1.01, COV = 0.11)

- Ellipsoidal head, axisymmetric collapse

$$p_o = \frac{F_y \, t}{r} (1 + 50 \, \varepsilon_y)$$

(experimental/theoretical result mean = 1.01, COV = 0.10)

- Torispherical head, asymmetric buckling

$$p_{cr} = \frac{285 \, F_y \, (1\text{-}125 \, \varepsilon_y)(r_t/2r)^{0.84}}{\left(\frac{2r}{t}\right)^{1.53} \left(\frac{R_s}{2r}\right)^{1.1}}$$

(experimental/theoretical result mean = 0.98, COV = 0.12)

- Torispherical head, plastic collapse

$$p_o = \frac{12.6\ F_y\ (1 + 240\ \varepsilon_y)(r_t/2r)^{1.04}}{(\frac{2r}{t})^{1.09}\ (\frac{R_s}{2r})^a}$$

for the limit pressure, where

$$a = \begin{cases} 0.79 & \frac{R_s}{2r} > 1 \\ 1.10 & \frac{R_s}{2r} < 1 \end{cases}$$

(experimental/theoretical result mean = 0.97, COV = 0.11)

Dynamic pressure. <Beyond scope of this review>.

Containment Uncertainty Analysis

Estimated material properties (actual not furnished).

Simplified method - minimum mean pressure resistance is 95 psig, controlled by hemispherical head.

Finite element analysis - failure pressure is 96 psig, controlled by membrane strain at cylinder/hemisphere intersection.

Dynamic and reliability results. <Beyond scope of this review>.

Conclusion

Mean failure pressure is 95 psig (approximately lognormal distribution with coefficient of variation of 0.16).

PWR - DRY CONTAINMENT - SPHERICAL

5.1 Cherokee (by Ames Laboratory) [5.1-1]

Objective

Uncertainty assessment of ultimate internal pressure resistance.

Containment Description

PWR, spherical, steel (Fig. 5.1-1).

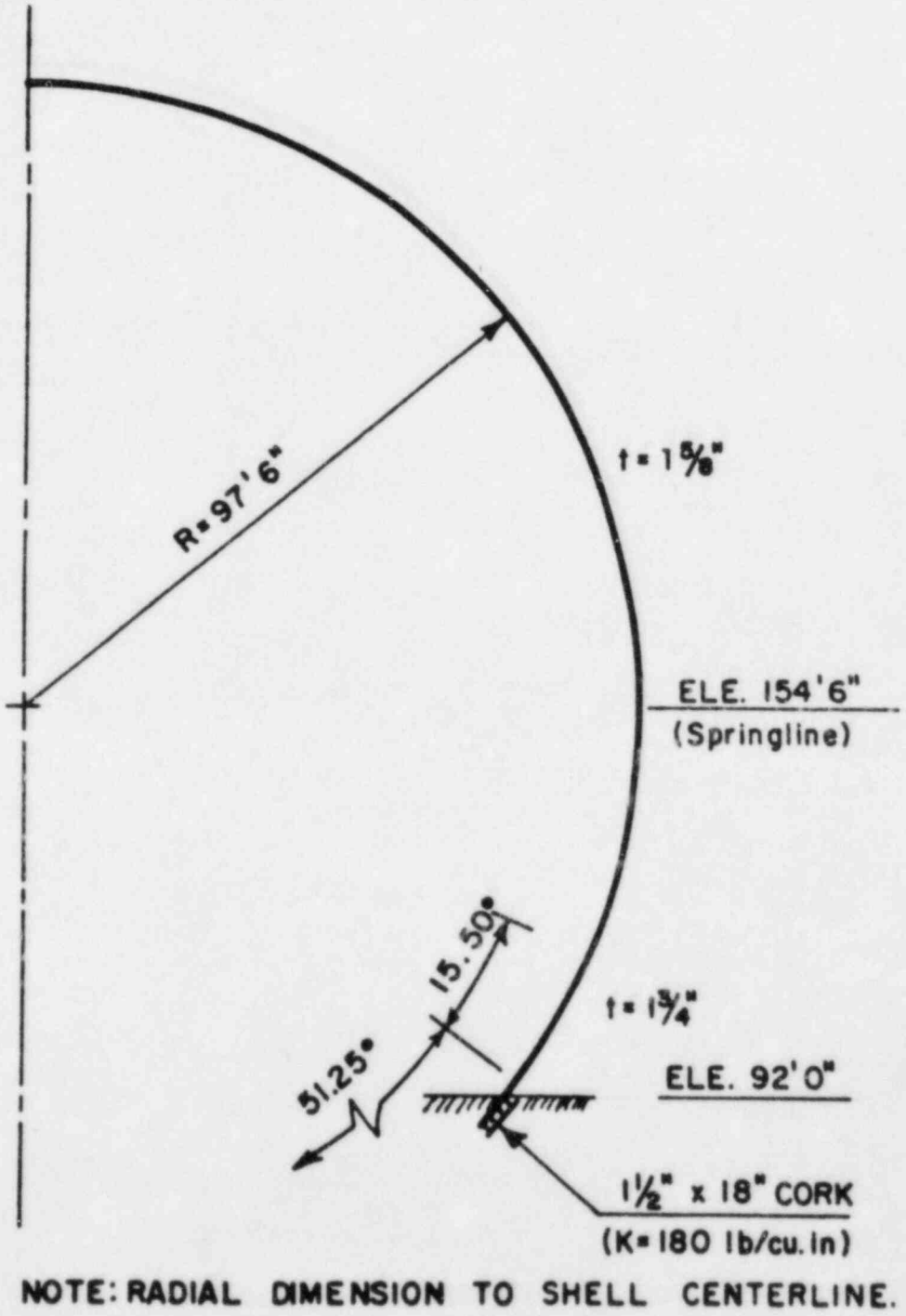

Figure 5.1-1 Cherokee Containment Vessel Geometry

Uncertainty Analysis, Failure Criteria, Finite Element Software and Calibration, Simplified Analysis Methods

See St. Lucie (Ames Laboratory).

Containment Uncertainty Analysis

Estimated material properties (actual not furnished).

Simplified method - minimum mean pressure resistance is 116 psig, controlled by membrane stress in sphere.

Finite element analysis - failure pressure is 117 psig controlled by membrane strain in the sphere.

Conclusion

Mean failure pressure is 116 psig (approximately lognormal distribution with coefficient of variation of 0.16).

PWR - ATMOSPHERIC CONTAINMENTS

6.1 Indian Point Containment (by Sandia National Laboratory) [6.1-1]

Objective

- Determination of the internal pressure at failure for units 2 and 3.
- Determination of the containment response to dynamic pressure <beyond the scope of this review>.

Penetrations

Study of Indian Point Unit 2 equipment hatch and personnel lock.

Failure modes:

- Steel reinforcement;
- Integrity of the steel liner plate against leakage.

Preliminary analysis <no details given> showed that because of the heavy reinforcement, failure at these two penetrations is unlikely to occur.

Containment Building

Reinforced concrete (Fig. 6.1-1).

Analysis

HONDO - dynamic finite element computer code.

Finite Element Model

Axisymmetric model ignoring penetrations.

Separate elements used for concrete, reinforcing steel and liner (7 elements throughout the thickness).

Elastic-plastic material idealization for steel liner plate and rebars. The hoop rebars were smeared into a continuous thin layer; which was then expanded into a much thicker layer (for dynamic analysis). The yield strength and elastic modulus were adjusted to account for this.

Soil model - elastic spring element.

Preliminary Calculation

Simple analysis using

$$p = \frac{t\sigma}{r}$$

p = pressure, r = radius, σ = stress, t (equivalent thickness) found from smearing the hoop rebars.

Assumes concrete has no capability to carry tensile loads.

Calculated maximum pressure (σ = ultimate strength) = 123 psig.

Another simple analysis:

$$\text{failure pressure} = \text{design pressure (47 psig)} \times \frac{\text{ultimate stress (90 ksi)}}{\text{yield stress (60 ksi)}}$$

$$\times \text{ load factor (1.5)} \times \frac{1}{\phi \text{ factor (.9)}} = 117.5 \text{ psig}$$

This analysis neglects the benefit of the seismic steel and the liner plate.

Model Calibration

Calibration of HONDO finite element program results with the structural integrity test (SIT) results.

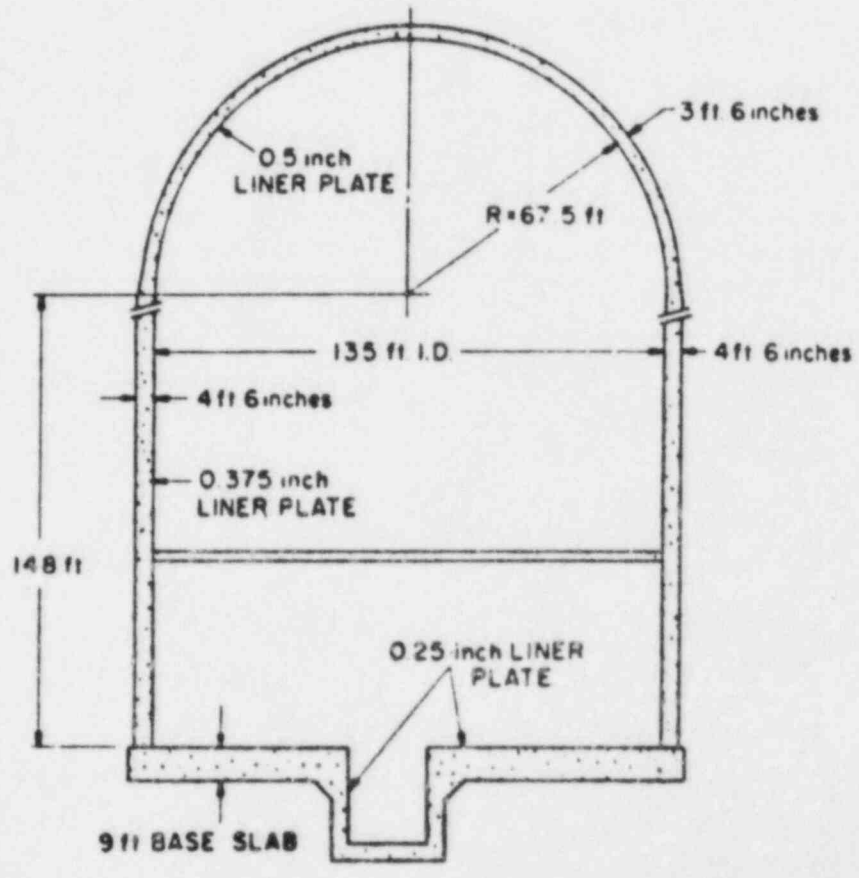

Figure 6.1-1 Indian Point Containment Building.

Pressure applied as ramp function.

Comparison showed that the measured and predicted radial displacement of a point removed from the base and dome differed noticeably.

Reducing the elastic modulus by 50% <no reason is given> and keeping the yield strength constant results in close results to the SIT results.

Static Results

Pressure loading applied as ramp function, plus gravity loads.

Radial displacement became unbounded at pressure = 108 psig.

Uplift of the containment corner was observed.

Discussion

Static solution was not completely achieved (see model calibration).

Building deformations start to increase at a very rapid rate indicating instability at pressure of 110 psig.

Finite element results agree with the simple (hand) calculations analysis.

Hand calculations assume uniformly strained rebars, at a pressure of about 120 psig, rebar strain of 7%, and the corresponding radial displacement of 4.7 ft.

Concrete will be extensively cracked long before this displacement.

Conclusion

Failure pressure for the Indian Point containment is approximately 110 psig.

6.2 Indian Point Containment (by Los Alamos) [6.2-2]

Objective

Prediction of the vessel internal pressure ultimate capacity.

Containment Building Design

Reinforced concrete (Fig. 6.1-1).

Structural Modeling

ADINA finite element code.

Two dimensional axisymmetric models. Penetrations (small or large) were not considered.

Soil - axisymmetric, discrete, compression only springs.

Concrete behavior - based upon tensile cracking, compression crushing and strain softening model. Concrete cracking was assumed to occur when the principle stress exceeds the uniaxial cutoff tensile stress and the original stiffnesses were reduced as:

shear reduction factor = 50%;
tensile stiffness reduction factor = 0.01%.

Concrete material properties are based upon a design value of 4 ksi compressive strength.

As built material properties of reinforcement material.

Ring elements used to idealized the smeared hoop reinforcement. Seismic steel projected unto hoop and meridional directions. Truss element used for meridional steel idealization.

Steel liner properties were assumed to be the same as the Zion liner plate actual properties.

Comparison with Structural Integrity Test (SIT)

Loads - dead weight and equipment plus incrementally applied internal pressure up to 54 psig (115% of the design pressure).

Finite element gives significantly greater displacement values than the measured one because of assumptions in concrete cracking model.

Containment Static Response and Failure

The solution is considered to be converged if unique values for the displacements <no details given> were reached at cylinder midheight node, apex of the dome, and outer corner of the base mat.

Pressure (psig)	Notes
30	First concrete cracking
100	First reinforcement yield
105	Liner first exceeds 0.3% strain
112	Lower bound failure pressure*
133	Upper bound failure pressure**

Pressure (psig)	Notes
118	Predicted failure pressure (shear and compression at base of sideway)

* Limit analysis of the shear carring capability of the base sidewall junction <no details given>.

** Limit analysis considering membrane failure of the cylinder sidewalls in the hoop direction.

Conclusion

Containment ultimate capacity is 118 psig. Failure caused by concrete crushing and cracking coupled with a loss of shear carrying capacity at the base of the cylindrical wall.

6.3 Indian Point Containment Vessel (by United Engineers and Constructions, Inc.) [6.3-1]

Objective

Evaluation of the capability to withstand conditions representative of a core melt accident.

Study Methodology

Capability is defined as the maximum combination of thermal and pressure required to produce a general yielding in the reinforced steel.

Predicting the weakest failure mode among all possible modes (both bursting and leaking).

Hand calculations to evaluate the capability at the following regions (failure modes):

- Membrane region of the dome and cylinder;
- Discontinuity - cylinder/dome and cylinder/basemat;
- Basemat;
- Large penetration - equipment hatch and personnel airlock;
- Small penetration;
- Liner plate.

Computer code used for liner/anchor system under thermal loads.

Containment Description - Configuration

Reinforced concrete vessel, Fig. 6.1-1.

Containment Description - Material Properties

Concrete - design minimum ultimate strength = 3 ksi.

Reinforcing steel - specified minimum F_y = 60 ksi and tensile strength = 90 ksi.

Liner plate - specified minimum F_y = 32 ksi and tensile strength = 60 ksi.

Design Criteria

<Beyond scope of this review>.

Analysis - Hand Calculations

Shell (membrane region):

- Used $\frac{pr}{t}$ (hoop) and $\frac{pr}{2t}$ (longitudinal);
- Includes liner and seismic rebars;
- General yielding state in tension, mean actual rebar yield stress used.
- Temperature has no effects unless high enough to change material properties;
- Results (controlling locations): 126 psig for both units.

Shell (discontinuity region).

- Base of the cylinder - classical beam on elastic foundation equations were used, fixed base, pressure capacities <no details given> are:

  149 psig (governed by moment capacity)
  131 psig (governed by shear capacity)

- Basemat - idealized with uniform foundation reaction with edge uplifting and compatibility with shell. Shear capacity will permit pressures greater than 126 psig <no details given>.

Liner and Liner Anchor Analysis

126 psi internal pressure combined with temperature below 300°F (temperature which a liner experienced during an accident, reference is

not available during the period of this work) will not result in loss of liner integrity.

Penetrations - Large Openings

Equipment and personnel locks investigated under pressure of 126 psig considering: membrane plus bending; anchorages to the concrete; and increased reinforcement near the opening.

Large penetrations regions are not critical because the predicted yielding is localized <no details given>.

Penetrations - Piping

Representative openings studied considering internal pressure pulse pipe reaction, and anchorages to concrete.

The study judged that these are not critical sections <no details given>.

Piping Penetration Assemblies

Three different piping types were investigated under internal pressure and thermal loading.

Load capability of the sleeves, the end plate and the end plate to process pipe weld were evaluated separately.

Maximum weld stress was limited to to 1.5 times the ASME allowable.

Containment wall growth deformation effects was not included.

Temperature on piping penetration welds was found to be the limiting factor <no details given>.

Electric penetrations based upon Westinghouse test can withstand pressures above these results from LOCA and will preserve integrity of the containment boundary up to a temperature of 400°F.

10 inch and 36 inch butterfly valves will withstand pressures of 202 psig at 300°F and 130 psig at 275°F because of air "buffer" injected between redundunt pair of valves.

Conclusions

Indian Point units 2 and 3 can withstand an internal pressure of 126 psig.

Cylindrical sections near the spring line is the critical region (membrane hoop forces).

Temperature has little or no effects on the containment capability.

PWR - SUB ATMOSPHERE

7.1 Maine Yankee Containment (by Sandia National Laboratory) [7.1-1]

Objective

Realistic prediction of the vessel ultimate static pressure capability.

Containment Building Description

Reinforced concrete with a steel liner, Fig. 7.1-1.

Finite Element Model

ADINA - finite element code.

Axisymmetric model (no penetrations considered) using three different types of elements:

- Two-dimensional solid element for concrete;
- Truss element for reinforcement steel;
- Shell element for liner plate;

Material properties - minimum specified values.

Concrete cracking - reduction of the original stiffness when crack forms perpendicular to maximum tensile principal stress:

shear stiffness reduction factor = 0.5
tensile stiffness reduction factor = 0.0001.

Longitudinal and hoop truss elements cross-sectional areas were adjusted according to the areas of the reinforcement per radian and between nodes, respectively.

Basemat - investigated two cases:

- Boundary condition as shown in Fig. 7.1-2;
- Nonlinear truss element with compressive stiffness only to model soil effects.

Analysis and Results

Loads - gravity load first applied followed by the internal pressure in load increments:

- Load increment of 0.5 psig results in nonconvergence solution with modified Newton method;
- Load increment was then reduced to 0.1 psig with no equilibrium iterations;

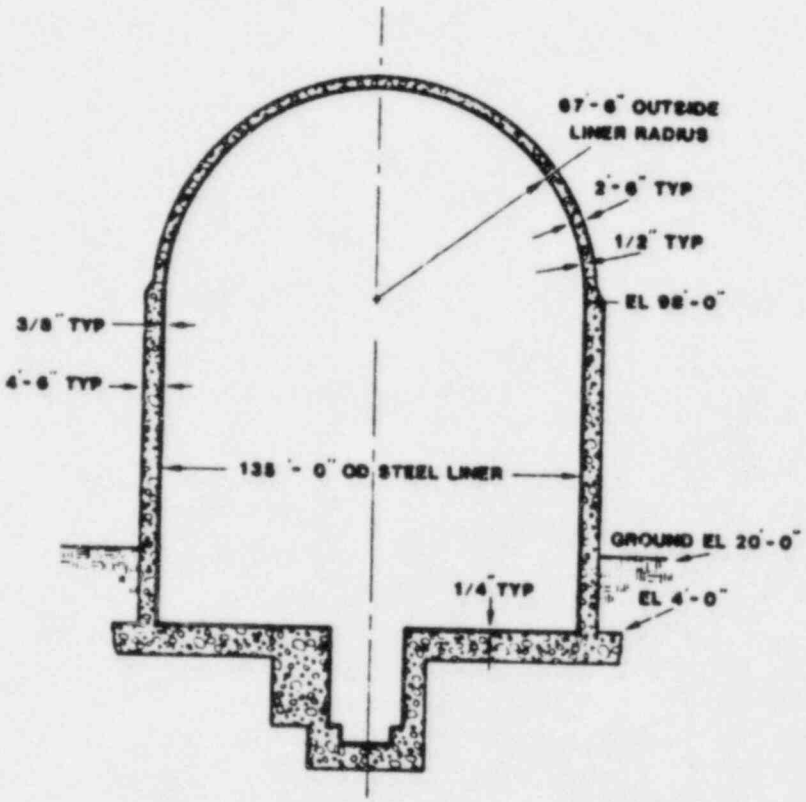

Figure 7.1-1 Maine Yankee Containment Structure

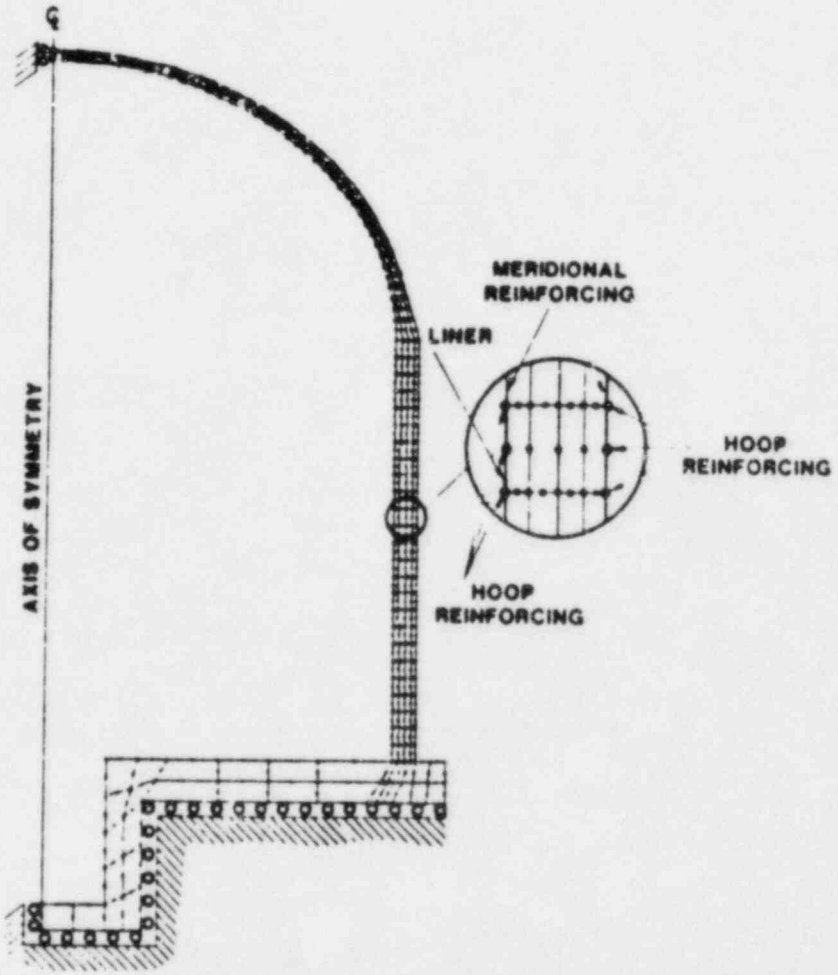

Figure 7.1-2 Axisymmetric Finite Element Model of the Maine Yankee Containment

Results for no basemat uplift are:

Pressure, (psig)	Notes
31	Linear behavior cracks formed over the entire cylinder and half way up to the dome.
73	First yielding in the liner at mid-cylinder height.
118	General yielding of hoop steel began (117 psig from hand calculation).
129	Solution was terminated because of numerical instability which resulted from the damage at the cylinder wall-base slab junction. General yielding of hoop, longitudinal reinforcement and liner occurred.

Results when basemat uplift was allowed - the behavior is similar to the previous case up to pressure of 73 psig. Concrete at the cylinder wall-basemat junction was severely damaged at 96 psig causing numerical instability to the solution.

- The differences in the solution of the above two basemat idealizations occur after 70 psig (see Fig. 7.1-3).
- Does a true structural failure correspond to this numerical instability? The answer apparently cannot be addressed with the current state-of-the-art [7.1-1].

Conclusions

If basemat uplift is allowed, failure due to severe damage in the cylinder wall base slab junction occurred at 96 psig. If basemat uplift is not allowed, failure due to general yield of rebars at 118 psig.

Bounds on the ultimate pressure capacity of the vessel and 96 psig and 118 psig.

8.1 Zion Containment Vessel (by Sargent and Lundy Engineers) [8.1-1, 8.1-2]

Objective

Ultimate internal pressure capacity for Probabilistic Risk Assessment (PRA).

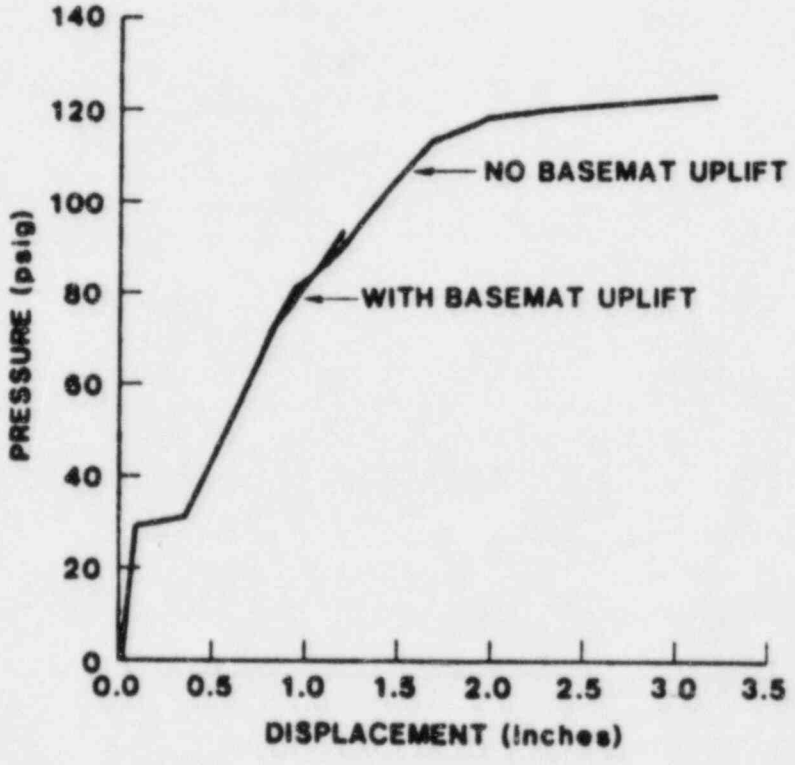

Figure 7.1-3 Radial Displacement of the Maine Yankee Cylinder Wall at Mid-Height

Configuration

Prestressed concrete vessel, Fig. 8.1-1.

Material Properties

In-place properties for concrete, reinforcing steel, post-tensioning steel, steel liner, and soil.

Actual average strength properties for reinforcing steel, steel liner, post-tensioning and soil were used in the containment strength calculations.

The concrete compressive strength, f'_c was expressed as the average value minus one standard deviation. Concrete tensile strength was taken as $6\sqrt{f'_c}$.

Best estimates of soil properties were used.

Failure Modes, Fig. 8.1-2

Assume no weld failure in the liner plate.

Primary failure modes are:

- Containment wall;
- Containment dome.

Secondary failure modes are:

- Cylinder/dome intersection;
- Cylinder/basemat intersection;
- Penetration.

Basemat failure is unlikely because continuous support by soil below.

Failure Criteria

Component	Limits
Tendon yielding strain	1%*
Shear failure	
Linear membrane strain	$15\ \varepsilon_y < \varepsilon_u/4$
Linear extreme fiber strain	$\varepsilon_u/2$

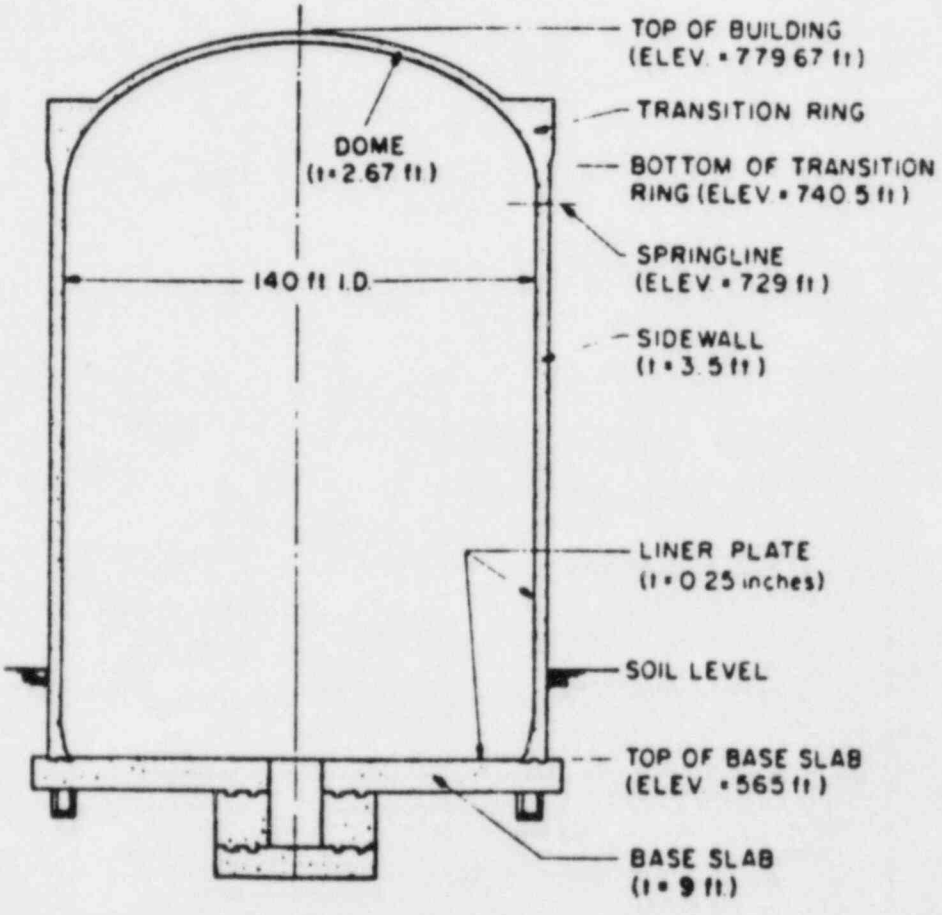

Figure 8.1-1 Zion Containment Building.

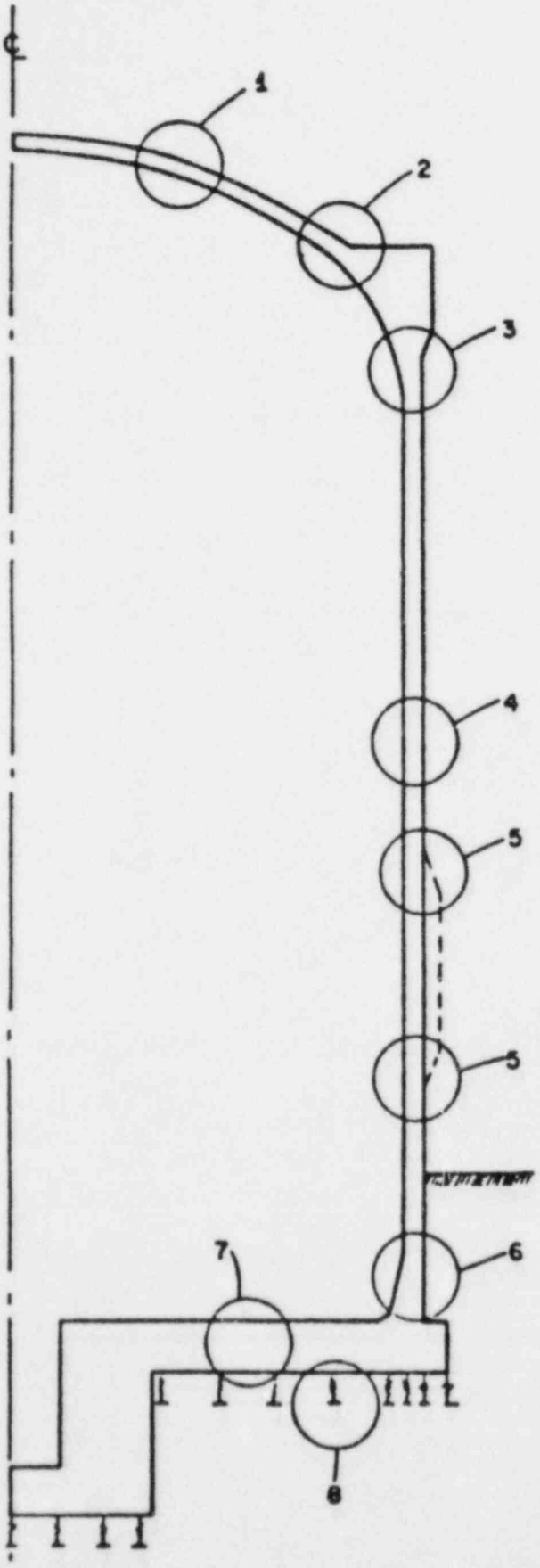

1 - DOME TENDONS

2 - DOME DISCONTINUITY (MOMENTS, SHEARS)

3 - CYLINDER DISCONTINUITY (MOMENTS, SHEARS)

4 - HOOP TENDONS, LINER, VERTICAL TENDONS

5 - EQUIPMENT HATCH FAILURE

6 - CYLINDER RESTRAINT (MOMENTS, SHEARS)

7 - BASE MAT REINFORCING AND SHEAR TIES

8 - SOIL PRESSURE

Figure 8.1-2 Containment Potential Modes of Failure

Component	Limit
Steel reinforcement strain	$10\ \varepsilon_y < \varepsilon_u/4$
Concrete compression	f'_c
Concrete tension	$6\ \sqrt{f'_c}$
Soil failure	F_u

where:

ε_y = Mean value of the yield strain.

ε_u = Ultimate strain, taken as the mean value minus one standard deviation.

f'_c = Defined in material properties section.

---

* Deformation of containment walls are unacceptable beyond this point because of interaction with adjacent buildings and gross mechanical damage to liner, penetrations, piping and equipment.

Analytical Techniques - Hand Calculations

Membrane equilibrium of cylinder and dome <no details given> at the following transition stages:

	Without Liner	With Liner
	(hoop forces in cylinder controls)	
• Concrete cracking	75 psig	75 psig
• Steel reinforcement yielding	110 psig	124 psig
• Post-tensioning yielding (1% strain)	120 psig	134 psig
• Post-tensioning ultimate	129 psig	143 psig

The above includes the effect of concrete creep and containment deformation on tendon stresses.

Radial displacement of the cylinder versus pressure shown in Fig. 8.1-3 is based upon strains at the above material stress state.

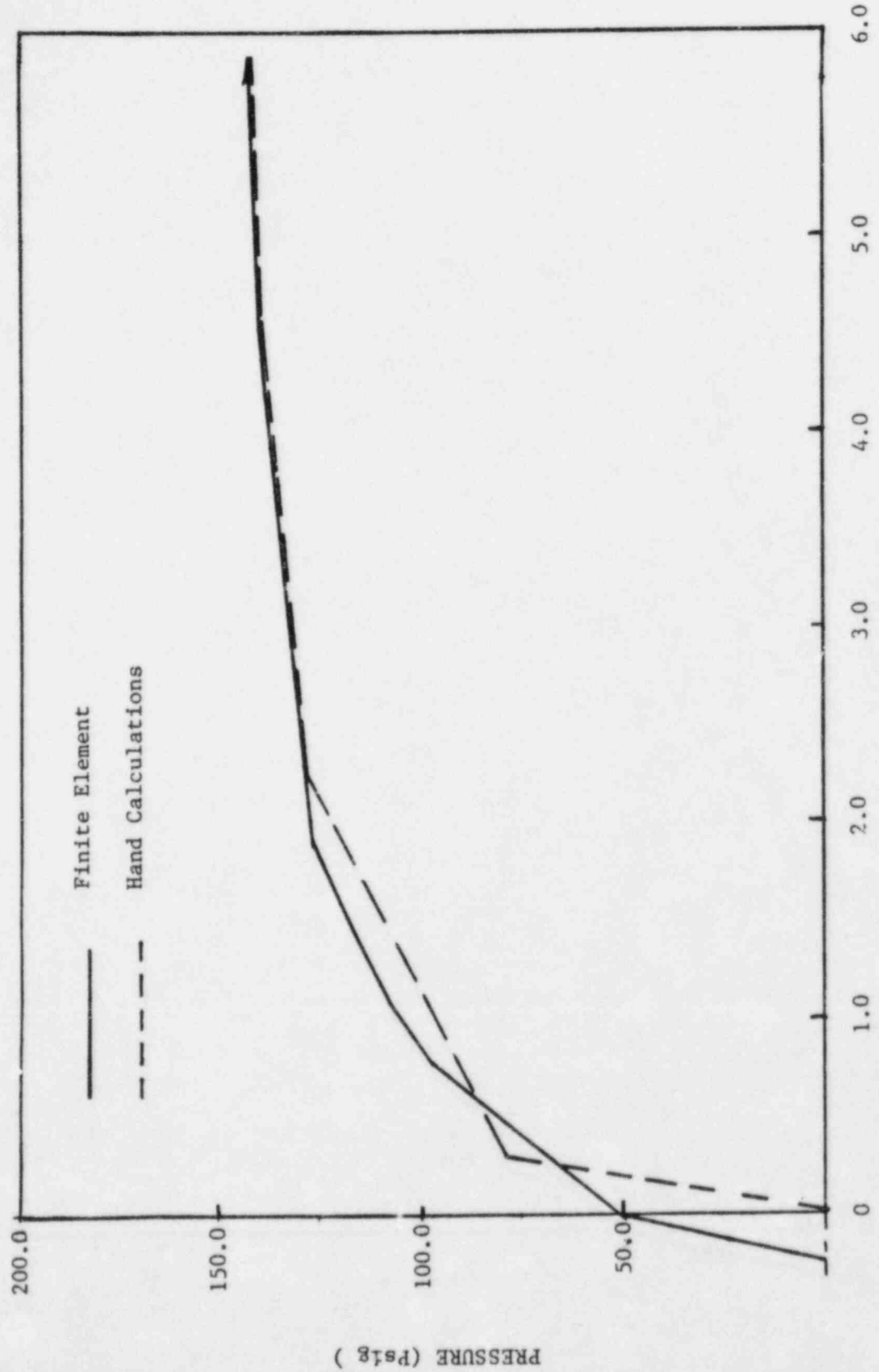

Figure 8.1-3 Internal Pressure Versus Radial Displacement of the Zion Containment

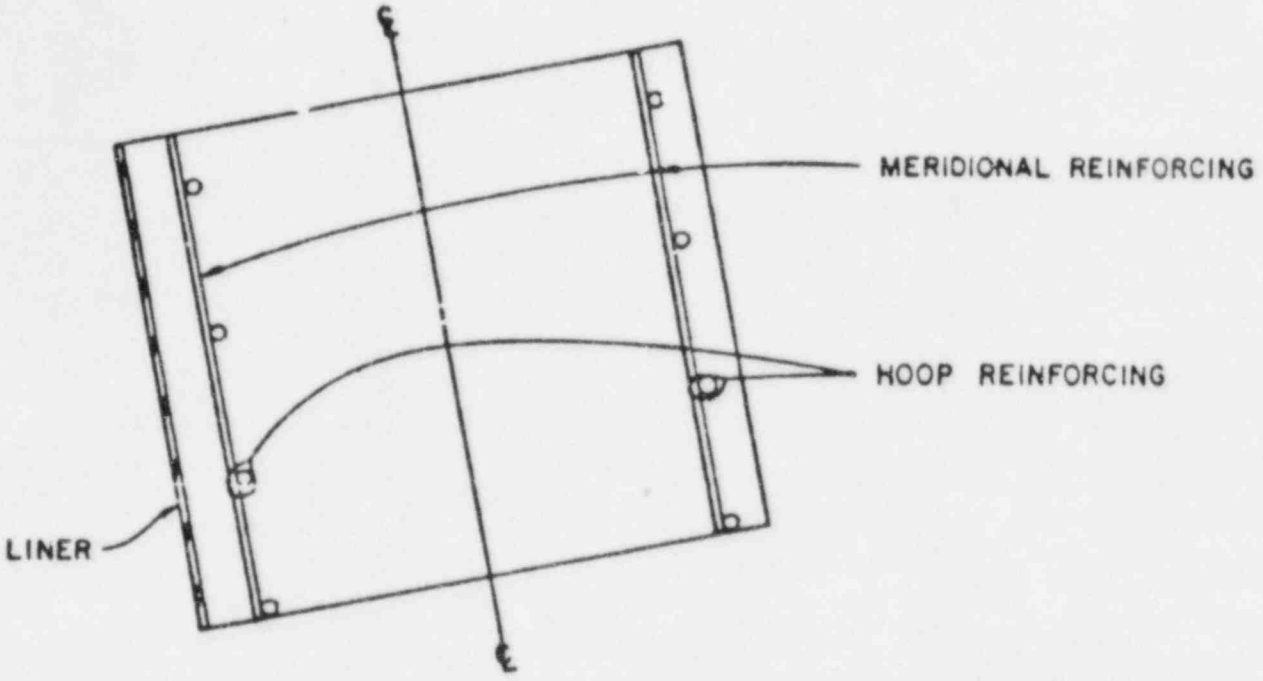

REINFORCED CONCRETE SHELL ELEMENT

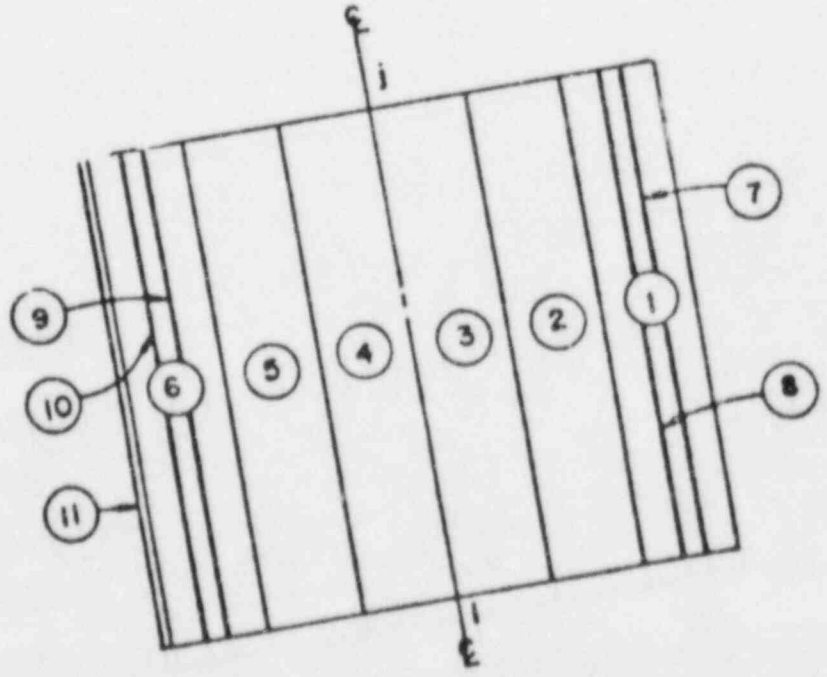

CONCRETE LAYERS 1 THRU 6

MERID. STEEL LAYERS 8 & 10

HOOP STEEL LAYERS 7 & 9

LINER LAYER 11

Figure 8.1-4 Layered Element for Nonlinear Finite Element Analysis

Analytical Methods - Finite Element

DYNAX - nonlinear analysis of thin shells and solids of revolution with concrete cracking and steel yielding (proprietory - no details given).

Finite element model includes:

- Cylinder, basemat, dome - multiple layers using axisymmetric shell element (details in Fig. 8.1-4);
- Tendons - trilinear idealization of nonlinear behavior beyond prestressed conditions;
- Prestress forces - represented by external pressure on cylinder and dome and concentrated forces at top and bottom of cylinder;
- Soil - axisymmetric, discrete, compression only springs.

Radial displacement of cylinder versus pressure is shown in Fig. 8.1-3.

Close to experimental results obtained from a 1:14 model (see later details). Experimental pressure was 110 psig at steel yielding and 159 psig at containment failure (hoop tendon failure).

Shear Failure Investigation

From the DYNAX run, six (1 through 6, Fig. 8.1-2) critical sections in the containment were examined.

Two additional sections, one on the side of the equipment hatch (hoop) and the other on the top (meridional) were studied. A finite element model used to determine the stresses around the equipment hatch <no details given> at pressure of 47 psig. The stresses were then modified to 134 psig internal pressure using the ratio of the prestressing forces corresponding to 47 psig and that of 134 psig (found from DYNAX finite element analysis). Conservative modification.

Analysis showed all various sections are safe for shear (using ASME BPV-III-2, CC-3421.4.11c). Crushing of concrete also does not occur at any section.

Large Penetration Investigation

The maximum reinforcing steel stress and concrete compressive stresses were within the limits at pressure level of 134 psig. Linear finite element analysis was proportioned to 134 psig. In-house program, TEMCO <no details given> was used to check steel and concrete stress.

Connection details between the large openings (equipment and personnel hatches) and the liner plate was also examined in details by Chicago

Bridge and Iron Company. Each steel element in both openings was investigated to determine its capacity based upon:

- Stability;
- Tensile or compressive yielding;
- Ability to maintain leak tightness.

Hand calculations based upon existing formulas showed that the strength of all steel elements are above 134 psig.

Liner Plate Strain Analysis

Two loading cases were investigated.

Temperature:

- Buckling analysis of individual panel (spacing between embedded anchors) for three different boundary conditions. In-house computer code used LAFD <no details given>;
- Hand calculation to determine the central hinge strain and the anchor force.

Temperature and pressure:

- Thermal load applied first and assumed to buckle liner with three plastic hinges formed;
- Applying internal pressure reverses the nature of the plastic moment from positive to negative at the hinges;
- Analysis showed formation of two additional hinges <no details given> at pressure of 61.0 psig;
- Maximum surface strain at pressure of 141 psi is one-third the liner material failure strain;
- Containment leak tightness is expected to be maintained at 134 psig internal pressure.

Confidence - Probability Calculations

Considered randomness of material yield strength.

Conclusions

Ultimate internal pressure capacity (hoop tendon yielding).

120 psig	without liner	(standard deviation = 4 psig)
134 psig	with liner	(standard deviation = 4 psig)

Temperature and temperature/pressure effects are not significant.

8.2 Zion Containment Vessel (by Los Alamos) [8.2-1, 8.2-2]

Objective

Prediction of the vessel internal pressure ultimate capacity.

Containment Building Design

Lightly reinforced - post-tensioned concrete structure, (Fig. 8.1-1).

Structural Modeling

ADINA finite element code.

Axisymmetric two dimensional model.

Neglected small penetrations effect.

Large penetration (equipment hatch) - separate three dimensional model.

Two dimensional shell element for the liner plate.

Ring elements for hoop steel and hoop tendons two nodes truss elements for meridional reinforcement and meridional tendons.

Soil - axisymmetric, discrete, compression only springs.

As built material properties were used for concrete, reinforcing steel, liner and post-tensioning steel.

Concrete behavior - based upon tensile cracking. Compression crushing and strain softening model.

Concrete cracking - reduction of the original stiffness when the principle stress exceeds uniaxial cutoff tensile stress as:

shear reduction factor = 50%
tensile stiffness reduction factor = 0.01%

Effects of reinforcement ties and stirrups are indirectly included by retaining a significant shear stiffness after cracks develop.

Comparison with Structural Integrity Test (SIT)

Loads:

- Dead weight and internal structures and equipment (approximated as an axisymmetric load);

- Prestressing;
- Internal pressure of 54 psig (115% of the design pressure).

Two dimensional finite element model results are generally very close to the SIT results. Small disagreements in cracking extent (concrete tensile strength).

Containment Static Response and Failure

The solution is considered to be converged if the displacements at cylinder midheight node, the apex of the dome and the outer corner of the basemat reach unique values <no details given>.

Pressure (psig)	Notes
85	First concrete cracking
none	First reinforcement yield
117	Liner first exceeds 0.3% strain (meridional direction)
105	Lower bound failure pressure*
134	Upper bound failure pressure**
125	Predicted failure pressure+

*Pressure at which more than half of the concrete at the wall-basemat junction loses its shear carrying capability.

**Based on limit analysis considering membrane failure of the cylinder sidewalls in the hoop direction.

+ Numerical instability at pressures beyond this point, base of cylinder wall.

Equipment Hatch Analysis

Three dimensional finite element using NONSAP-C code.

Finite element model (penetration, wall and buttress), Fig. 8.2-1. <No results are given.>

Conclusion

Containment ultimate capacity is 125 psig (failure caused by high shear and moment and the cylinder basemat junction).

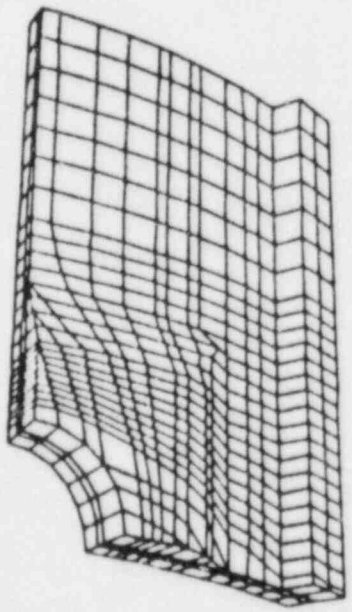

Figure 8.2-1 Finite Element Mesh for 3-D Analysis of the Zion Equipment Hatch

9.1 Bellefonte Containment (by Sandia National Laboratory) [9.1-1]

Objective

Realistic prediction of the vessel internal pressure ultimate capacity.

Configuration

Prestressed concrete - no base slab, built on rock (Fig. 9.1-1).

Finite Element Model

ABAQUS finite element code.

Axisymmetric model:

- Axisymmetric continuum element (concrete, tendons and rebars);
- Three node shell element (liner plate);
- Nonaxisymmetry due to penetrations and steel variation were ignored.

Concrete constitutive model - Chen and Chen model:

- Crushing - concrete loses all of its strength instantaneously;
- Cracking - material strength is lost in direction orthogonal to crack direction;
- Unloading portion of $\sigma - \varepsilon$ curve is used to control how quickly the strength is lost.

Material properties - actual properties based on test data.

Analysis and Results

Loads - prestressing forces followed by internal pressure.

Prestressing - gradual application as equivalent thermal loads so that nonlinear behavior of the concrete could be followed.

Internal pressure - 1 psi increments (fixed number of iterations at each load stop)

Pressure, (psig)	Notes
110	First concrete cracking (dome).
120	First yielding of the liner in the dome.

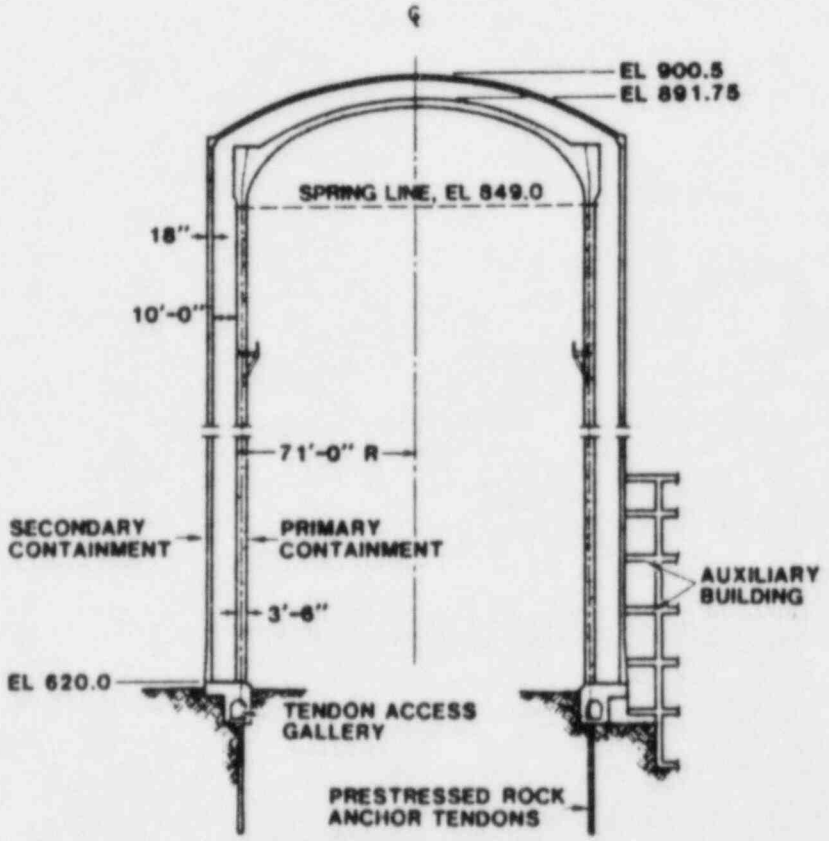

Figure 9.1-1 Bellefonte Containment Structure

Pressure (psig)	Notes
130	Dome tendons yielded accompanied with gross cracking in the adjacent concrete.

Hand calculations <no details given> to estimate the pressure associated with cylinder wall general yielding gave pressure of 139 psig.

Uncertainty associated with dome tendon failure mode because tendon placement is actually nonsymmetric.

Conclusions

Failure of Belleforte vessel is approximately:

130 psig (lower bound)	yielding of dome tendons
139 psig (upper bound)	cylinder wall general yielding

Failure of other components were not addressed.

10.1 Oconee Containment (by Sandia National Laboratory) [10.1-1]

Objective

Estimation of the vessel ultimate strength under internal pressure.

Containment Description

Prestressed, <no containment geometry given>.

Failure Criteria

General hoop yielding of cylindrical shell.

Material Properties

Minimum allowable yield strength.

Analysis Method

Hand calculation based on equilibrium at yield of rebars, liner and tendons.

Conclusion

Estimated general yielding pressure of cylinder = 151 psig.

11.1 Calvert Cliffs Containment (by Sandia National Laboratory [11.1-1]

Objective

Estimation of the vessel ultimate strength under internal pressure.

Containment Description

Prestressed, PWR <no containment geometry given>.

Material Properties

Minimum allowable yield strength.

Failure Criteria

General hoop yielding of cylindrical shell.

Analysis

Hand calculation based on equilibrium at yield of rebars, liner and tendons.

Conclusion

Estimated general yielding pressure of cylinder = 124 psi.

MARK III CONTAINMENTS

12.1 Perry (by Ames Laboratory) [12.1-1]

Objective

Uncertainty assessment of ultimate internal pressure resistance.

Containment Description

Mark III, Steel (Fig. 12.1-1)

Uncertainty Analysis, Failure Criteria, Finite Element Software and Calculation, Simplified Analysis Methods

See St. Lucie (Ames Laboratory).

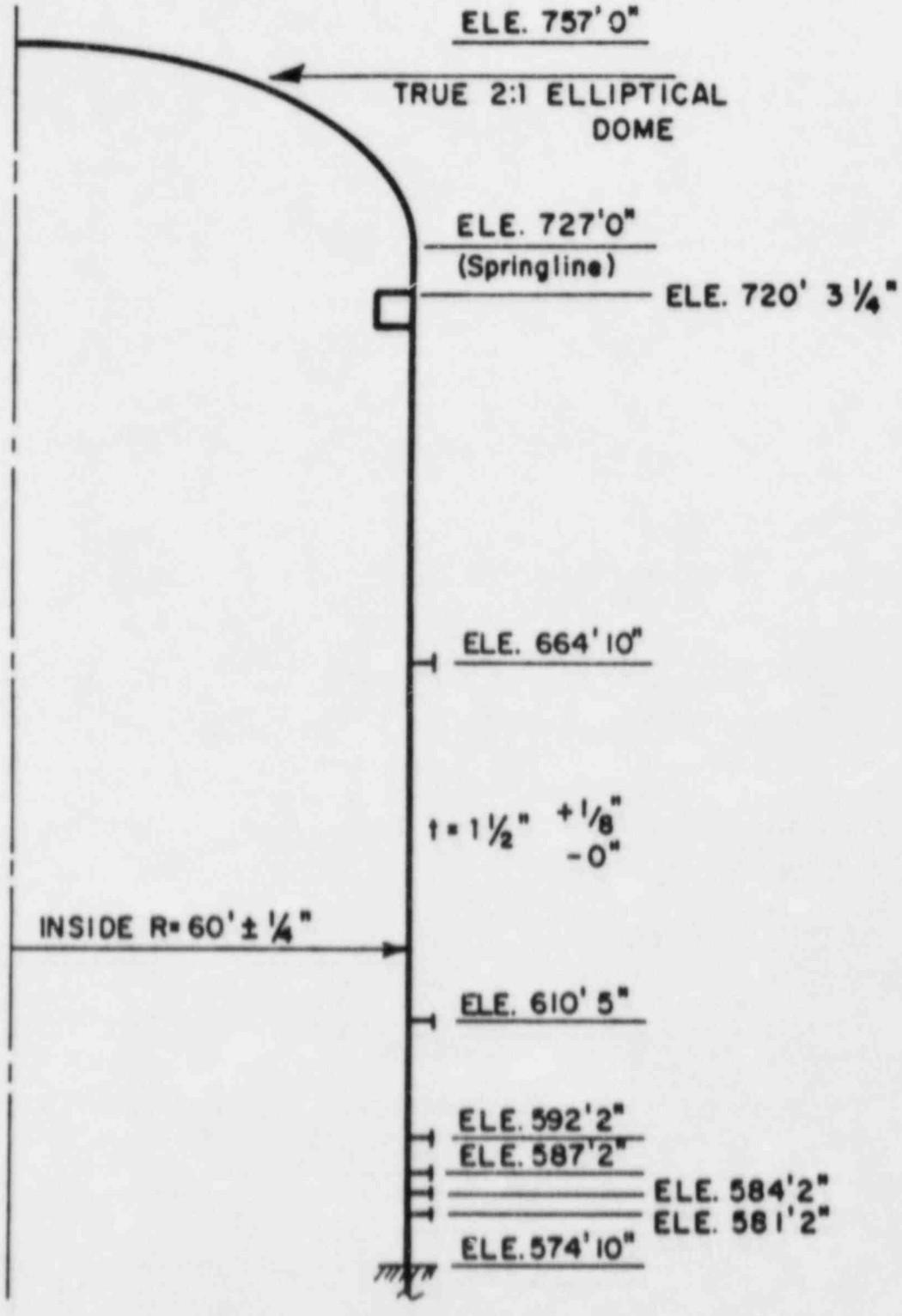

Figure 12.1-1 Perry Containment Vessel Geometry

Containment Uncertainty Analysis

Actual material properties, as furnished by owner.

Simplified method - minimum mean pressure resistance is 100 psig as controlled by asymmetric buckling of the cylinder/ellipse knuckle.

Finite element analysis - failure pressure is 112 psig as controlled by maximum membrane strain at knuckle (compression). (Buckling not permitted in finite element analysis.)

Conclusion

Mean failure presure is 100 psig (approximately lognormal distribution with coefficient of variation of 0.14).

13.1 Grand Gulf Containment (by Brookhaven National Laboratory) [13.1-1, 13.1-2]

Objective

Predicting failure under uniform internal pressure cased by hydrogen burn.

Containment Structure

Mark III, reinforced concrete vessel, Fig. 13.1-1.

Failure Criteria

Maximum allowable strain in liner and plastic yielding of reinforcements.

Material Model

Steel - von Mises plasticity model with isotropic strain hardening.

Concrete - Chen and Chen plasticity model up to fracture which is described by a dual failure criteria:

- Stress based criterion - Chen and Chen loading surface reaches concrete ultimate;
- Strain based criterion - strains reach failure surface in strain space.

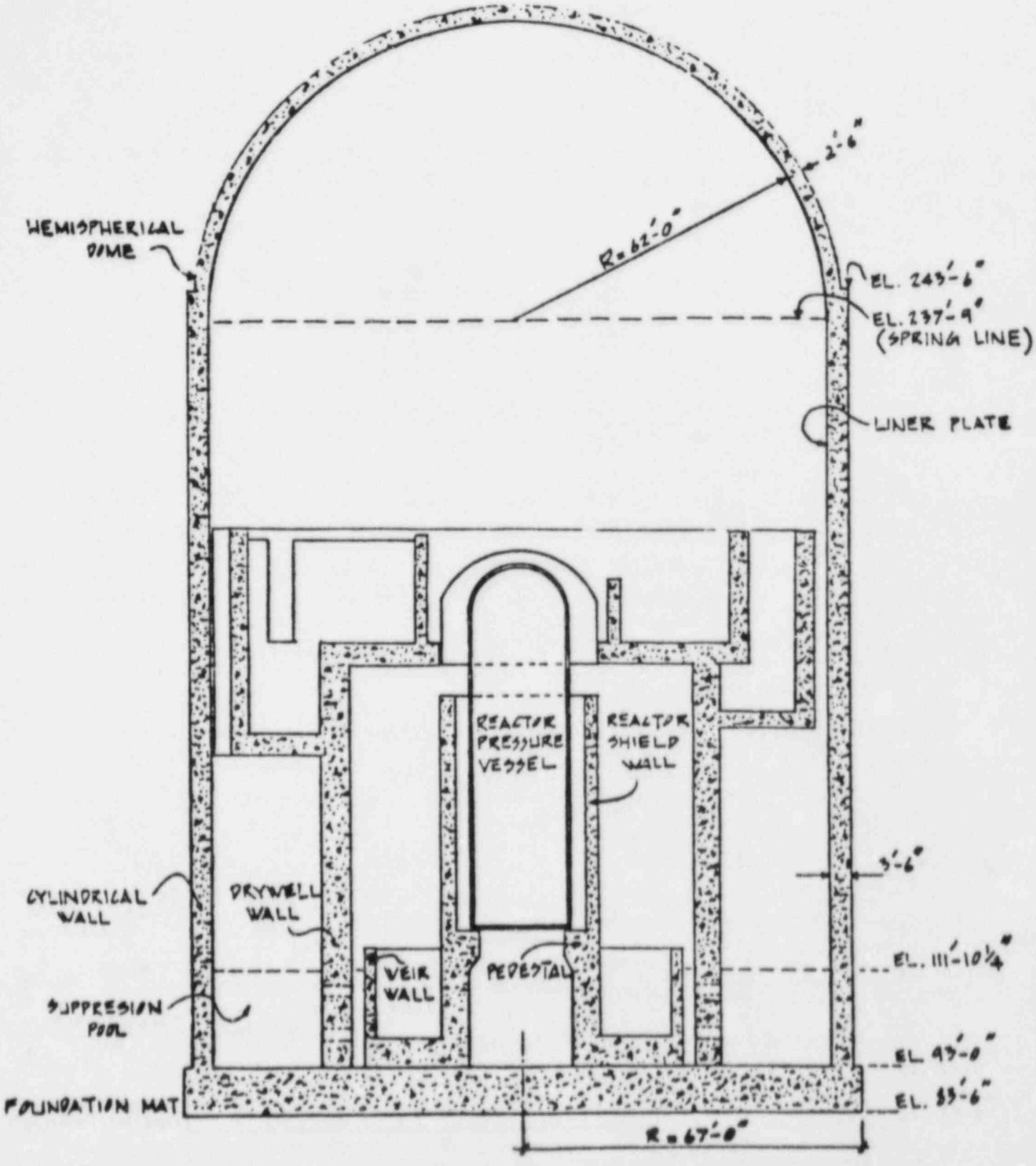

Figure 13.1-1 Schematic Drawing of the Grand Gulf Mark III Containment

Failure can occur in two modes:

- Crushing - the stresses are redistributed to the neighboring material, or;
- Cracking - tensile stresses and a fraction of shear stresses acting on the crack plane are redistributed.

Smearing and de-smearing procedure - hetrogeneous reinforced concrete is replaced by homogeneous material.

- Smearing - equivalent linear and nonlinear stiffness is formulated in terms of the stiffness matrices of steel and concrete.
- De-smearing - inverse of smearing procedure to calculate concrete and steel stress and strain to assess steel yielding and concrete fracture.

Sample Problems

Implosion of concrete cylinder test - analysis compares very closely to average experimental results.

Reinforced concrete beam - experiment somewhat stiffer, probably due to interlocking of cracked concrete.

Shear panel - good agreement.

Finite Element Model of the Containment Structure

NFAP - general purpose finite element program with nonlinear capability.

Axisymmetric model - 8 noded layered axisymmetric element (Fig. 13.1-2).

Penetrations ignored - strengthened by additional reinforcement.

Soil - structure interaction was ignored. Base of the foundation mat was assumed to be fixed.

Nonlinear material and geometric behavior.

Bi-linear stress - strain relation for reinforcement steel and liner plate. Liner and reinforcement material data are based on Ref. 13.1-3.

Concrete material properties, see Fig. 13.1-3. Stiffness reduction factor where crack found:

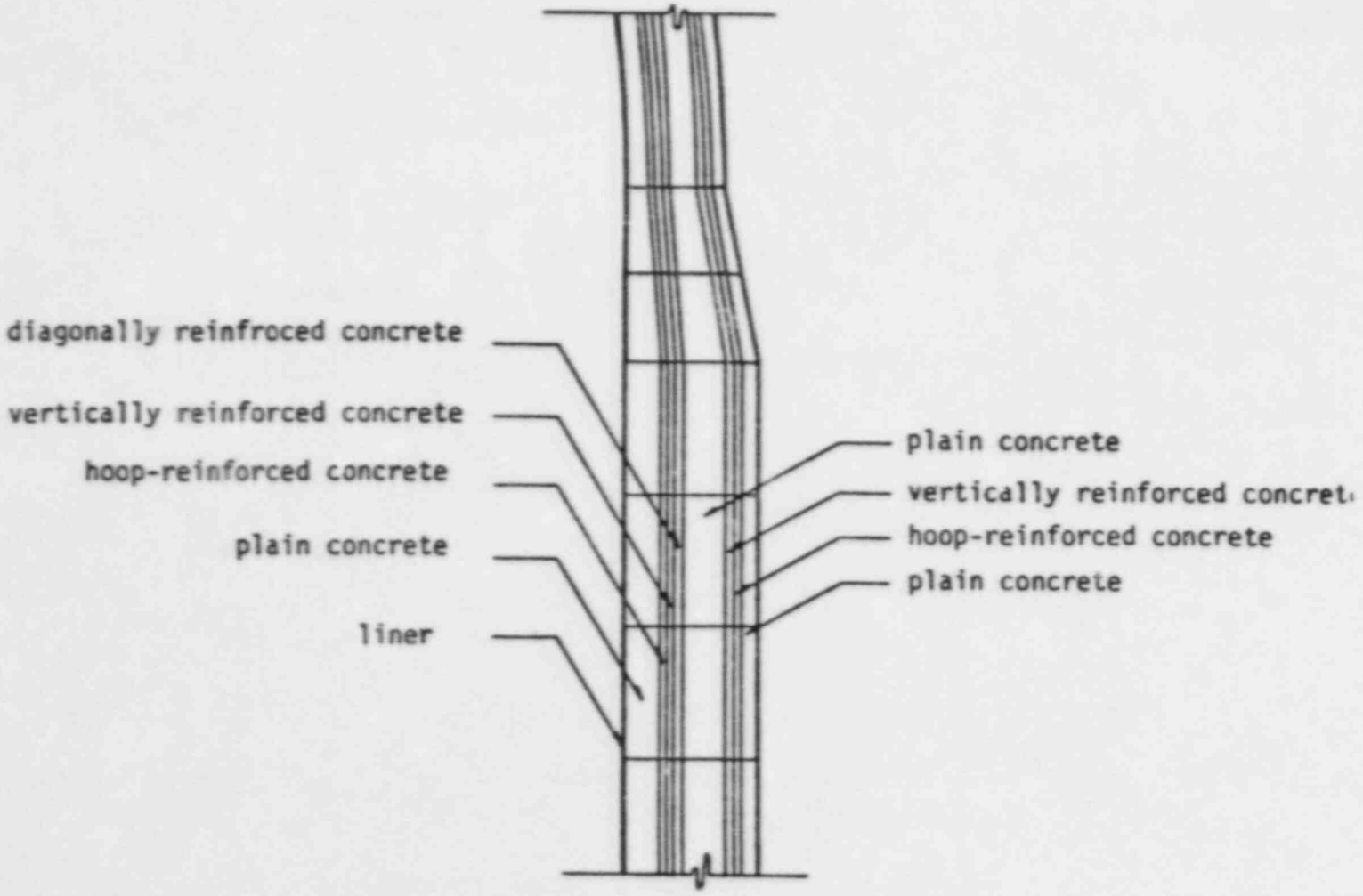

Figure 13.1-2 Different Element Layers in the Cylindrical Wall of the Containment

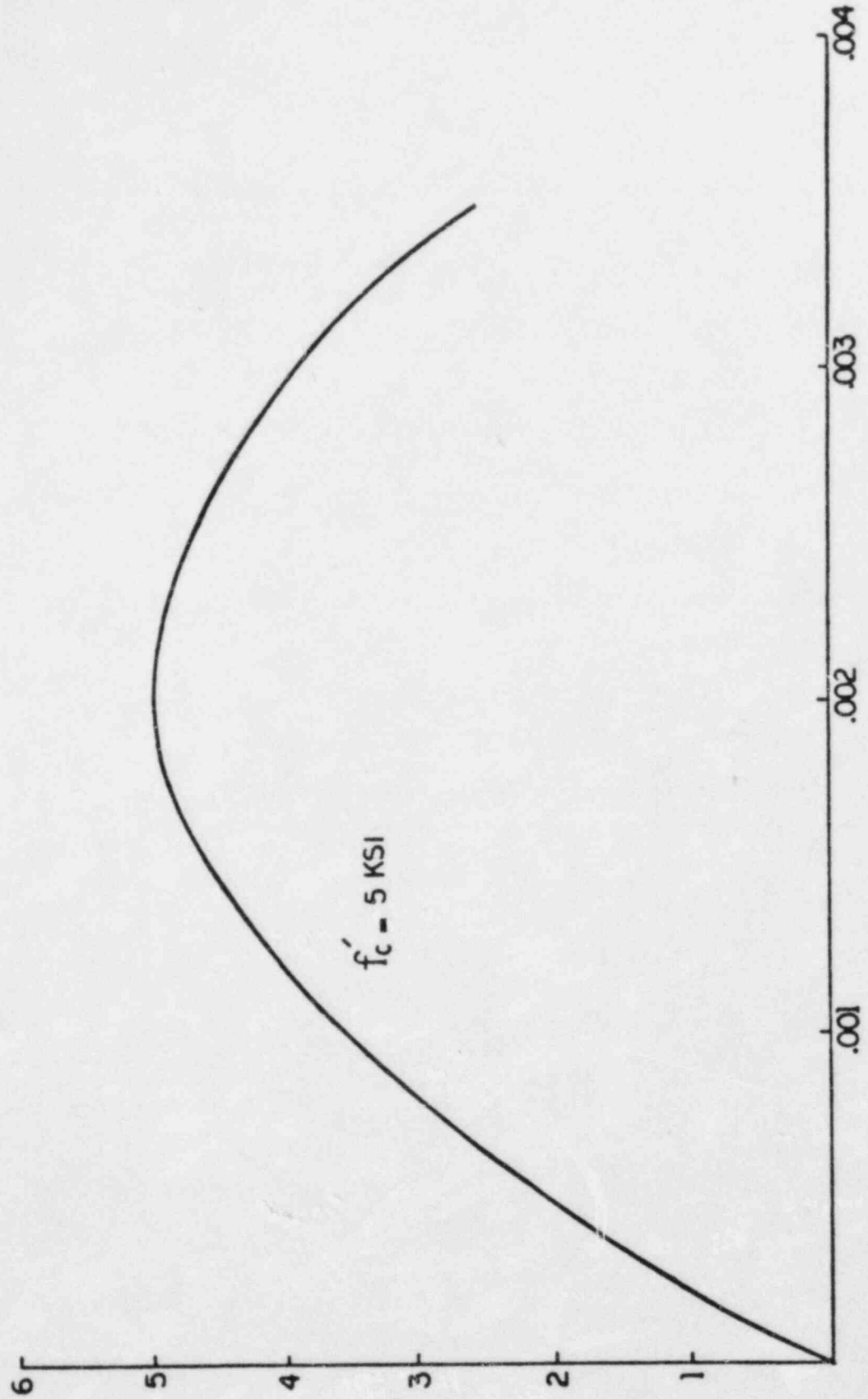

Figure 13.1-3 Uniaxial Stress-Strain Curve for Plain Concrete in Compression

Direction	Factor
Normal	10^{-5}
In plane shear	0.5

Loads - dead weight and quasi-static pressure, incrementally applied (full Newton-Raphson at higher pressures).

Analysis Results - Overall Deformation Pattern

Pressure (psig)	Behavior
Up to 35	Linear
between 38-40	Large section of concrete cracks and liner yields
51	Initiation of yielding in hoop reinforcement

Analysis Results - Concrete Cracking

Cracking is governed by strain criteria (0.015%).

Pressure (psig)	Crack Pattern
36	Hoop cracks by hoop stresses
37	Meridional cracks by meridional stresses
40	Hoop and meridional cracks cover the entire cylinder
47	Hoop cracks appeared in the hemisphere
52	Hoop cracks cover the structure

Analysis Results - Basemat/Cylinder Junction

Pressure (psig)	Behavior
37	Meridional cracks
40	Liner yields
52	Liner strain is 0.265%

Analysis Results - Cylinder Wall Below Spring Line

Pressure (psig)	Behavior
35	Linear
40	Liner yield
51-52	Hoop reinforcement yield
52	Solution terminated (convergence problems)
53-53.5	Estimated yielding of diagonal rein.orcement

Rough estimates showed that liner hoop strain increases rapidly beyond pressure of 52 psig <nc details given>. At 54.5 psig, the liner hoop strain is 0.9%.

Conclusion

Failure pressure of the containment.

40 psig	Large section of concrete cracking and liner yield.
52 psig	Hoop reinforcement yield.
53.5 psig	Diagonal reinforcement is fully plastic.
54.5 psig	Large displacement (6 - 7 in.) corresponds to 0.9% strain.

Liner carries 18% of hoop stress resultant at 52 psig.

MARK II CONTAINMENTS

14.1 WPPSS (by Ames Laboratory) [14.1-1]

Objective

Uncertainty assessment of ultimate internal pressure resistance.

Containment Description

Mark II, Steel (Fig. 14.1-1).

Uncertainty Analysis, Failure Criteria, Finite Element Software and Calibration, Simplified Analysis Methods

See St. Lucie (Ames Laboratory).

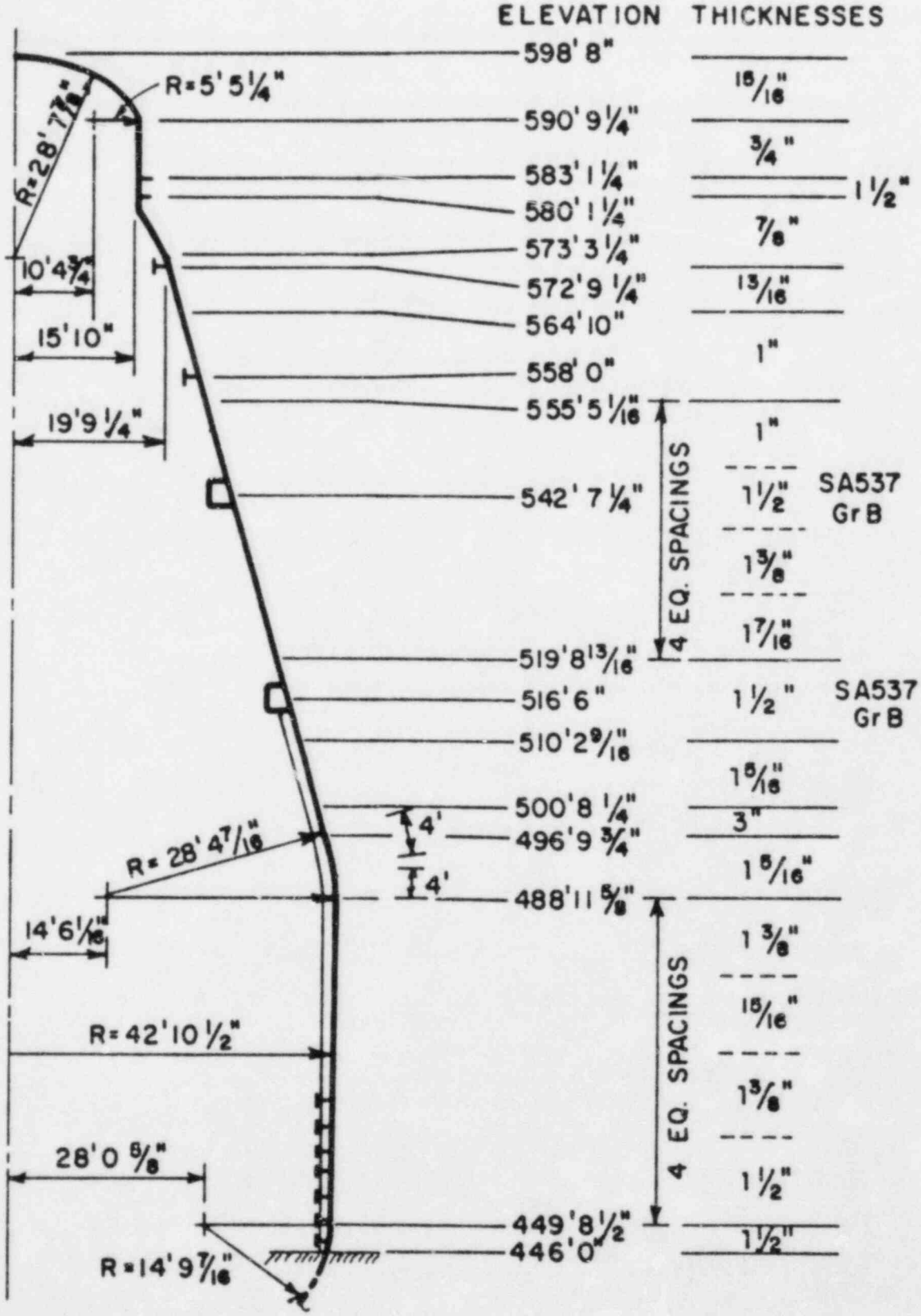

Figure 14.1-1 WPPSS Containment Vessel Geometry

Containment Uncertainty Analysis

Simplified method - minimum mean pressure resistance is 133 psig, controlled by limit pressure in lower circumferentially unstiffened cylinder.

Finite element analysis - failure pressure is 134 psig controlled by membrane strain in the lower circumferentially unstiffened cylinder.

Conclusion

Mean failure pressure is 133 psig (approximately lognormal distribution with coefficient of variation of 0.17).

15.1 Limerick Containment (by General Electric/Science Application Inc.) [15.1-1]

Objective

Ultimate pressure capacity of the containment for Probabilistic Risk Assessment study.

Containment General

Containment arrangement

- Reinforced concrete, Mark II vessel, (Fig. 15.1-1).

Criteria

- Ultimate capacity is defined as internal pressure which causes a general yielding (hoop or shear reinforcement or liner plate).
- Material properties are taken from construction test records.

Containment Ultimate Pressure Capacity

Idealization of the lower containment (wet well) wall as infinite cylinder neglecting all restraints provided by base slab, diaphragm slab and discontinuities. This idealization yields lower bound ultimate pressure. The model consists of hoop steel, meridional rebars, inclined reinforcement, liner and concrete.

Equilibrium and strain compatibility of the model were established using the Bechtel in-house computer program (CECAP) <no details given>.

General yielding state was reached at pressure of 120 psig, and the hoop reinforcement are the highly strained rebars.

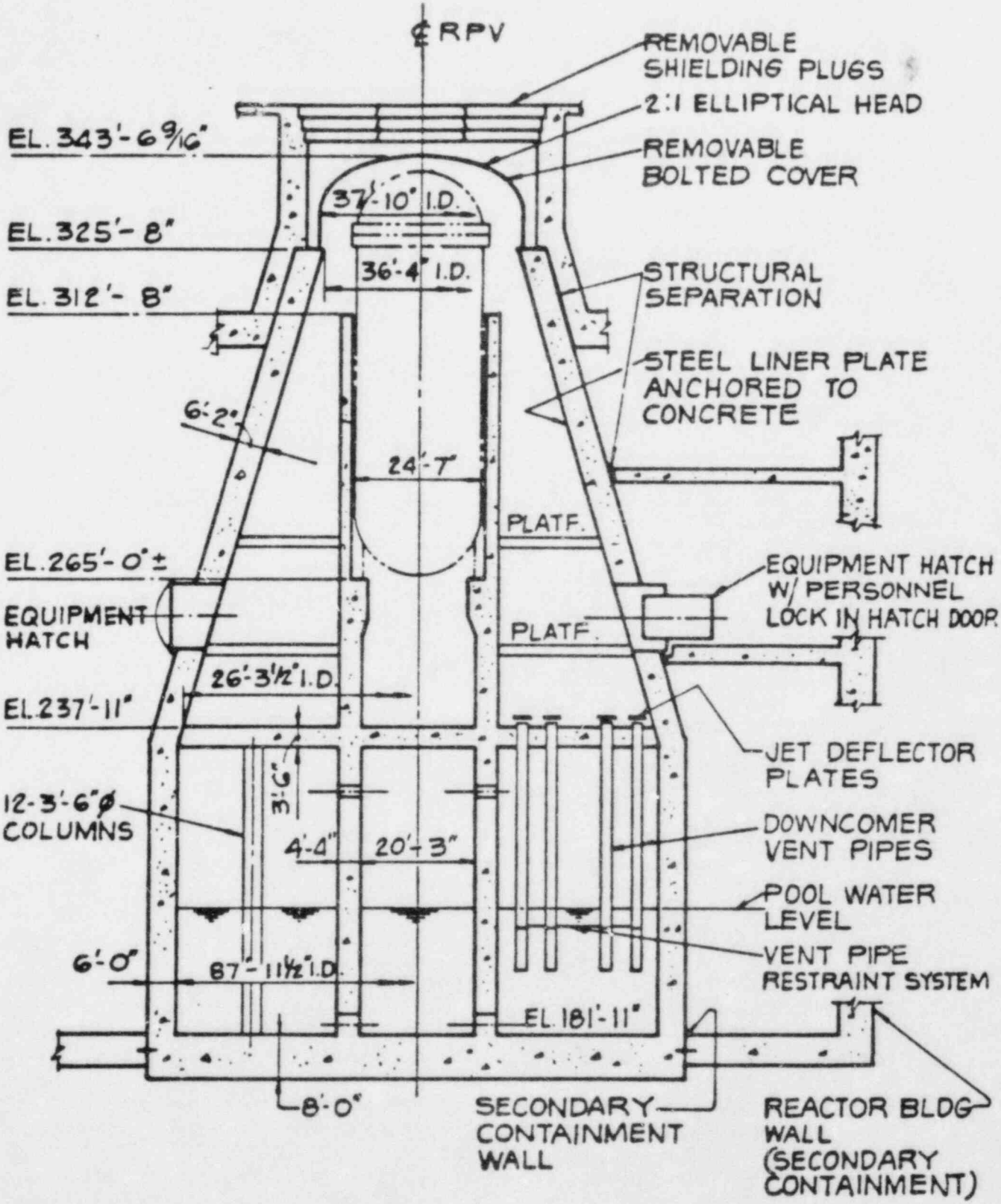

Figure 15.1-1 Limerick Containment General Arrangement

Finite element calculation:

- Axisymmetric model of the containment used in the FINEL computer program <no details given>;
- Concrete tension cracking is considered;
- Dead and live load as well as internal pressure were considered. No temperature effects were investigated;
- Middle section of the cylinder is the most strained section at 120 psig, but no component has yielded;
- Hoop rebars at the cylinder midheight and the shear reinforcement at the wall-base junction are at yield at 150 psig pressure;
- Critical section considered are shown in Fig. 15.1-2.

Summary

Containment wall - diaphragm containment wall is overstressed <no details given> at 170 psig.

Simple equilibrium analysis showed yielding of the reinforcement anchoring the top head of the structure of 170 psig (no details given).

Ultimate pressure capaciiy determined to be 140 psig after consideration of assumptions and accuracies of the two analyses.

Refueling Head and Hatch Pressure Capacity - Chicago Bridge and Iron Investigation

Refueling head

- Critically stressed areas are shown in Fig. 15.1-3.
- Calculate membrane stresses are less than the yield stresses at pressure of 120 and 160 psig along with temperature of 340°F and 70°F (no details given).
- Flange face deflection exceeds CBI's original criteria for leaktight joint and gasket. No quantative figure was established for possible leakage rate.

Hatches

- Analysis of equipment and personnel hatches showed that the stresses are below yield strength at 120 psig (no details given).

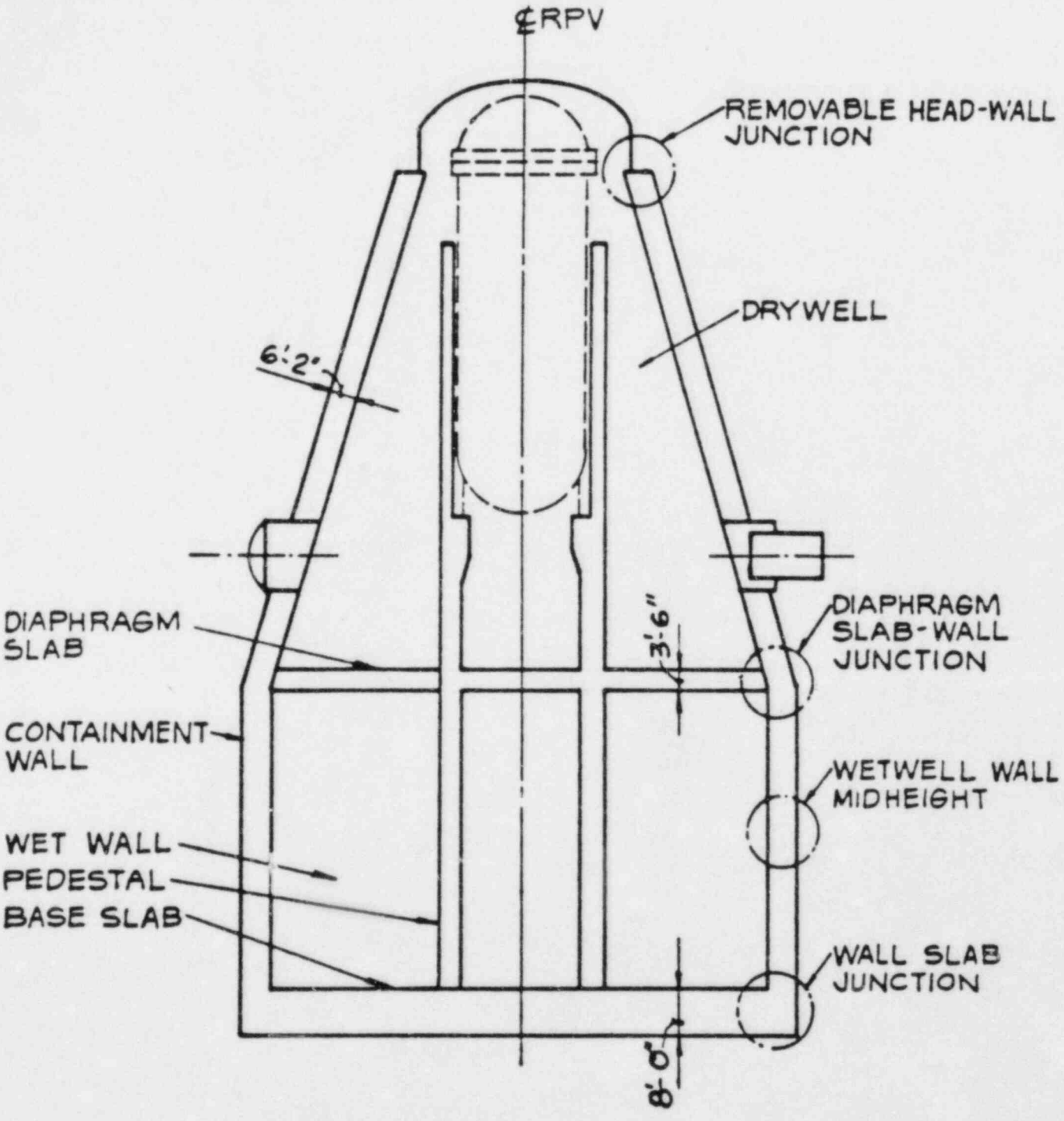

Figure 15.1-2 Location of Critical Section

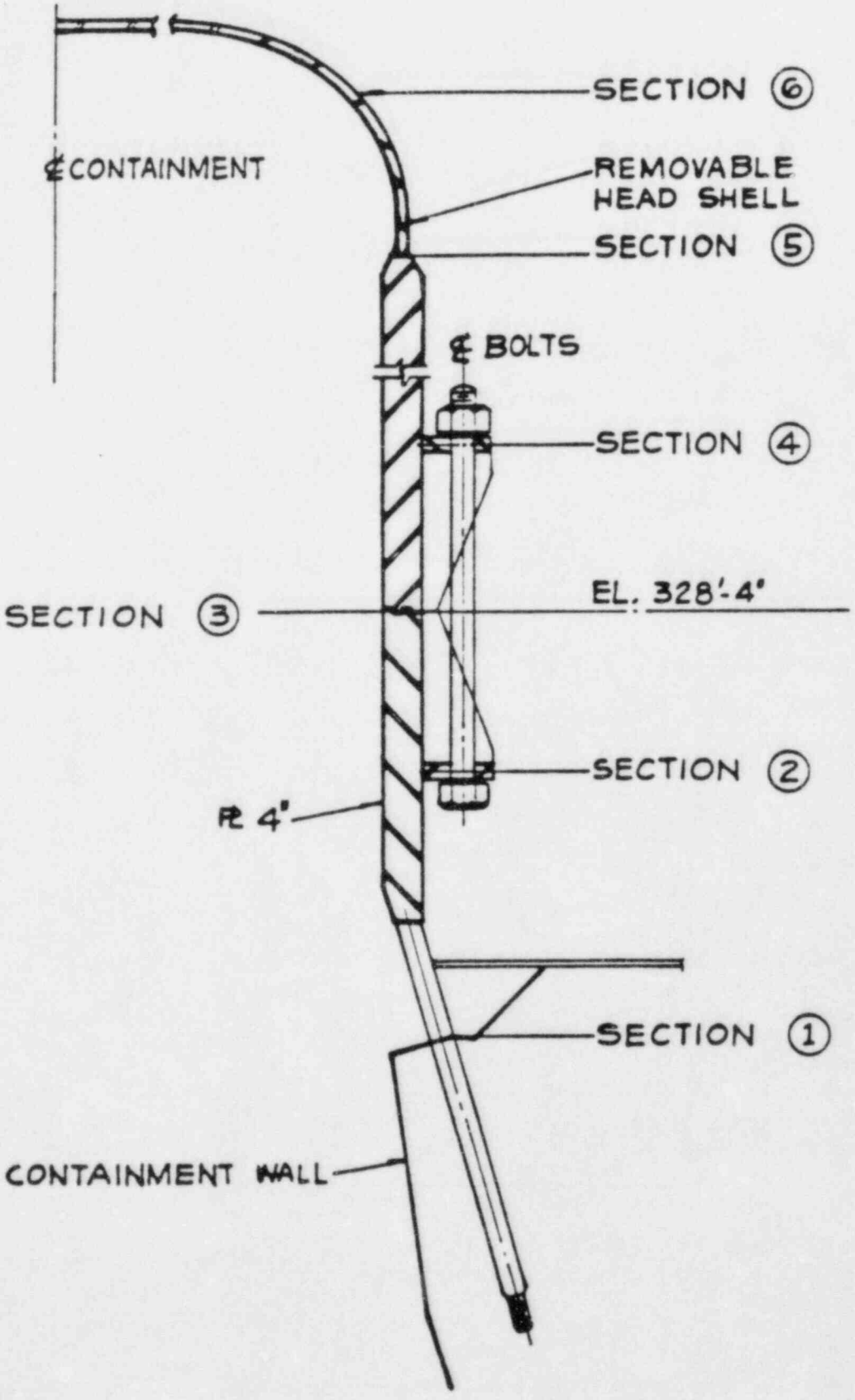

Figure 15.1-3 Removable Head Wall Junction

- Refueling head manway and suppression chamber access hatch experience stresses in excess of yield at 160 psig.
- Equipment hatch and personnel airlock eyebolt support welds indicated stresses above yield at 160 psig.

Penetration and Primary Boundary Value Pressure Capacity Investigation

No values are expected to fail below 300 psig (based on manufacturer's recommendations).

Lowest pressure where excessive leakage might occur is in the 150-200 psig range (based on manufacturer's recommendations).

Conclusion

The containment ultimate capacity is 140 psig.

MARK I CONTAINMENTS

16.1 Browns Ferry (by Ames Laboratory) [16.1-1]

Objective

Uncertainty assessment of ultimate internal pressure resistance.

Containment Description

Mark I, Steel (Fig. 16.1-1).

Uncertainty Analysis, Failure Criteria, Finite Element Software and Calibration, Simplified Analysis Methods

See St. Lucie (Ames Laboratory).

Containment Uncertainty Analysis

Simplified method - minimum mean pressure resistance is 117 psig, controlled by the limit pressure at the cylinder/sphere intersection in the dry well.

Finite element analysis - failure pressure is 128 psig controlled by membrane strain at the cylinder/sphere intersection in the dry well.

Conclusion

Mean failure pressure is 117 psig (approximately lognormal distribution with coefficient of variation of 0.16).

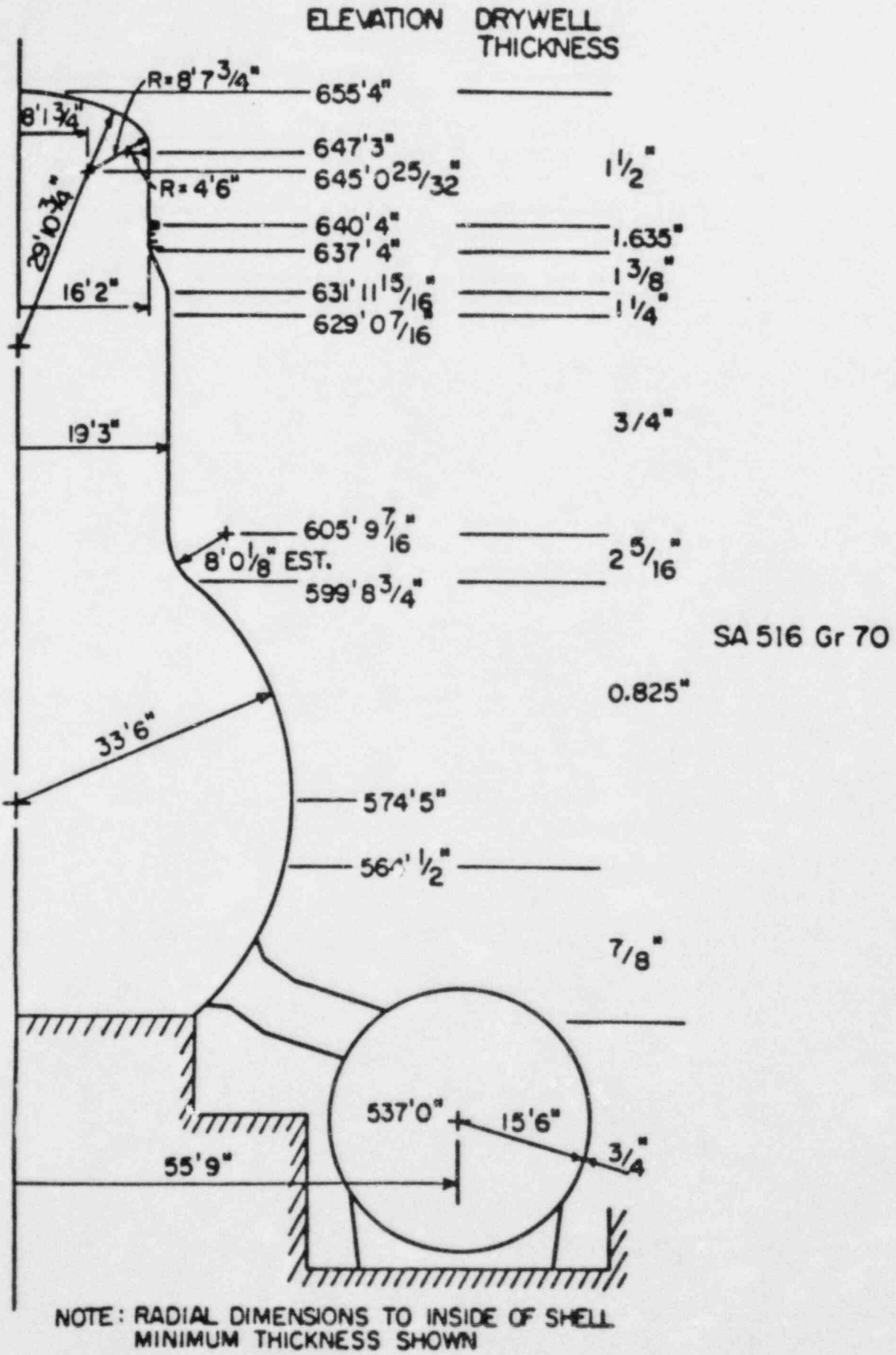

Figure 16.1-1 Browns Ferry Containment Vessel Geometry

17.1 Peach Bottom Containment (by Sandia National Laboratory) [17.1-1]

Objective

Estimation of the containment ultimate strength under internal pressure.

Containment Description

Mark I, steel vessel, see Fig. 17.1-1.

Material Properties

Minimum allowable yield strength.

Failure Criteria

General yielding of the vessel.

Estimated Pressure (hand calculations)

Pressure (psi)	Section (Fig. 17.1-1)
260.5	A
123.0	B
141.8	C
123.0	E
insufficient information	D

Conclusion

Ultimate strength capability of the peach bottom = 123 psi, controlling locations are the neck area and the suppression pool.

17.2 Peach Bottom Containment (by Battelle's Columbus Laboratory) [17.2-1]

Objective

Best estimate of ultimate strength.

Containment Failure - Mode and Pressure Level

MONSAS program (analysis summarized in WASH-1400, [1.6-1 in Appendix II]).

Failure Locations

Inner diameter of the toroidal suppression chamber.

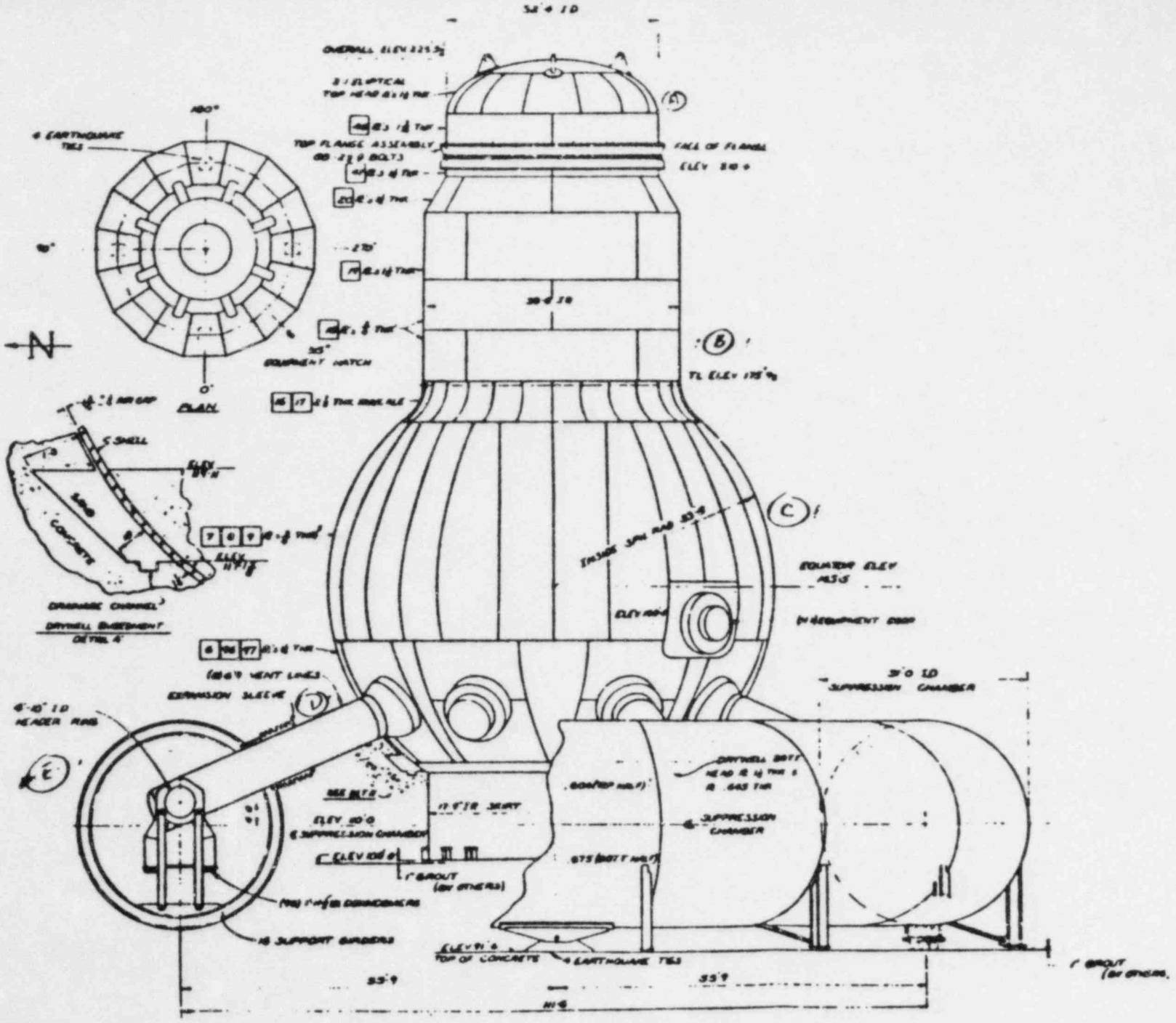

Figure 17.1-1 Peach Bottom Containment Vessel

Knuckle region between cylindrical and spherical portions of the drywell.

The expansion joint of the vent between the drywell and the suppression chamber.

Drywall supporting system.

Burst pressure is predicted as 250 psig. Actual failure pressure adopted as 175 ± 25 psig.

REFERENCES FOR APPENDIX I

1.1-1 Greimann, L., et al., "Reliability Analysis of Containment Strength," Report to U.S. NRC, NUREG/CR 1891, IS-4753, August 1982.

1.1-2 Gill, S.S., "The Limit Pressure for a Flush Cylindrical Nozzle in a Spherical Pressure Vessel," International Journal of Mechanical Science, Vol. 6, 105-115, 1964.

1.1-3 Dinno, K.S. and Gill, S.S., "Limit Pressure for a Protruding Cylindrical Nozzle in a Spherical Pressure Vessel," Journal of Mechanical Engineering Science, 7 (3), 259-270, 1965.

1.2-1 Tsai, J.C. and Orr, R.S., "Probabilistic Failure Modes and Locations in Containments Subjected to Internal Pressurization," Proceedings of the Workshop on Containment Integrity, Vol. II of II, NUREG/CR-0033, SAND82-1659, 201-226, October 1982.

1.2-2 Orr, R., Oral presentation at ACRS Meeting, September 1980, Slides reprinted in NUREG/CR-1891.

1.3-1 Greimann, L., Letter report to Dr. F. P. Schauer, NRC, Washington, January 1980, Reprinted in NUREG/CR-1891.

1.4-1 Hubbard, H.W., Letter report to Dr. R. L. Tedesco, July 1980, Reprinted in NUREG/CR-1891.

1.5-1 TVA, Oral presentation at ACRS Meeting, September 1980, Slides reprinted in NUREG/CR-1891.

1.6-1 Bagchi, G., Memorandum to F.P. Schauer, NRC, August 1980, Reprinted in NUREG/CR-1891.

1.7-1 Zudans, Z., Letter report to Dr. E. Saujo, NRC, August 1980, Reprinted in NUREG/CR-1891.

2.1-1 Greimann, L., et al., "Reliability Analysis of Containment Strength," Report to U.S. NRC, NUREG/CR 1891, IS-4753, August 1982.

2.2-1 Tsai, J.C. and Orr, R.S., "Probabilistic Failure Modes and Locations in Containments Subjected to Internal Pressurization," Proceedings of the Workshop on Containment Integrity, Vol. II of II, NUREG/CR-0033, SAND82-1659, 201-226, October 1982.

3.1-1 Greimann, L., et al., "Probabilistic Seismic Resistance of Containments," Report to U.S. NRC, NUREG/CR-3127, 1983.

3.2-1 Jung, J., "Response of the Watts Bar, Maine Yankee and Bellefonte Containments to Static Internal Pressurization," Proceedings of the ANS/ENS International Meeting on Light Water Reactor Severe Accident Evaluation, August 28 - Sept. 1, 1983, Cambridge, MA.

4.1-1 Greimann, L., et al., "Reliability Analysis of Steel Containment Strength," Report to U.S. NRC, NUREG/CR-2442, June 1982.

5.1-1 Greimann, L., et al., "Reliability Analysis of Steel Containment Strength," Report to U.S. NRC, NUREG/CR-2442, June 1982.

5.1-2 Greimann, L. and Fanous, F., "Simplified Methods for the Inelastic Analysis of Stiffened Shells," Transactions of SMIRT 7, Paper No. J 3/2, Chicago, IL, USA, August 1983.

6.1-1 Murfin, W.B., "Report of the Zion/Indian Point Study: Volume 1," Report to the U.S. NRC, NUREG/CR-1410, SAND80-0617/1, August 1980.

6.2-1 Butler, T.A. and Fugelso, L.E., "Response of the Zion and Indian Point Containment Buildings to Severe Accident Pressure," Report to the U.S. NRC, NUREG/CR-2569, LA-9301-MS, May 1982.

6.3-1 "Containment Capability of Indian Point Power Plant Unit Nos. 2 and 3 for Internal Pressure Load," A study prepared for the Power Authority of the State of New York and Consolidated Edison by United Engineer and Constructors, Inc.

7.1-1 Jung, J., "Response of the Watts Bar, Maine Yankee and Bellefonte Containments to Static Internal Pressurization," Proceedings of the ANS/ENS International Meeting on Light Water Reactor Severe Accident Evaluation, August 28 - Sept. 1, 1983, Cambridge, MA.

8.1-1 Walser, A., "Primary Containment Ultimate Capacity of Zion Nuclear Power Plant for Internal Pressure Load," Proceedings of the Workshop on Containment Integrity, Vol. II of II, Prepared for the U.S. NRC, NUREG/CP-0033, SAND-82-1659, 263-318, October 1982.

8.1-2 "Zion Probabilistic Safety Study," Appendix 4.4.1, "Primary Containment Ultimate Capacity of Zion Nuclear Power Plant for Internal Pressure Load," A study prepared for Commonwealth Edison Company by Sargent and Lundy Engineers, Project No. 6102, November 1980.

8.2-1 Butler, T.A. and Fugelso, L.E., "Response of the Zion and Indian Point Containment Buildings to Severe Accident Pressure," Report to the U.S. NRC, NUREG/CR-2569, LA-9301-MS, May 1982.

8.2-2 Butler, T.A., "Failure Modes for Concrete Nuclear Containment Buildings," Advances in Containment Design and Analysis, ASME/ANS Joint Conference, July 26-28, 1982, Portland, Oregon.

9.1-1 Jung, J., "Response of the Watts Bar, Maine Yankee and Bellefonte Containments to Static Internal Pressurization," Proceedings of the ANS/ENS International Meeting on Light Water Reactor Severe Accident Evaluation, August 28 - Sept. 1, 1983, Cambridge, MA.

10.1-1 Jung, J., "Analysis of Containments," Memo to Steve Hatch, Sandia National Laboratory, June 1983.

11.1-1 Jung, J., "Analysis of Containments," Memo to Steve Hatch, Sandia National Laboratory, June 1983.

12.1-1 Greimann, L., et al., "Reliability Analysis of Steel Containment Strength," Report to U.S. NRC, NUREG/CR-2552, June 1982.

13.1-1 Sharma, S., et al., "Failure Evaluation of a Reinforced Concrete Mark III Containment Structure Under Uniform Pressure, "Report to the U.S. NRC, NUREG/CR-1967, BNL-NUREG-51543, AN.DR., September 1982.

13.1-2 Sharma, S., Reich, M. and Chang, T. Y., "Nonlinear Finite Element Analysis of Reinforced Concrete Mark III Containment Under Pressure and Gravity Loads," Transaction of SMIRT 7, Paper No. J 2/8, Chicago, IL, USA, August 1983.

13.1-3 Annual Book of ASTM Standards, Part 4, American Society of Testing and Materials, 1971.

14.1-1 Greimann, L., et al., "Reliability Analysis of Steel Containment Strength," Report to U.S. NRC, NUREG/CR-2442, June 1982.

15.1-1 "Ultimate Pressure Capacity of Limerick Primary Containment," Study in support of Risk Assessment of Limerick Generating Station, conducted by General Electric/Science Application, Inc., Final Report, October 1981.

16.1-1 Greimann, L., et al., "Reliability Analysis of Steel Containment Strength," Report to U.S. NRC, NUREG/CR-2442, June 1982.

17.1-1 Jung, J., "Analysis of Containments," Memo to Steve Hatch, Sandia National Laboratory, June 1983.

17.2-1 Battelle Columbus Laboratory, "BMI-2104 Draft Report for Peer Review," (Previously identified as NUREG 0956).

APPENDIX II - RELATED WORK

1. Work Conducted in the U.S.A.

1.1 Containment Integrity Program (by Sandia National Laboratory) [1.1-1, 1.1-2, 1.1-3, 1.1-4, 1.1-5, 1.1-6]

Objective

Design, test and analyze three 1/30 scale and one 1/8 scale models of steel containments under internal pressure.

Small Steel Models

Construction and experimental effort <beyond scope of this review>.

MARC - general purpose finite element program with geometric and material nonlinearities and finite strain.

Finite element model of containment:

- Truss stress - strain curve;
- Maximum strain of 15%;
- Axisymmetric shell elements;
- Axisymmetric solid elements near base ring;
- Rigid ring-to-shell attachment.

No experimental results published but predicted deflected shape approximately matches observed shape on a check out model.

Finite element model of personnel lock in a complete hemisphere:

- Axisymmetric shell elements;
- Constrained and unconstrained personnel lock;
- Failure pressure greater than unpenetrated hemisphere.

Finite element analysis of equipment hatch in complete hemisphere:

- Equipment hatch doors buckled at pressure below general membrane yielding;
- Confirmed by hand calculations <no details given>.

Large Steel Model

Work is in planning stages. No analysis to date.

Concrete Models

Work is in planning stages. No analysis to date.

1.2 Failure Modes (by Offshore Power Systems) [1.2-1]

Objective

Identify containment failure modes.

Definition of Containment Failure

Failure must be defined in terms of leakage exceeding predetermined limits <no details given>.

Possible modes include failure to isolate, penetration seals and gaskets, isolation values, cracks in steel liner.

Brittle failure would be catastrophic and could occur with shear failure in concrete, e.g., cylinder/basemat junction and periphery of equipment hatch opening.

Failure Analysis of Leakage Rates

Failure modes and locations are plant specific.

Analysis of typical panel from Sequoyah, McGuire and Floating Nuclear Plant containments with ANSYS (see Sections 1.2, 2.2 in Appendix I and, 1.5 in Appendix II):

- Panel bounded by rings and stringers;
- One-quarter symmetry;
- Each containment panel gave different results.

BOSOR5 analysis of Floating Nuclear Plant by Bushnell (see Ref. 1.5-2 in Appendix II of this review for a summary of this work).

Probabilistic Analysis of Containment Failure

Recommended procedure:

(1) Establish leakage rates to be analyzed <no details given>;

(2) Perform analysis of overall containment <no details given>;

(3) Classify containment segments: cylindrical or conical membrane shell; double curvature membrane shell; base slab; head/cylinder junction; cylinder/base slab junction; equipment hatch; personnel locks; mechanical penetrations, and electrical penetrations;

(4) Estimate probabilistic density function of leakage rate versus internal pressure. Use data from containment tests at design pressure. <No details given.>

(5) Add the leakage rate combination of each region. Develop the possibilty density function as a function of pressure <no details given>.

Uncertainty associated with estimates, therefore need upper and lower bound probabilities to quantify uncertainty.

1.3 Punching and Radial Shear Problems in Reinforced Concrete Containment [1.3-1]

Objective

Investigation of punching and radial shear problems.

Punching (Peripheral) Shear

Definition of action and loading caused by:

- Localized radial loads produced by support reaction, pipe break or other similar loads;
- Localized plus internal pressure (biaxial loads).

Current design approach:

- ASME - Section III, Division 2 provisions based on elastic stress basis;
- Design of shear reinforcement - carry any shear in excess of v_c;
- Difficult task to place the punching shear reinforcement, particularly around openings.

Recent Experimental Results

Cornell University research:

- Biaxial tension in slab has little effect on shear capacity;
- Suggested strength.

$$v_c \text{ (psi)} = (6 - 1.5 \frac{f_s}{f_y}) \sqrt{f'_c} \qquad f_s < 0.9 f_y$$

Great Britain tests - test results are above Cornell test results (the reasons are not known).

Proposed design criteria:

- Tentative design expression (consistent with other ACI punching shear expressions);

$$v_c \text{ (psi)} = (4 - \frac{f_s}{f_y}) \sqrt{f'_c} \qquad f_s < 0.9 f_y$$

- Pre-existing cracks do not degrade punching strength.

Design Implications and Safety

Containment design according to ASME should be able to resist higher punching loads in cases where biaxial tension levels are moderate or high.

Much of the currently required reinforcement could be eliminated without raising safety concerns.

Additional research is needed.

Radial Shear

Complex situation near the containment wall basemat intersection, critical section, may be above the base.

Current design approach, ASME code, conservative. The redundanary furnished by hoop steel at the critical sections are not properly accounted for.

Analytical and experimental program is needed in this area.

1.4 Ultimate Internal Pressure Capacity of Concrete Containment Structure (by Sargent and Lundy) [1.4-1]

Objective

Capacity of a BWR Mark III containment and a PWR reinforced concrete containment.

Containment Description

Reinforced concrete, Mark III (Fig. 1.4-1) and prestressed concrete, Mark II (Fig. 1.4-2).

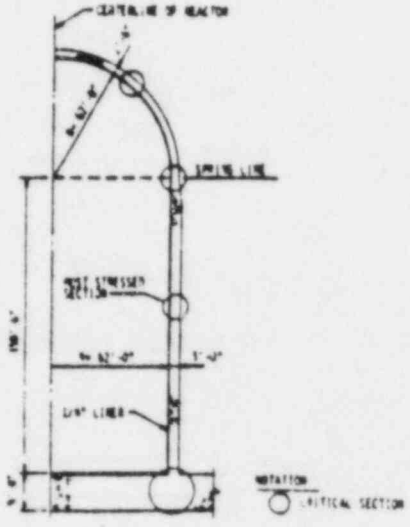

Figure 1.4-1 BWR Mark III Reinforced Concrete Containment

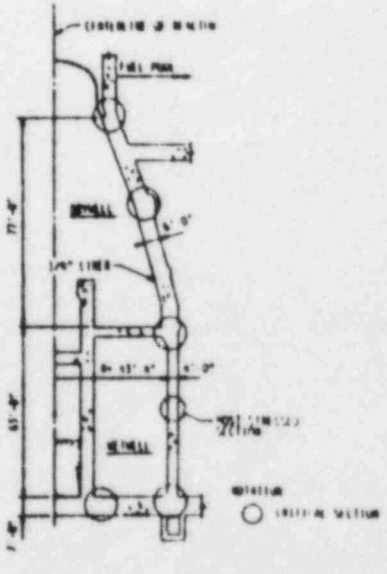

Figure 1.4-2 BWR Mark II Prestressed Concrete Containment

Possible Failure Modes, Failure Criteria, Hand Calculations, and Finite Element Analysis

(Analysis techniques appear to be very similar to Zion, Sec. 8.1 in Appendix I).

Discussion of the Results

Containment response to pressure increase - see Figs. 1.4-3 and 1.4-4.

Failure occurred at cylinder midheight for both Mark II and Mark III at pressures of 228 and 95 psig, respectively.

Additional components (equipment hatch, personnel locks, electrical penetrations, steel drywell head, etc.) check <no details given>. Personnel airlock in Mark II has capacity of 150 psig and equipment hatch in Mark III has a capacity of about 80 psig.

Liner strains are sufficiently low at 150 psig and 80 psig, respectively, to retain leak tightness.

Conclusions

Hand calculations are adequate for membrane sections at the pressure boundary.

1.5 Floating Nuclear Plant [1.5-1, 1.5-2]

Objective

Investigation of the vessel capacity under internal pressure.

Containment Description

Stiffened steel cylindrical shell with torispherical dome, Fig. 1.5-1.

Analysis of Floating Nuclear Plant (by Offshore Power System) [1.5-1]

ANSYS - finite element program.

Typical panel - shell skin framed by the stringer and ring stiffness. (Similar to Sequoyah, Sec. 1.2 in Appendix I.)

Analysis was carried out to initial yield stress of 38 ksi.

Results

Pressure - radial displacement, see Fig. 1.5-2.

Analysis of Floating Nuclear Plant (by Lockheed Research Laboratory) [1.5-2].

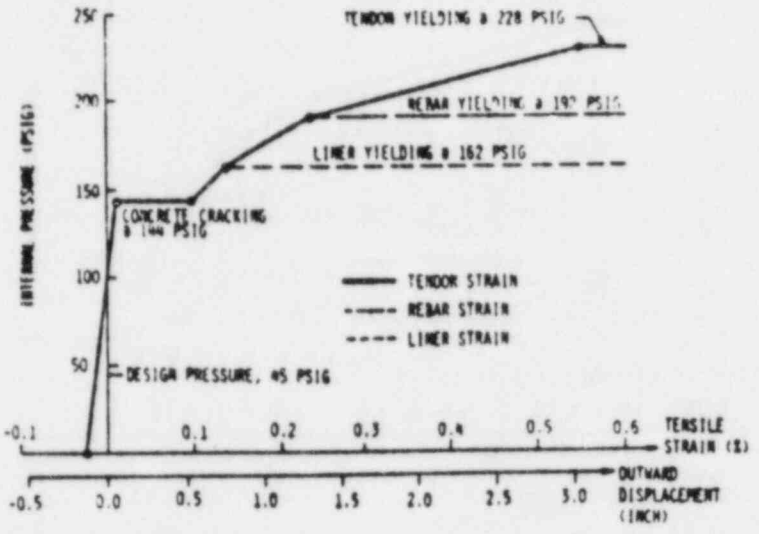

Figure 1.4-3 Response of BWR Mark II Prestressed Concrete Containment at the Most Stressed Section

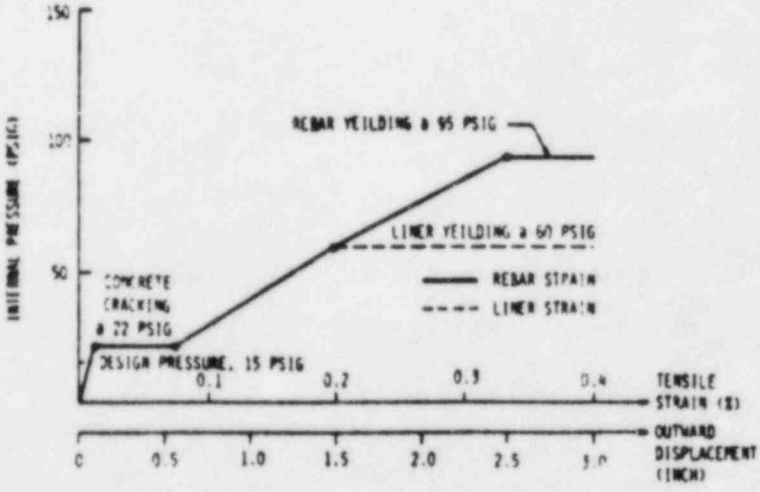

Figure 1.4-4 Response of BWR Mark III Reinforced Concrete Containment at the Most Stressed Section

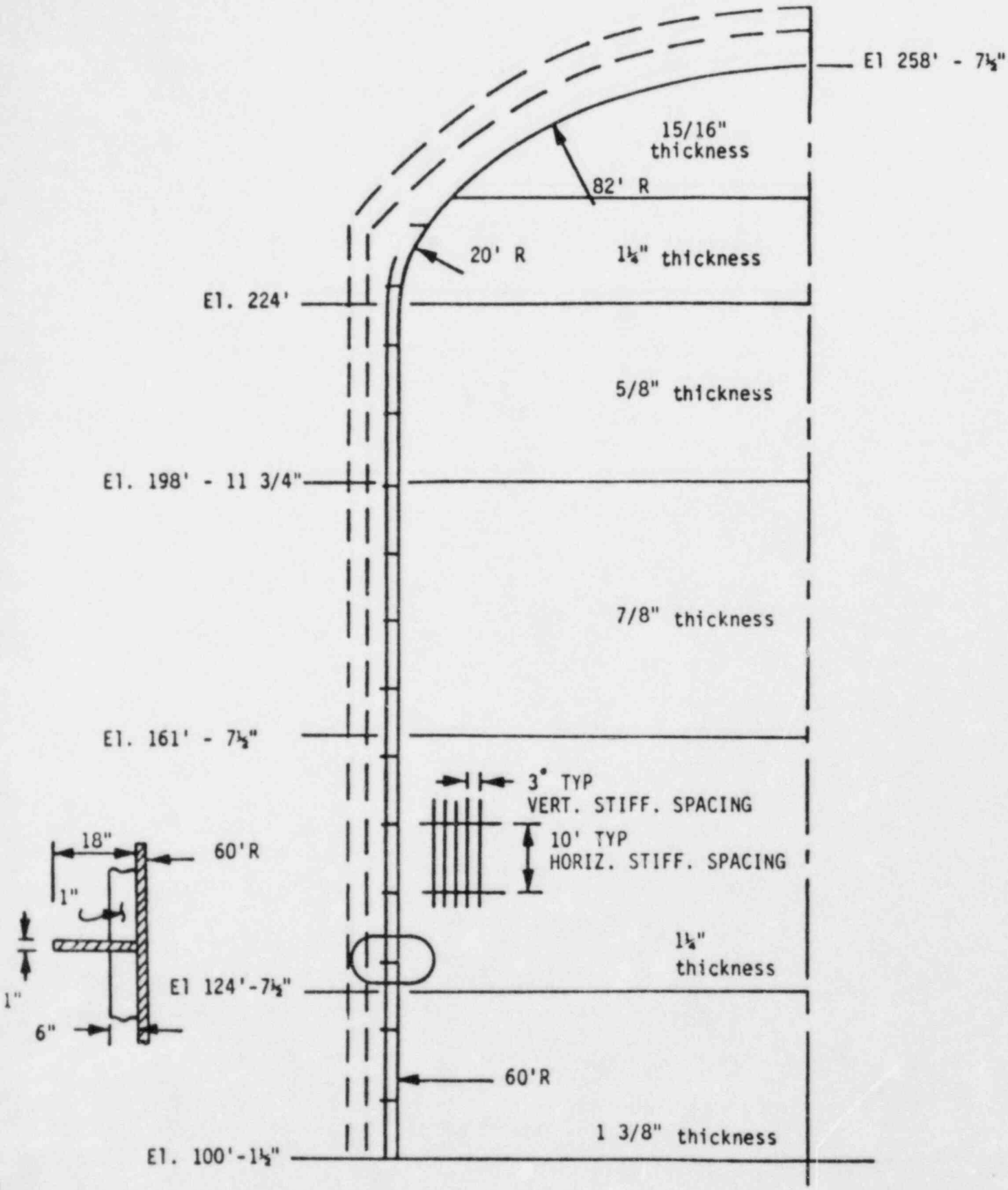

Figure 1.5-1 Floating Nuclear Plant Containment Vessel

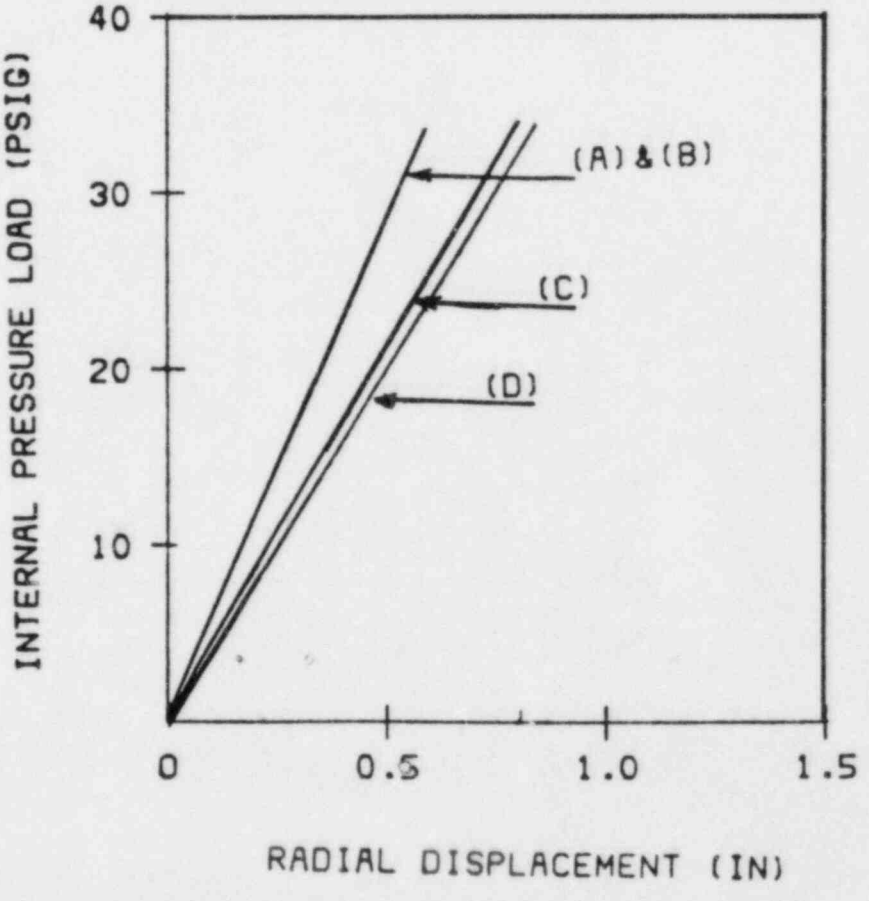

Figure 1.5-2 Pressure-Displacement Curve for Floating Nuclear Plant Containment

Buckling Analysis

BOSOR5 - buckling of elasic-plastic complex shells of revolution under axisymmetric loads, deformation theory, large prebuckled displacements.

Plastic Buckling Under Internal Pressure

Axisymmetric collapse occurred in the 5/8 in. plate (about 45 psi) before nonsymmetric buckling of the torispherical head (between 65 and 70 psi, Fig. 1.5-3).

Modal and dynamic analyses of Offshore Power System are also reported in [1.5-2] <beyond the scope of this work>.

1.6 WASH 1400 [1.6-1]

Summary and Conclusion

The objective is to determine the thresholds and modes of failure of PWR and BWR when subjected to loads greater than the design values.

PWR - subatmospheric reinforced concrete containment.

BWR - lightbulb and tours vapor suppression containment.

Predicted failure pressures:

Containment	Failure Pressure (psig)	Failure Mode
PWR	100 ± 15	Yielding of reinforcing steel and/or crumbling of concrete in upper cylinder of dome.
BWR	175 ± 25	Upper part of the toroidal suppression chamber.

Other highly stressed locations in the PWR are the torodial knuckle between spherical and cylindrical part of the drywell, thin part of the sphere, the expansion joint between the drywell and vents, and the weld discontinuity.

Failure pressure is a continuous normally distributed variable, probability of failure is 0.5 at nominal failure pressure and approaches unity as loading approaches ultimate strength.

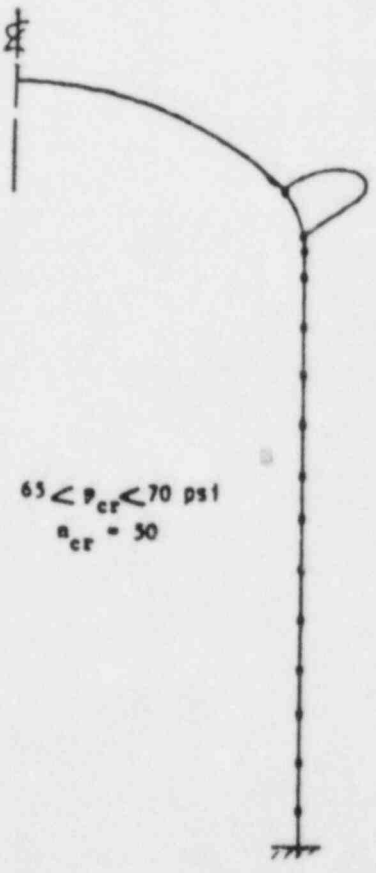

Figure 1.5-3 Floating Nuclear Plant Containment Buckling Mode Predicted Using BOSOR5

Discussion: PWR Containment

Reinforced concrete - flat base, vertical cylinder covered with hemispherical dome and is lined with steel plate.

Determination of failure load requires considering interaction among liner, concrete and steel rebars. Concrete transmits forces to steel.

Integrity of liner must be maintained, must be ductile, especially at discontinuities.

Ideal ultimate strength of the containment based on liner and rebars ultimate strength is 150 psig. Failure at 140 psig is certain, therefore, failure below this load should be considered.

Design of concrete containment is based on nominal safety factors of 1.67.

Mast (see later discussion) suggests that ultimate strength will be reached when rebars yield. Strains beyond yield results in separation of steel from concrete and extensive concrete cracking.

- For structure designed for 45 psig loads to ultimate containment strength of 75 psig without liner and 92 psig with liner as 107 psia.

Battelle's Columbus Laboratories (BCL) Analysis

- Concrete fails first before steel - containment is over-reinforced. Most of the load is taken by the innermost layer of reinforcement, when concrete fails to distribute the applied pressure among the various layers.

- Failure would take place approximately halfway between yield and ultimate strength of liner and rebars (75 psig or 90 psia).

The 107 psia (Mast's prediction) is more realistic.

The nominal failure pressure can be taken as the mean of these two values or 100 psia.

Possibility of failure near penetrations should be considered. A weak point can be developed near an opening where good bond between steel and concrete cannot be achieved due to the congested large amount of reinforcement required around an opening, making concrete placement difficult.

Penetration anchorage to the containment reinforcement important.

Failure near the apex of the dome is also possible, depending on closure detail. Locally low material strengths could occur.

For the concrete containment, the failure pressure based upon the above discussion, Mast's and BCL analyses is 100 ± 15 psia.

The error band accounts for the uncertainties involved in the analysis, such as material properties, variation in the material, and workmanship.

Evaluation of failure size is difficult but it would be large enough to defeat the primary function of the vessel.

Discussion of BWR Containment

Normal design pressure is 56 psia.

Computer stress analysis on a typical drywell by BCL and the results are given in latter section.

BCL analysis showed that the inside upper part of the suppression chamber tears is the most highly stressed region.

Factors involved in developing a failure criteria of BWR containment are material construction, expected quality control, type of loading and constraints on the system.

Failure criteria based on the ultimate material strength results in ultimate pressure of 250 psia.

Reasonable failure criteria is halfway between yield and ultimate because of uncertainties in welds. Also, free expansion would be limited by internal structures.

Predicted failure is thus 175 ± 25 psia with rapid depressurization likely.

Expansion joints on vent pipes from drywell to suppression pool could be weak, as low as 125 psia.

Sealing gaskets at top closure of the dry well does not generally constitute a structural weak link and is made extra strong.

Error band includes uncertainties due to failure mode, material properties, and workmanship.

Ultimate Strength of Containment Structure (by Mast, Consulting Engineering)

Loading Conditions at Accident

To predict the point of failure in pressure at temperature and pressure rise.

Design Basis

pressure = 45 psi, temperature = 150°F, safety factor = 1.67

Effect of Increasing Internal Pressure

General - increasing pressure results in increase in membrane stresses and increase in radial shear at discontinuities.

Conditions at the yield point of reinforcement - since stress in reinforcement at the design pressure is 30 ksi, internal pressure of 75 psi results in yielding.

Concrete cracked and crack width (based on membrane shear test not radial) equals 0.03 inches.

Radial shear failure around large penetration appears to be more imminent than at the other boundaries.

Penetration sleeves are provided with shear lugs. These can prevent sleeve slipping only before cracking but may not be effective at high pressure with extensive cracking.

Hooked anchors or welded straps for connecting penetration sleeves to reinforcement could eliminate this weak link.

Ultimate Strength of the Liner

Liner is ductile - designer should evaluate if liner will hold until structural failure.

The point of greatest weakness of the liner is its anchorage to the base. Questionable whether liner can follow rotations and translations under gross deformations.

Based on the assumption that all components are designed by ultimate strength method - there should be no weak link and the structure can withstand pressure of 75 psig with factor of safety of one.

Conditions at Ultimate Strength of the Reinforcement

Extrapolating the yield pressure to predict ultimate strength is wrong because of the large strains associated with strain hardening.

Shear capacity due to aggregate can not be developed across a crack, therefore must depend entirely on radial shear.

At the stage of progressive cracking weak links will form where high radial shear with insufficient reinforcement.

At the end of strain hardening, cracks become wider and strains imposed on the liner most likely will cause the liner to tear.

Ultimate Strength of Concrete in Shear

Effect of Internal Temperature

Temperatures less then 340° are not enough to result in any losses of concrete shear capacity.

Conclusions

Predicted failure pressure is 80 psi due to (1) yielding of reinforcement, crack width will be 1/2 in., and liner will tear or, (2) if liner ductile enough, radial shear.

Other possible weak links:

- Yielding of reinforcements;
- Penetration sleeves connections;
- Yielding of reinforcement around penetrations;
- Cylinder/base junction.

Containment Failure Modes Study (by Battelle's Columbus Laboratories)

The objective is to determine the pressure level and the failure mode of the vessel.

The predicted pressure by BCL is close to that found by Mast.

Failure mode for reinforced concrete vessel follows:

- Concrete between steel layers fails first resulting in separation at the planes where the concrete is weakest;
- Failure of inner layer of rebars and liner is not certain.

Bounds on containment resistance:

- Lower bound - corresponds to yielding of rebars and liner - the calculated yield pressure is 63.6 psig.
- Upper bound - rebars and liner at ultimate - calculated ultimate pressure is 87.5 psig.

Reinforced Concrete Containment Structure

As pressure increases, reinforcing bars on inner surface become more highly stressed than those on outer.

First major sign of distress will be massive concrete shear failure as concrete crumbles away from outer reinforcement.

Liner and inner reinforcing layer act together and their load carrying capacity controls the failure pressure.

Yielding of liner and rebars will accelerate crumbling of concrete.

Strain hardening will commence to accommodate further increase in internal pressure.

Based on the maximum, distortion energy failure criteria and assuming the longitudinal stresses in liner is one half the circumferential stress, the lower and upper bound for the pressure are 63.6 and 87.5 psig, respectively, (using minimum specified strengths).

A good estimate of the failure pressure is the average of these bounds.

Steel Containment Structure

Two phases for the analysis:

- Computer analysis of the entire structure (axisymmetric model);
- Failure calculations based on the stress concentrations in the individual components.

Computer Calculations for Axisymmetric Pressure Vessel

MONSAS computer code - nonlinear (large deformation) elastic analysis.

Axisymetric model - neglect penetration with local effects.

Wall thickness has to be estimated because the lack of the provided details.

Boundary conditions, see Fig. 1.6-1 - p lb/in. accounts for the effects of the containment head.

Containment wall elastic properties are taken as specified in ASME.

Analysis was accomplished for 62 psig internal pressure and 281°F temperature.

High bending stresses at shell discontinuities.

Burst Pressure Calculations for Individual Components

ASME formulas were used to predict the burst pressure for each individual component. Assumed single load application, adequate welds,

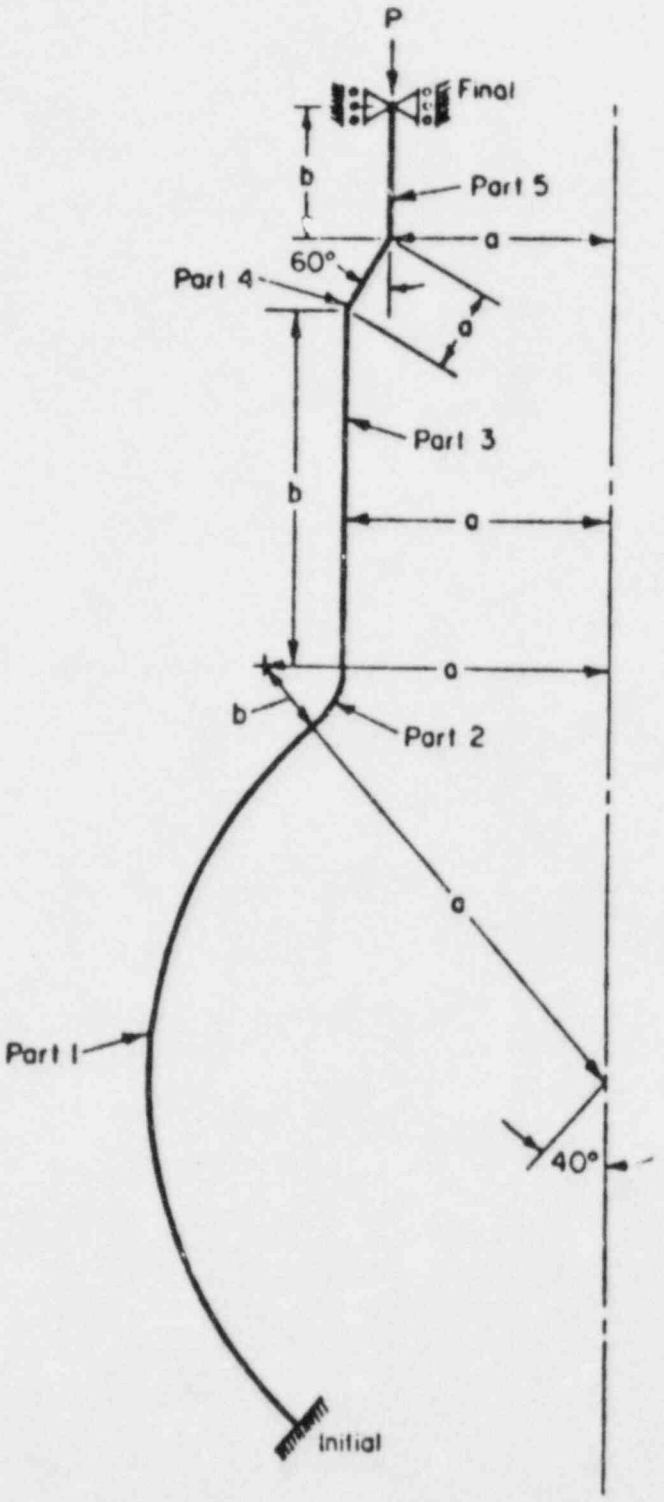

Part No.	a, inches	b, inches
1	402.0	---
2	303.0	72.0
3	231.0	314.5
4	231.0	74.0
5	194.0	35.914

Figure 1.6-1 Axisymmetric Model for Steel Shell Computer Analysis

Part (see Fig. 1.6-1)	Pressure (psig)
1	300
2	250
3	260
4	375
5	620

Failure would occur in the toroidal knuckle.

Discussion and Recommendations for the Reinforced Concrete Containment

Uncertainties in the analysis for the reinforced concrete containment are deemed to be as follows:

- Excess in reinforcement causes difficulties in achieving proper compaction of concrete;
- Development length requirement for the rebars;
- Ignoring the effects of seismic on the vessel capacity;
- Shear cracking around personnel lock;
- Liner yield strength actual value was not used.

Uncertainties in the analysis for the steel stems from lack of some specific design details.

Details of reinforcement around pipe penetration should be included to predict more accurate value for failure.

1.7 MARK III Standard Plant (by General Electric) [1.7-1, 1.7-2]

Objective

Ultimate strength assessment.

Containment Description

Mark III, Steel - Fig. 1.7-1.

Introduction

Assumed to be built to ASME quality.

Penetration assumed to be properly reinforced and do not control.

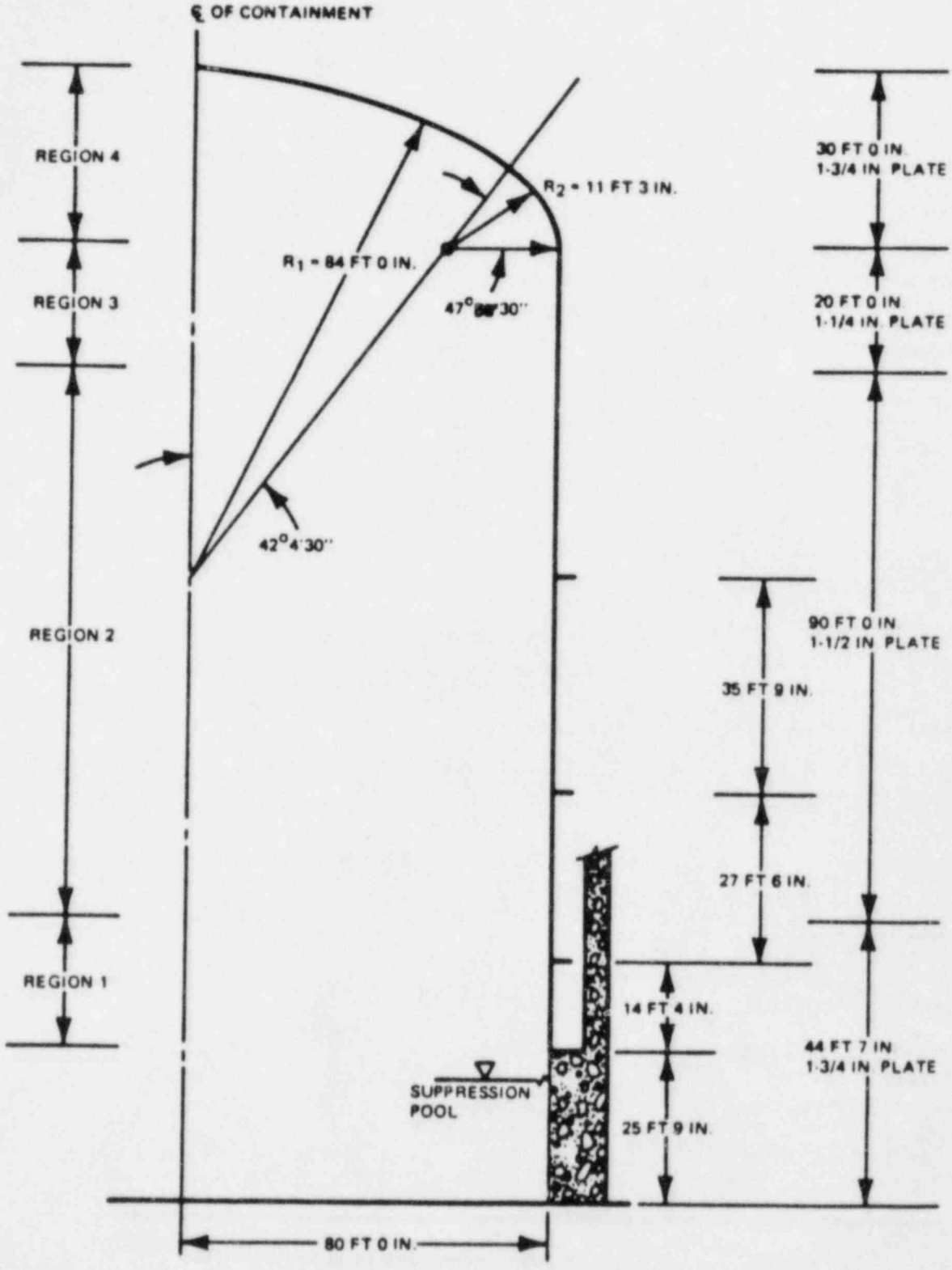

Figure 1.7-1 Dimensions of the Standard Mark III Containment Shell Having Two-Center Torispherical Dome

Steel is ductile.

Welds meet ASME requirements and have strength and ductility at least equal to base metal.

Penetrations through reinforced concrete assumed to be adequately reinforced and at least as strong as the unpenetrated section.

Loads can be considered static.

Stress Distribution

Axisymmetric, finite element shell model (ASHSD).

Internal pressure loads and temperature increase of 80°F.

Highest shear stress in knuckle region, (hoop stresses in compression and meridional stresses in tension in knuckle region).

Pressure Carry Capability of Containment Vessel

ASME Level A stress intensity limit (S_{mc} from Table I-10.1, ASME Section III).

Check primary membrane, P_m, local membrane, P_L, bending stress, P_b, and secondary Q.

Compression limit for hoop stress in knuckle from Fig. VII-1101.2 of ASME, Section III, is 14 ksi. Pressure capability, Level A, = 15 psig (controls).

Pressure capability = 16 psig if S_{mc} is used with ASHSD results.

ASME Level C stress intensity limit. Stability check not required.

ASHSD results to give pressure limit as 30 psig, Level C, controlled by torispherical shell (knuckle).

Lower Portion of Containment Shell

Lower 25 feet of steel shell backed by 5 feet of reinforced concrete, connected to a 3-foot thick reinforced concrete shield building (8 feet total concrete).

Hoop stress in containment shell (derived as if shell were two layers of steel - containment shell layer and reinforcing steel layer).

Using ASME, Level A limits gives pressure capability of 75 psig, as controlled by inner layer of steel (containment shell).

ASME, Level C limit is 141 psig, controlled by containment shell at yield.

Containment Anchorage System

Anchor bolts allowable stress is 0.5 S_{ult} for Level A. Total bolt area times allowable stress gives Level A pressure as 62 psig.

Level C (bolts at yield) pressure is 104 psig.

Concrete allowable bearing stress for factored load category from CC. 3421-9, ASME Section III, Division 2. Allowable concrete stress times total bearing plate area gives the containment anchorage capability as governed by concrete bearing stress to be 72 psig.

For service load category, allowable is 35% of this or 25 psig.

Cracking may result in welds between basemat liner and containment shell but no substantial drainage of pool water will occur.

Drywell Wall and Root Slab

External pressure loads <beyond scope of this review>.

Thick wall cylinder stresses with concrete stress limited to 0.5 f'_c for service category loads and 0.6 f'_c for factored category loads (ASME Section III, Division 2, CC. 3431-1). Gives limits of 136 and 272 psig, respectively.

Slab modelled as rectangular plate with three edges built in and fourth free. Used linear plate theory to find maximum moment which is set equal to ultimate moment capacity of slab. Pressure found as 163 psi.

Straight line theory of stress and strain for slab moment [CC. 3500, 8] gives service load category pressure of 67 psig and factored loads category pressure of 112 psig.

Slab shear checked by [CC 3521.2, 8]. Gives factored load capacity of 111 psig and 51 psig for service load category.

Drywell Head

External pressure <beyond scope of this review>.

ASHSD axisymmetric shell analysis - Level A stress intensity limit gives 116 psig capacity and 160 psig for Level C.

ASME buckling capacity, Level A, is 178 psig for the head portion and 75 psig for the cylindrical skirt.

Possible Failure Modes of Containment Vessel Shell

Containment vessel limited by structural integrity of torispherical dome (see previous analysis).

Axisymmetric, plastic yielding and asymmetric buckling are possible failure modes.

Plastic yielding - use average of upper bound and lower bound solution obtained by Shield and Drucker corresponding to a limit mechanism (some details given but not reproduced here). Limit pressure found by numerical iteration to be 38 psig (using S_y corresponding to 80°F temperature increase).

Asymmetric buckling - gives 61 psig, therefore yielding controls.

Probability of fracture at design pressure is near zero since containment requirements for material design, fabrication, examination, inspection, and testing for metal containments have been met.

"Unzipping" will occur because of welding pattern and stiffener locations <no details given>.

Cracking may occur on knuckle region of pressures beyond calculated pressure capacity but will be arrested by welds or stiffeners. Dynamic pressurization cracking may not be arrested.

Probability of Loss of Containment Integrity

Knuckle of torispherical head controls. With actual (estimated) yield stress, mean containment capability is 51 psig for plastic yield.

Yield may not cause loss of integrity. Loss of integrity will occur when ultimate tensile strength is reached or a crack is developed.

Using actual properties for ultimate tensile strength, mean pressure at ultimate is 69 psig.

The probability of cracking is assumed to vary linearly between S_y and S_{ult}. (Zero at 51 psig and one at 69 psig).

For 50% failure probability, containment dome capacity is 59 psig.

Conclusions

Loss of containment integrity would occur in torispherical dome, with gradual depressurization.

Other portions will remain intact.

1.8 Buckling of Heads (by Los Alamos) [1.8-1]

Objective

Conduct experiments to determine margin-to-failure of 2:1 torispherical and ellipsoidal heads under internal pressure.

Preliminary Analytical Modeling

BOSOR5 finite difference program for buckling at axisymmetric shells.

Analytical Results

As specified geometry and material properties head (plastic) buckling predicted between 56 and 58 psi (n = 37).

Imperfections have small effect, as does strain hardening, in this particular case.

BOSOR5 applied to actual as-built model with corrections to account for plastic strain during spinning. Buckling predicted between 54 and 56 psi.

Experimental Techniques

<Beyond scope of this review.>

Experimental Results

Only two stress-relieved heads have been tested. Buckling occurred at 46 psi and 64 psi with n between 12 and 15 (±16% from analytical).

As pressures increased into post-buckling regime, buckles deepened but never became sharp. Cracks occurred in expoxy bonding head to support ring at 50 and 100 psi, but no leakage of head material.

1.9 Ultimate Internal Pressure Capacity of Reinforced Concrete MARK III Containment (by Bechtel) [1.9-1]

Objective

Ultimate capacity of BWR Mark III containment.

Containment Description

BWR, Mark III, concrete (see Fig. 1.9-1).

Finite Element Analysis

FINEL - proprietary computer code.

Axisymmetric model (neglect all penetrations because adequately reinforced.)

Concrete tension cracking and steel yielding are included.

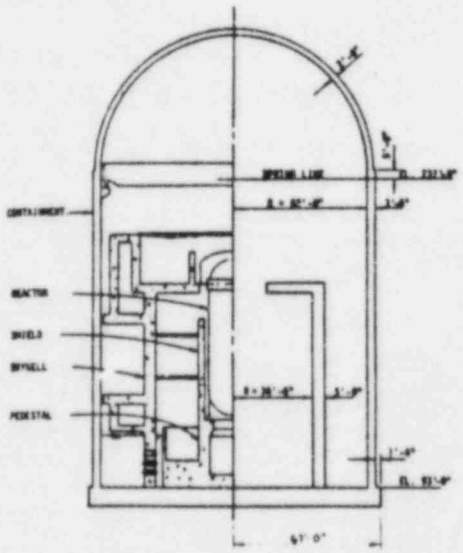

Figure 1.9-1 Containment Structure

Quadrilateral elements are used for concrete and liner. Unidirectional elements are used for reinforcing steel.

Minimum specified material properties are used.

Convergence is based on small change in strain between two cycles.

Internal pressure is treated as quasi-static load and incrementally after initial weight loads.

Analysis Results

Ultimate pressure coresponds to general yielding state.

Critical section was found to be in the cylinder near the springline where liner yields first followed by inner hoop rebars and then outer hoop steel.

Ultimate pressure was found to be 56 psig.

Using actual material strength, the mean ultimate capacity is 67 psig. The lower and upper bounds are 62 and 70 psig, respectively.

1.10 Leakage Through Electrical Penetrations (by Sandia) [1.10-1]

Objective

Assess potential leakage of electrical penetration assemblies and recommend test program.

Background and History

Electrical penetrations have evolved into more reliable. Leakage has been detected in 0.42% of the installed electrical penetrations better than other penetration types.

Existing Capabilities

Five test apply to severe accidents:

- Conax - 1100°F, no leakage;
- D.G. O'Brian - 280 psi at 382°F and 550°F, no leakage;
- Viking - 500°F, no leakage;
- Westinghouse - 1090°C, integrity maintained.

Generally, unlikely to leak at 350°F and 100 to 120 psig.

Penetration Failure Modes - Leakage

High temperature in seal materials may reduce material properties which may promote leaking.

Organic seals (plastic, rubber) - susceptible to heat.

Inorganic seals (glass, ceramics) - good heat resistance.

Metal seals - mechanical and melted.

Structural interaction - leakage induced by deformation of supporting structure, especially important for large penetration (personnel locks and equipment hatches) which were not covered in this work. ASME design factor of 3 on ultimate tensile stress.

Leakage by two methods.

- Through the seal - permeation, function of diffusion and solubility of gas in seal material, affected by temperature;
- Past the seal - "through a clear passage", depends on creep, temperature.

Theoretical prediction unreliable.

Postulated Failure Modes in Generic Containments

Large dry - Bellefonte:

- Ultimate capacity of containment building is 139 psig;
- 42 Conax and 27 Westinghouse electrical penetrations;
- Potential for leaks is extremely low because massive concrete wall acts as heat sink to keep outside below temperature limits.

Ice Condenser - Watts Bar

- Ultimate capacity of shell between 120 and 170 psig but equipment hatch predicted to fail at 140 psig;
- Predicted containment and penetration temperature is 340°F. Leakage potential relatively small since electrical penetration qualified to 340°F.

Mark I BWR - Browns Ferry

- Containment failure pressure estimated at 160 psig;

- High temperatures in accident scenarios.

Another source predicts threshold leaking at 400°F and gross leaking at 500°F. Current work questions assumptions on actual thermal response - find temperatures in range of 150°F to 400°F.

No failure of electrical penetration since temperatures less than 350°F. Equipment hatch seal is a potential leakage source.

Recommendation for Testing

Recommend testing 6 electrical penetration designs and continue work on containment integrity (temperature effects).

1.11 Post-tension Concrete 3-D Analysis [1.11-1]

Objective

Develop and demonstrate modeling techniques for determining ultimate internal pressure capacity for post-tensioned containment.

Containment Building Description

Post-tensioned reinforced concrete (Fig. 1.11-1).

Nominal material properties.

Failure Criteria

Tendons reach ultimate stress.

Structural Model

Three dimensional finite element model of dome (30 degree section with symmetry boundary conditions (Fig. 1.11-2)).

No penetrations.

ADINA program with 3-D solid elements

Stiffness reduction after cracking: 0.001 for normal stiffness and 0.5 for shear.

Cylinder tendons - elastic plastic trusses with initial strain constrained to mid-section of concrete.

Dome tendons - three separate tendon sets modelled with special uniaxial 3-D shell elements constrained to concrete.

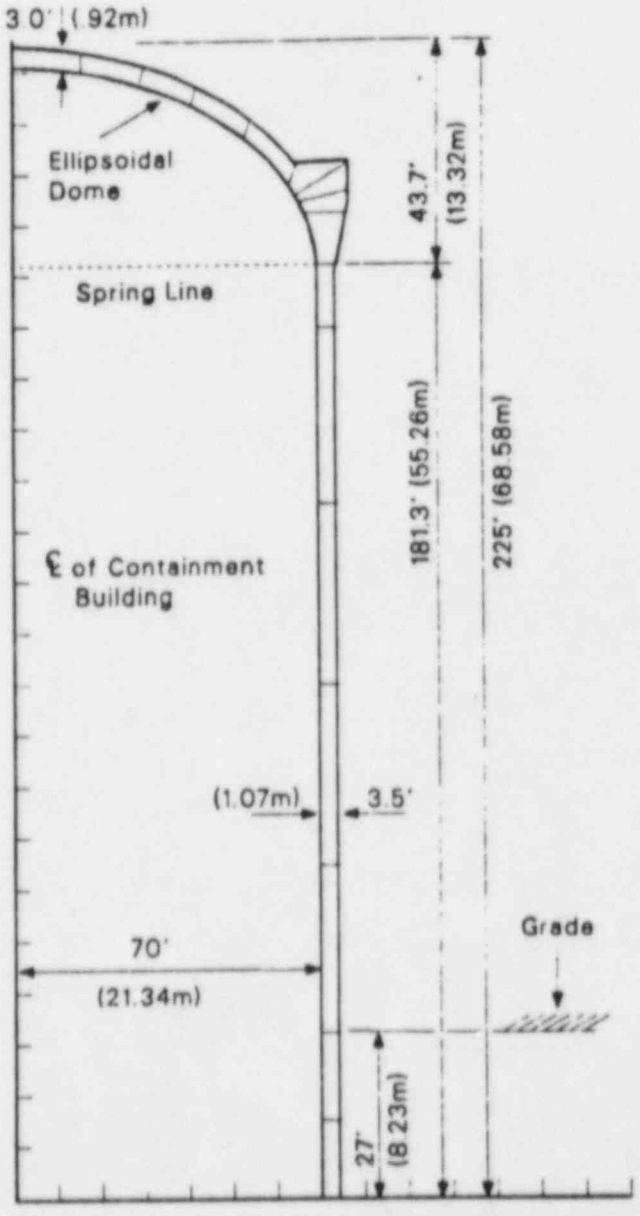

Figure 1.11-1 Containment Vessel Geometry

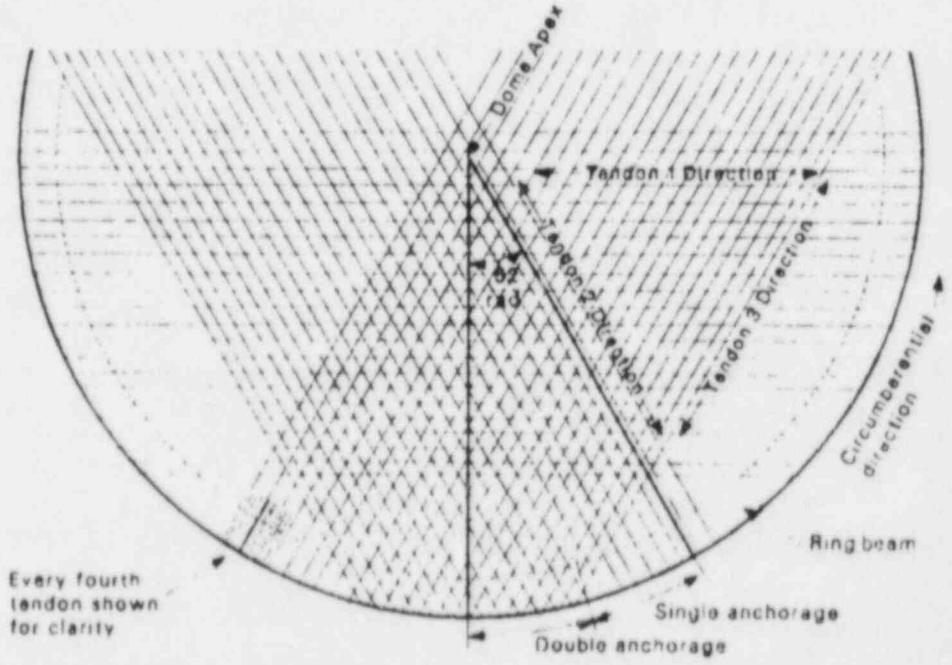

Figure 1.11-2 Dome Tendon

Reinforcing steel modelled by truss elements constrained to concrete.

Liner modelled as elastic-plastic 3-D shell constrained to concrete.

Symmetry boundary conditions.

Applied Loads

Initial prestress followed by gravity load followed by pressure increments.

Pressure incremented until "solution appeared to become unreliable" at 100 psi.

Pressure (psi)	Notes
73	Liner yield
85	Concrete cracked.
90	First rebar yield.
98	Concrete crushing.
99	Ties in ring beam yield. Tendon yield.

Conclusions

Three-dimensional analysis important. Concrete cracking in ring beam appeared to be accentuated by unsymmetrical anchorage of post-tensioning.

At 99 psi, ring beam totally crushed or cracked by tendons only 25% of the way from yield to ultimate. Tendons would probably pull out.

Need finer mesh near ring.

2. Work Conducted in Canada

2.1 Behavior of Prestressed Containment Under Over-Pressure Conditions (University of Alberta) [2.1-1, 2.1-2, 2.1-3, 2.1-4, 2.1-5]

Objective [2.1-1]

Experimental and analytical program to investigate the behavior of prestressed containment under over-pressure conditions.

Test Model [2.1-2]

1:14 scale prestressed model of the prototype vessel, Figs. 2.1-1.

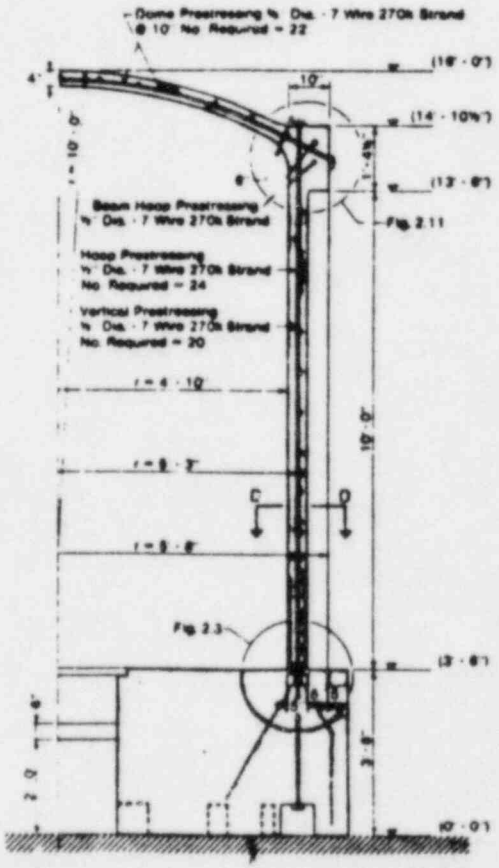

Figure 2.1-1 Vertical Section Through test Structure

Post-Tensioning and Instrumentation

<Beyond the scope of this review.>

Testing

Water used to develop the internal pressure of the test structure.

Test was accomplished in several stages.

Observed Behavior and Mode of Failure

Pressure (psig)	Notes
40	First meridional and hoop.
80	Extensive cracks and bulging of cylinder walls.
130	Crack pattern is shown in Figs. 2.1-2, 2.1-3
142-145	Vertical tendons and one horizontal ring beam tendons fractured.
159	One vertical tendon and one horizontal tendon at midheight fractured resulting in model failure (Fig. 2.1-4).

Buttresses provide significant stiffening to outward movement and influence crack pattern [2.1-5].

Analytical Investigation of the Tested Model [2.1-3]

Analysis of the tested model utilizing inelastic finite difference technique using BOSOR5 computer code.

Idealization of the shell structure using a series of segments joined with or without eccentric links.

Two analytical models referred to as Models A and B were considered.

Model A

Elastic-perfectly plastic properties for the reinforcement.

Piecewise linear approximation of the prestressed stress-strain relation found from test.

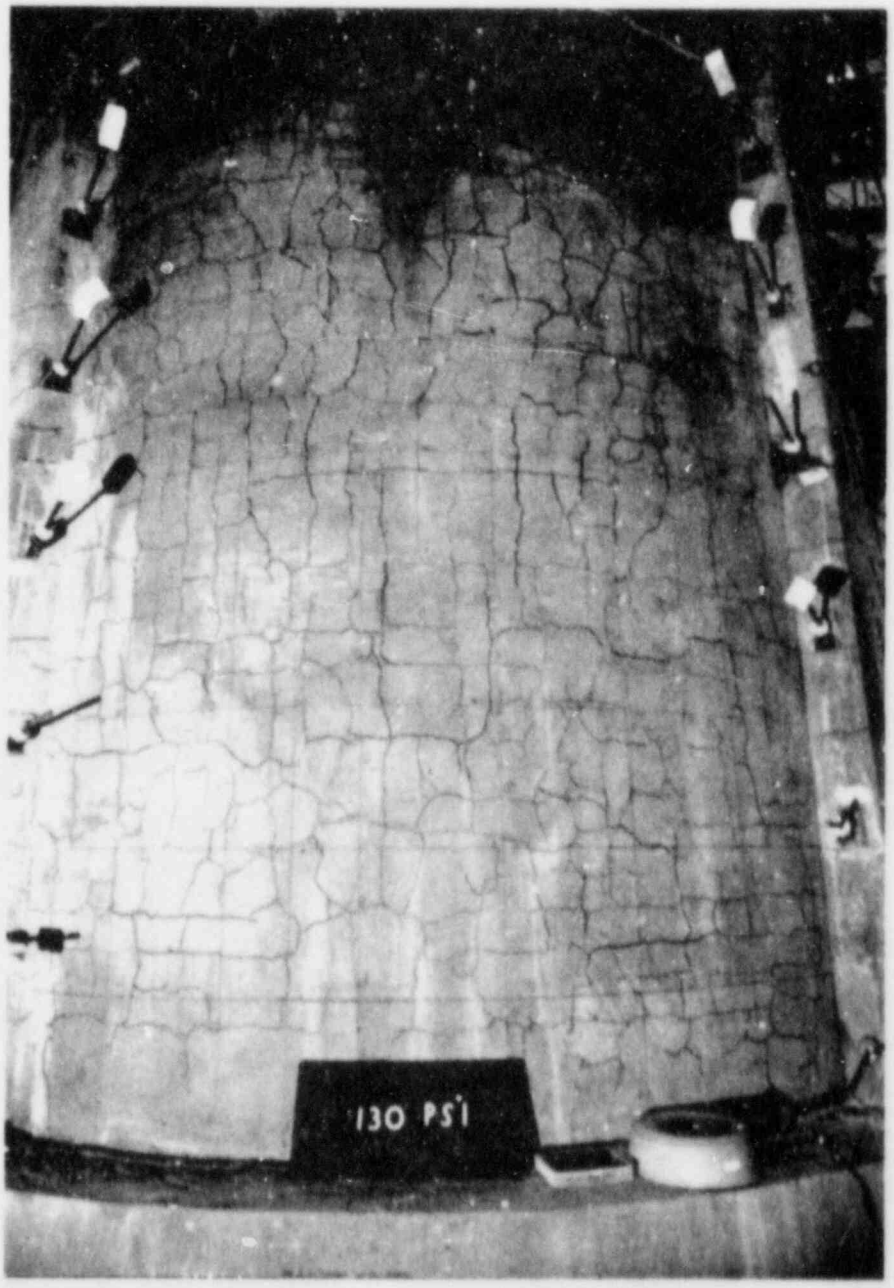

Figure 2.1-2 Cylinder Wall Cracking at 130 psig

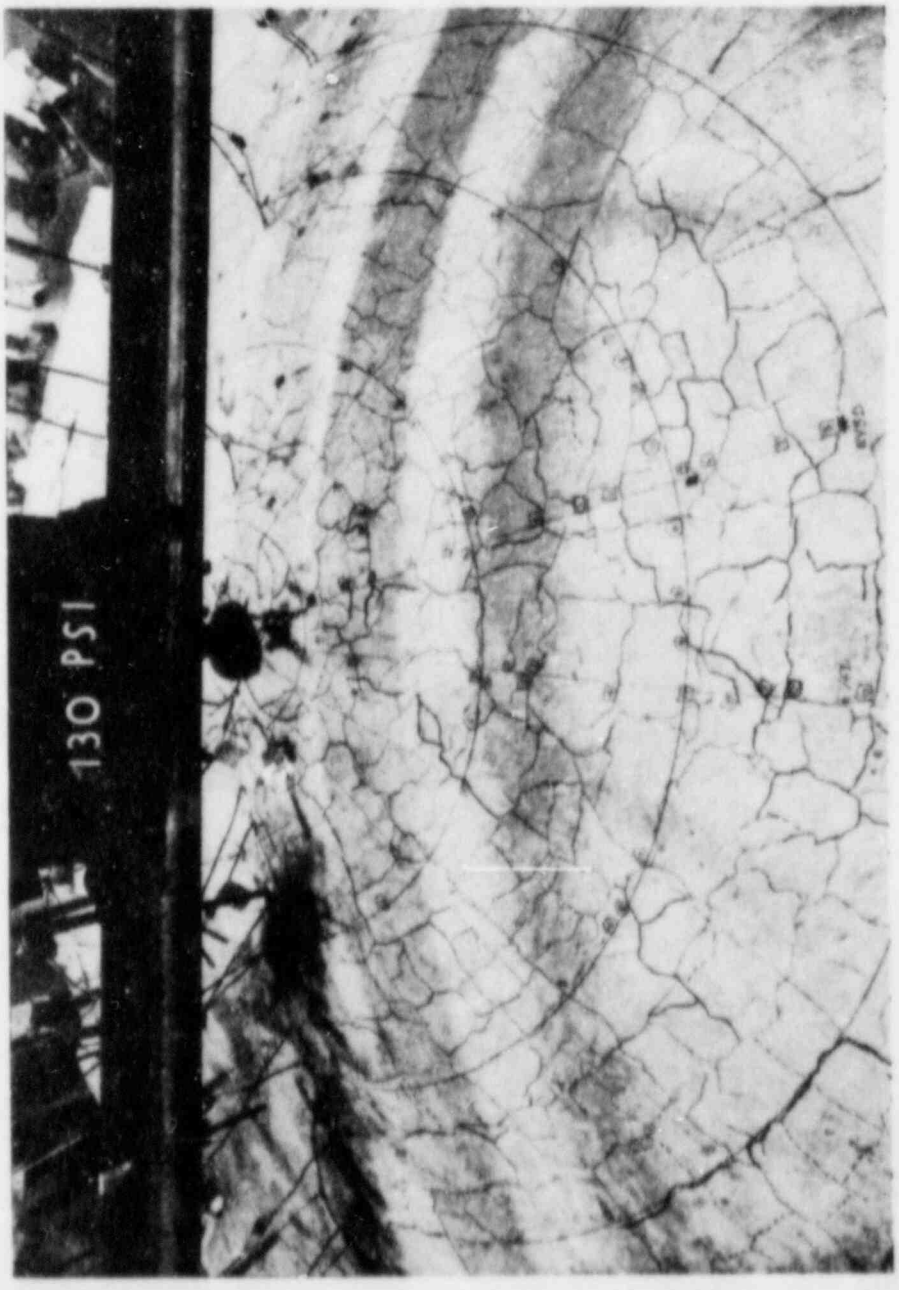

Figure 2.1-3 Dome Cracking at 130 psig

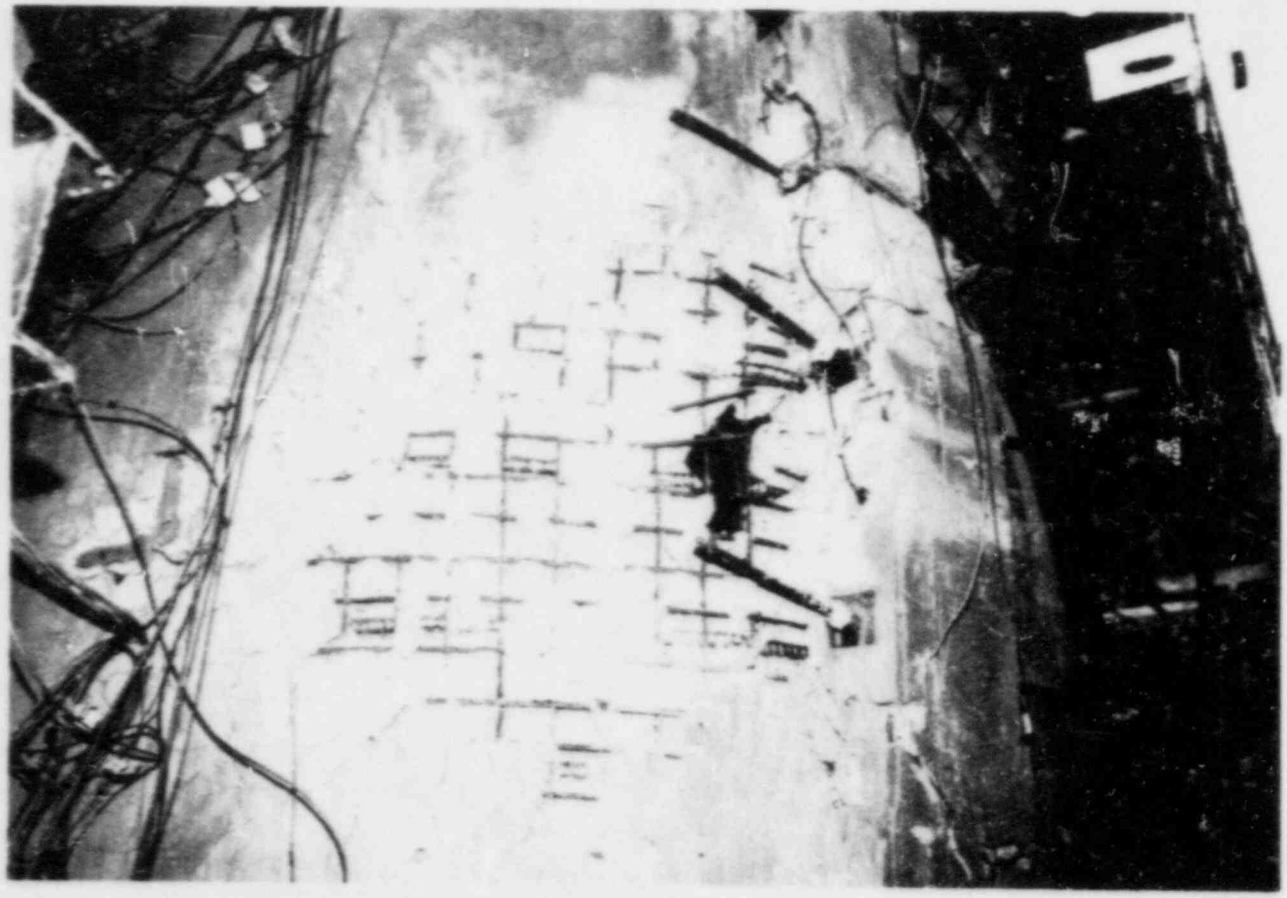

Figure 2.1-4 Failure Region

Equivalent external pressure used to simulate prestressing effect.

Concrete properties [2.1-4]:

- Based on test results of large scale wall segments;
- Tension cutoff would tend to overstimate strains and displacements;
- Equivalent stress-strain relation is given in Fig. 2.1-5(a) (includes degrading stiffness);
- Concrete cracking strength equal 50% of a 6 inches split cylinder tensile strength.

Numerical instability at pressure of 108 psi.

Model B

Modification of Model A.

Sudden termination of dowels produced cracking and stress concentration problem.

Tapering the effective area of the dowels over their development length would be more realistic to model the development of the dowels.

One continuous reference surface used on the model to avoid eccentric connections between the segments.

Concrete stress-strain is shown in Fig. 2.1-5(b)

Rebars and tendons properties were taken as in Model A.

Comparison of Analytical and Experimental Behavior - Model B

Measured results agree with those predicted by the BOSOR5 analysis.

The analysis became unstable at pressure = 133.75 psig.

Initiation and distribution of cracking from BOSOR appears to correspond resonably with test observations.

At 133.75 psig internal pressure - the stresses in the wall tendons were 90% (hoop), 93% (vertical) and in the dome was 95%.

2.2 Cracking of Prestressed Concrete Containments Due to Internal Pressure [2.2-1]

Objective

Study (analytical and experimental) the development of cracking, crack

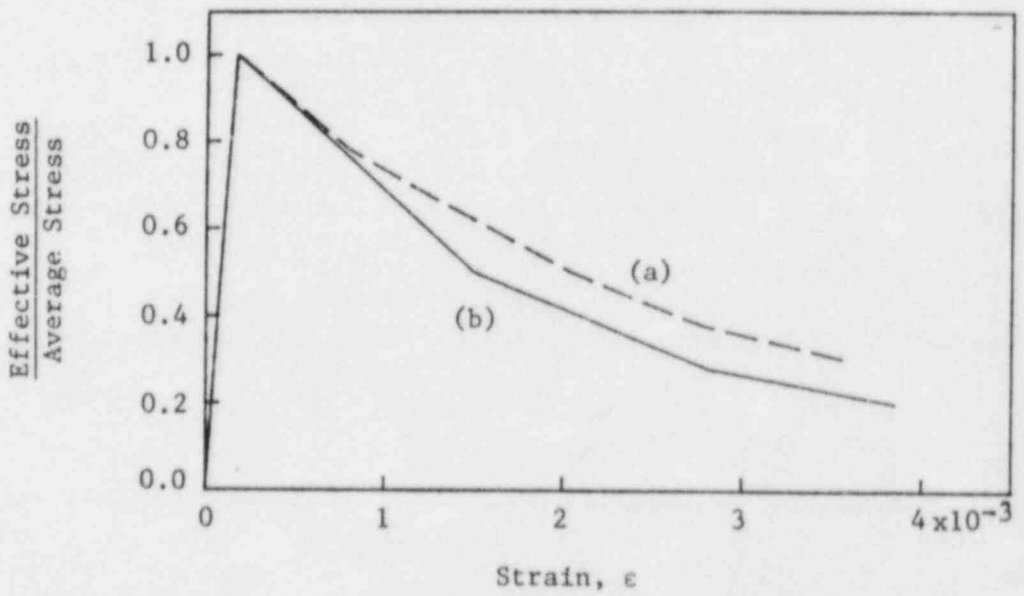

Figure 2.1-5 Effective Tensile Stress-Strain Relationship Used BOSOR5

width and leakage through cracks in an overpressurized prestress vessel.

Wall Segment Tests

1:4 scale wall segments represent various locations in a vessel.

Loads applied by pulling on the reinforcement and prestressing.

Determination of Crack Spacings

Cracks coincide with reinforcing bar locations.

Crack spacing is independent of the concrete cover.

Surface cracks follow transverse bars if these bars are spaced at between 0.5 to 1.0 times the expected crack spacing.

Crack propagation and rules for computing crack spacing.

Computed Mean Crack Width

Outlined procedure to compute crack widths.

Comparison of Computed and Measured Crack Widths

Mean of measured to computed values = 1.07 with a coefficient of variation = 0.347.

Application of Cracking Analysis

Outlined procedure to determine crack width of a prototype containment.

3. Work Conducted in Japan

3.1. Behavior of Reinforced Concrete Containment Models Under Thermal Gradient and Internal Pressure [3.1-1]

Objective

Experimental study to investigate the effect of thermal gradient on a containment ultimate strength capacity.

Test Models

Shape, dimensions, reinforcement, (Fig. 3.1-1).

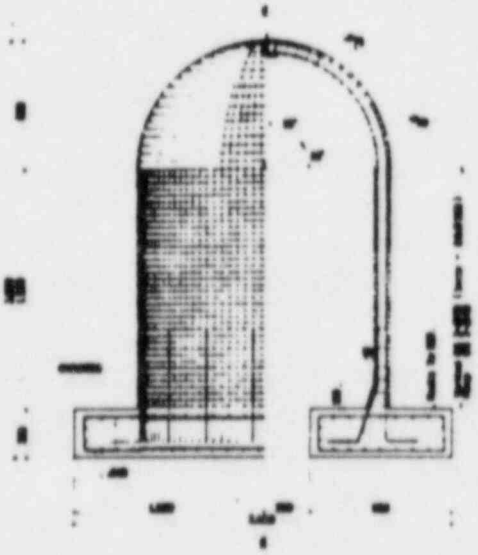

Figure 3.1-1 Test Model and Reinforcing Arrangement

Test Method

Equipment, procedure and method of measurement.

Two models under:

- Internal pressure;
- Internal pressure plus temperature gradient through wall.

Test Results and Considerations

Model 1 - small cracks at 3.5 kg/cm^2, hoop reinforcement yield at 7 kg/cm^2, failed by punching shear around hole at top of dome.

Model 2 developed cracks while thermal cycling. Same failure mode.

Splitting tensile strength can be used for membrane cracking.

FIP-CEB Model Code accurately predicts crack patterns.

Initial rigidity reduced in Model 2 because of thermal cracking.

Approximate hand methods proposed for calculating thermal forces in cracked structure.

Conclusions

The proposed method to calculate the thermal stress showed good agreement with test results.

Thermal loads reduce the section effective stiffness because of its self-relieving characteristics.

Thermal effects play a negligible role in containment ultimate strength.

3.2 An Experimental and Analytical Study on Radial Shear of Reinforced Containment Under Pressure and Thermal Effects [3.2-1]

Objective

Experimental study to estimate the radial shear of shell wall at the junction of base mate subjected to pressure and thermal effects.

Test Model

1:12 scale models of prototype reinforced concrete containment (Fig. 3.2-1).

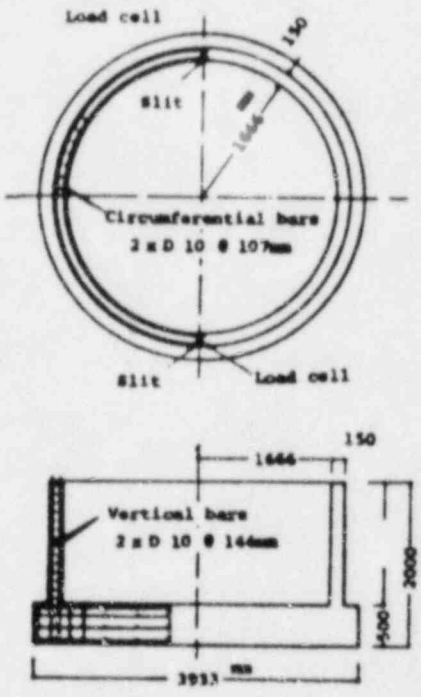

Figure 3.2.1 Test Model and Arrangement of Reinforcement

Three types differ in the vertical and circumferential reinforcement ratio.

Test Method

Equipment <beyond the scope of this review>.

Experimental Results

Concrete cracking - crack pattern and propagation history described.

Temperature distribution given.

Hoop force distribution:

- Yielding of hoop rebars started at the top of the wall;
- Hoop force distributions are similar in both pressure and pressure plus thermal loading cases.

Ultimate strength and failure modes:

- Cracks in the inner surface followed by yielding of the vertical steel at same location;
- Theoretical shear strength calculated is higher than experimental results.

Transition of base shear stresses:

- Shear stress increases monotonically from zero up to the yield pressure of the circumferential rebars;
- Rapid increase in the base shear after yielding of all hoop rebars;
- Thermal component of the base shear decrease with crack formation.

Nonlinear Axisymmetric Finite Element Analysis

Finite element model:

- Incremental loading;
- Concrete cracking with account of tensile stress between cracks. Degrading concrete strength after cracking is included;

- Bi-linear stress-strain relation for rebars;
- Vertical bars simulated with thin plate elements. Solid elements for concrete.

Cracking caused some irregularities in numerical solutions.

Conclusions

Influence of residual shear stresses on ultimate strength and failure mode was not observed.

Nonlinear finite element results indicated good agreement with test results.

3.3 Design Method of Shell Wall End of Reinforced Concrete Containment Vessel (RCCV) Against Radial Shear [3.3-1]

Objective

Experimental investigation to propose a reasonable design method for the shear reinforcement at wall basemat junction in MARK III containments.

Model

1:12 scale model (Fig. 3.3-1) simulating internal pressurization.

Experimental Results

Concrete cracking and deflection:

- Vertical cracks occurred along vertical rebars;
- Horizontal cracks (by membrane tension) appeared near the model wall top.

Ultimate strength and failure modes:

- Reinforcement yield first at wall/base juncture due to bending. Then yielding of hoop bars progressing slowly downward. Agreed with hand calculations;
- Ductile behavior in the ultimate state due to the contribution of circumferential rebars;
- Shear reinforcement has little effect on the ultimate pressure;

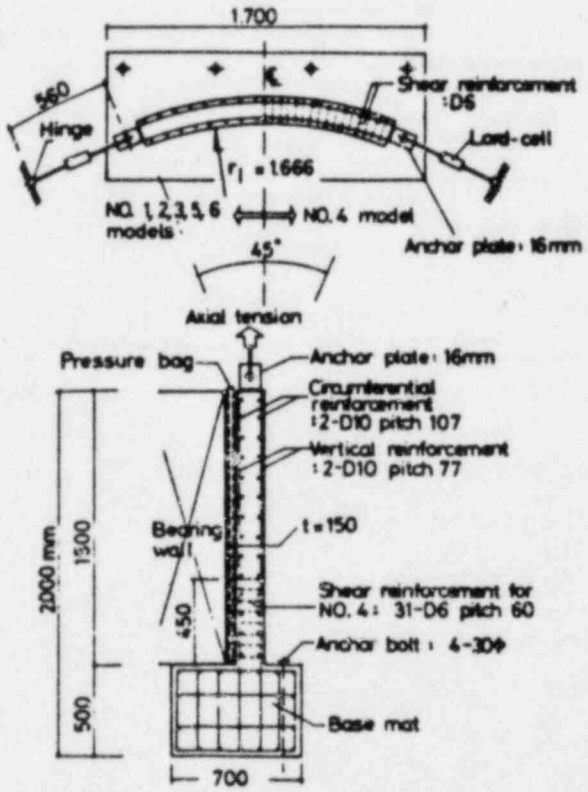

Figure 3.3-1 One-Twelfth Scale Junction Model of RCCV

- Shear failure will not be ahead of the hoop yield under conditions similar to the models.

Base shear stresses:

- Measured base shear follows the elastic shell solution;
- Base shear in the ultimate state reached at 1.3 times the elastic solution.

Design of Junction Against Radial Shear

Suggested design relation should predict the base shear when hoop steel yields.

Measured shear (during tests) lies between the base shear calculated when hoop steel reaches yield and tensile strength.

Conclusions

Models without shear reinforcement provide a significant strength margin. Current design code underestimates radial shear strength.

4. Work Conducted in Poland

4.1 Results of Strength Tests on a 1:10 Model of Reactor Containment [4.1-1]

Objective

Experimental study on a model of a PWR containment to be built.

Model Configuration and Test Program

Prestressed concrete model (Fig. 4.1-1).

The model was built using material identical with those of the prototype.

Test was divided into two stages:

- By applying pressure not more than 1.15 the design pressure value (elastic behavior);
- Destructive test (nonlinear stage investigation).

Elastic Phase Test

No cracks were observed

Linear behavior (strains proportion to load).

Measured results compared with those found using shell theory analysis <no details given>.

Noticeable difference between measured and predicted hoop strain caused by ignoring the effect of the buttresses in the analytical solution.

Nonlinear Behavior of the Model

Pressure* (psig)	Notes
34.70	Cracks appeared near the buttresses.
43.40	Horizontal cracks were observed.
66.5	All wall cracked and hoop reinforcement yielded.
75.2	Failure pressure (near the opening and wall entrys).

* Does not include the water pressure before pressurization (different between upper and lower portion = 8.7 psig).

Cracked model - Fig. 4.1-2

Conclusions

Theoretical calculated pressure based on limit strength of prestressing and reinforcement yielding <no details given> are:

Theory	Test	
71	--	without liner
89.6	83.8*	with liner

* At the bottom of the model.

5. Work Conducted in United Kingdom

5.1 Nonlinear Analysis of Prestressed Concrete [5.1-1]

Objective

Comparison between experimental (model test)/theoretical prediction of a prestressed concrete ultimate internal pressure capacity.

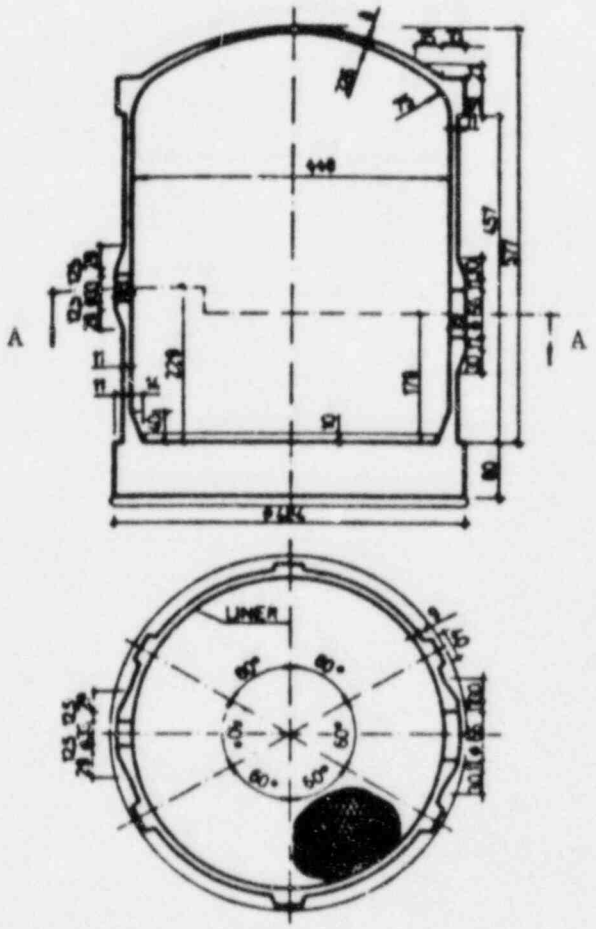

Section A-A

Figure 4.1-1 Containment Model

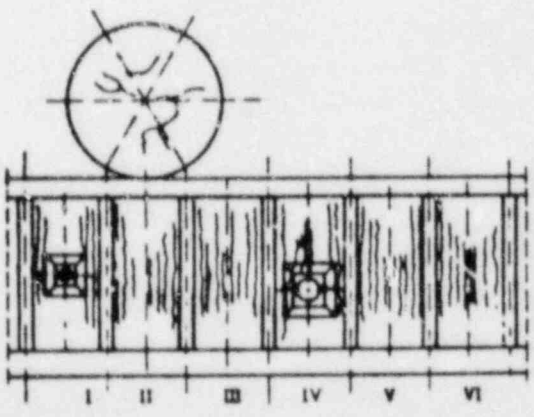

Figure 4.1-2 Diagram of Cracking of Model External Surface After Tests.

Model Test

General - prestressed 1:12 micro concrete vessel, Fig. 5.1-1

Instrumentation <beyond the scope of this review>.

Containment model was considered to reach the ultimate load when:

- Deflection in the model crown corresponding to a 25 mm deflection of the prototype;
- Crack width across a meridian equal to 5 mm/meter.

Analytical Model

Nonlinear finite element analysis (geometric and material nonlinear behavior).

Axisymmetric eight noded isoparametric quadrilateral ring element.

Prestressing effects were simulated as external pressure.

Converged solution is reached when the residual forces became insignificantly small.

Three yield criteria, von Mises, Tresca and Drucker-Prager were used to investigate their effect on the vessel inelastic behavior.

Comparison of Experimental and Theoretical Results

Deformation - see Fig. 5.1-2. No test results are available beyond 1.45 kg/cm^2 internal pressure.

Drucker-Prager yield criteria yields the largest deviation in the deformation when compared to linear analysis.

Geometric nonlinearity affects the response depending upon the yield criteria used.

Conclusion

Failure pressure is 2.12 kg/cm^2 (crown deformation and strain reached the critical values).

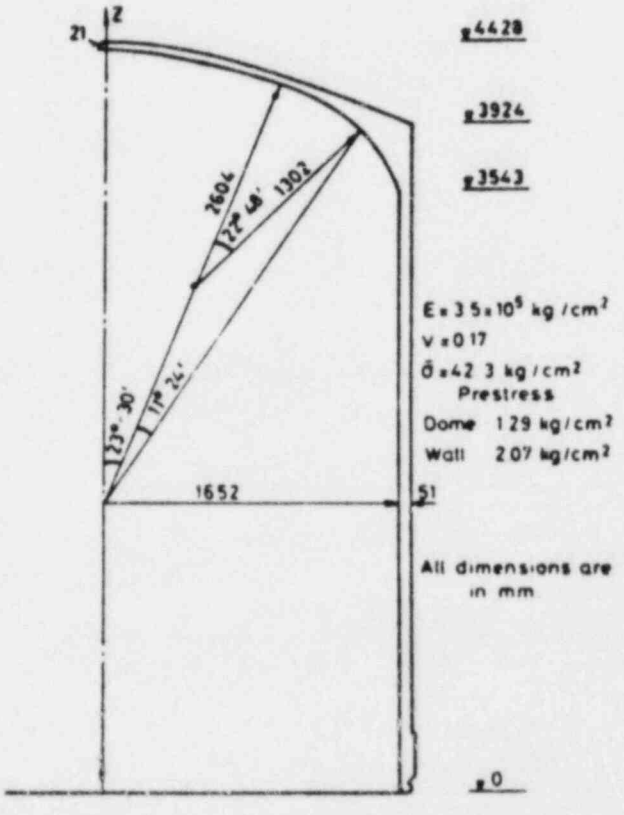

Figure 5.1-1 Model of the Containment Vessel

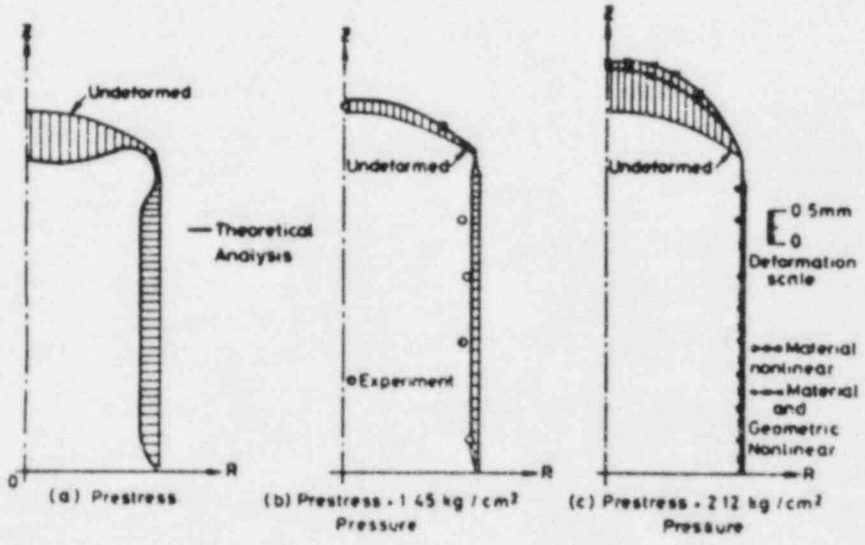

Figure 5.1-2 Deformation of the Containment Vessel (Experimental Results Shown Wherever Available)

6. Work Conducted in the Federal Republic of Germany

6.1 Dynamic Stresses of LWR Containment [6.1-1]

Objective

To analyze dynamic stresses and strains of LWR containment.

Computer Programs

Programs for dynamic analysis of thin shells <beyond scope of this review>.

ROTNEM - nonlinear membrane model for computation of stress and strains in PWR containment during quasi-static internal pressurization, axisymmetric loads, and large displacments.

Local high bending stresses are reduced by plastic hinges.

Results

Dynamic <beyond scope of this review>.

Spherical containment (German PWR) - Fig. 6.1-1.

Henky material flow for biaxial stress state.

Results up to 3% strain.

Further Development

Plans to include deviations from perfect shape for dynamic analysis.

Plan to verify ROTNEM with experiments on their circular sheets with and without thickened inclusions.

7. Work Conducted in France

7.1 Study of the Behavior of Containment Buildings of PWR-type Reactor, Until Complete Failure in Case of LOCA [7.1-1]

Objective

Nonlinear axisymmetric analysis of the behavior of PWR 900 and 1300 MWe containment buildings under LOCA pressure and temperature loadings.

Method of Calculation

Nonlinear finite element analysis using INCA program, axisymmetric model.

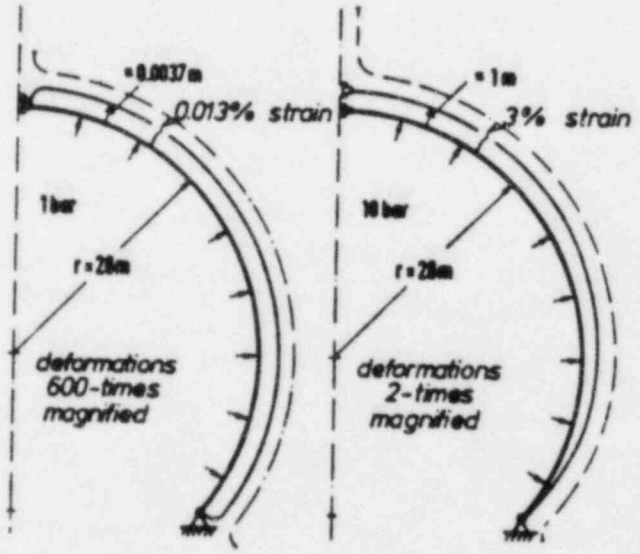

Figure 6.1-1 PWR-Containment With Rigid Nozzle
Under Internal Pressure.
(— displacements, – – meridional strains)

Concrete model - three yield surfaces:

- Crack damage - maximum principle stress;
- Shear damage - Drucker-Prager (Mohr - Coulomb) criterion;
- Hydrostatic compaction with hydrostatic stress.

Metal model - plasticity model with von Mises yield crite: ion.

Isoparametric (quadrilateral and triangular element) for concrete, shell element for steel skin, special elements for prestress and reinforcement.

Loads

Weight of the structure, vertical and horizontal prestress, weight of the internal structures, accidental loads (temperature and pressure).

Results

Deformation of structure - Figs. 7.1-1, 7.1-2, 7.1-3 and 7.1-4.

Plastification of metals:

- PWR 900 MWe - rupture of cylinder and dome prestressed steel;
- PWR 1300 MWe - rupture of dome prestressed steel.

Conclusion

Good prediction for complete ruin but point of through fracture of concrete not well predicted.

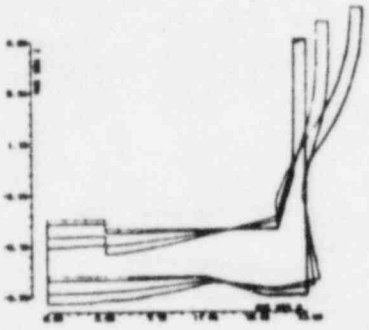

Figure 7.1-3 PWR 900 MWe - Deformed Shapes at Times 0,14 and 28 hours

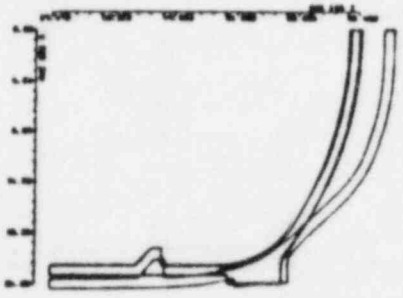

Figure 7.1-1 PWR 1300 MWe - Deformed Shapes at Time 0,9 and 14 hours

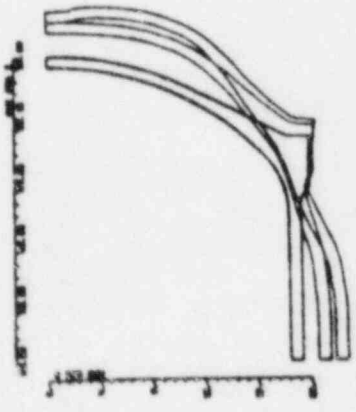

Figure 7.1-4 PWR 900 MWe - Deformed Shapes at Times 0,18 and 27 hours

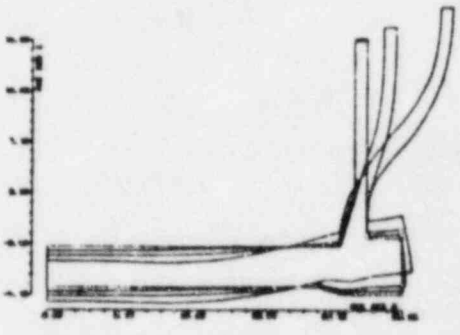

Figure 7.1-2 PWR 1300 MWe - Deformed Shapes at Times 0,12 and 28 hours

REFERENCES FOR APPENDIX II

1.1-1 Blejwas, T.E., et al., "Containment Integrity Program FY82 Annual Report," Report to the U.S. NRC, NUREG/CR-3131/1, SAND83-0417, March 1983.

1.1-2 Blejwas, T.E. and Horschel, D.S., "Analysis of Steel Containment Models," Proceedings of the Workshop on Containment Integrity, Vol. II of II, NUREG/CR-0033, SAND82-1659, 201-226, October 1982.

1.1-3 Blejwas, T.E., von Riesemann, W.A., and Costello, J.F., "The NRC Containment Integrity Program," Transactions of SMIRT 7, Paper No. J1/1, Chicago, IL, August 1983.

1.1-4 Woodfin, R.L. and Dennis, A.W., "Techniques Used in Static Pneumatic Pressure Experiments on Models of Generic Steel Containment Building," Transactions of SMIRT 7, Paper No. J6/2, Chicago, IL, August 1983.

1.1-5 Woodfin, R.L. and Dennis, A.W., "Results Obtained from Static Pneumatic Experiments on Models of a Generic Steel Containment Building," Paper No. J6/3, Transactions of SMIRT 7, Chicago, IL, August 1983.

1.1-6 Horschel, D.S. and Blejwas, T.E., "An Analytical Investigation of the Response of Steel Containment Models to Internal Pressurization," Transaction of SMIRT 7, Paper No. J6/4, Chicago, IL, August 1983.

1.2-1 Tsia, J.C. and Orr, R.S., "Probabilistic Failure Modes and Locations in Containments Subjected to Internal Pressurization," Proceedings of the Workshop on Containment Integrity, Vol. II of II, NUREG/CR-0033, SAND82-1659, 365-382, October 1982.

1.3-1 White, R.N. and Gergely, P., "Punching and Radial Shear Problems in Reinforced Concrete Containments," Proceedings of the Workshop on Containment Integrity, NUREG/CR-0033, SAND82-1659, 109-122, October 1982.

1.4-1 Krishnaswamy, C.N., Namperumal, R. and Al-Dabbagh, A., "Ultimate Internal Pressure Capacity of Concrete Containment Structures," Transactions of SMIRT 7, Paper No. J3/6, Chicago, IL, August 1983

1.5-1 Tsia, J.C. and Orr, R.S., "Probabilistic Failure Modes and Locations in Containments Subjected to Internal Pressurization," Proceedings of the Workshop on Containment Integrity, Vol. II of II, NUREG/CR-0033, SAND82-1659, 365-382, October 1982.

1.5-2 Meller, E. and Bushnell, D. "Buckling of Steel Containment Shells, Task 1a: Dynamic Response and Buckling of Offshore Power Systems' Floating Nuclear Plant Containment Vessel," NUREG/CR-2836, Vol. 1, Part 1, December 1982.

1.6-1 "Reactor Safety Study: An Assessment of Accident Risks in the U.S. Commercial Nuclear Power Plants," WASH-1400, U.S. Atomic Energy Commission, Appendix E, August 1974.

1.7-1 Gou, P.F. and Love, J.E., "Pressure Carrying Capacity of the Containment Structural System of the Mark ILI Standard Plant," Proceedings of the Workshop on Containment Integrity, Vol. II of II, Prepared for the U.S. NRC, NUREG/CP-0033, SAND-82-1659, 263-318, October 1982.

1.7-2 Gou, P.F. and Love, J.E., "Determination of Pressure Carrying Capability of the Containment Structural System for the Mark III Standard Plant," Transactions of SMIRT 7, Paper No. J2/6, Chicago, IL, USA, August 1983.

1.8-1 Fiy, G., Bennet, J.G., Baker, W.E. and Babcock, C.D., "Esperiments Designed to Assess the Margin-to-Failure of Steel Containment Susceptible to "Knuckle" Buckling," Transactions of SMIRT 7, Paper No. J3/5, Chicago, IL, August 1983.

1.9-1 McGaughy, J.P., Lin, F.T. and Sen, S.K., "Ultimate Internal Pressure Capacity of a Reinforced Concrete Mark III Containment," Transactions of SMIRT 7, Paper No. J3/9, Chicago, IL, USA, August 1983.

1.10-1 Sebrell, W., "The Potential for Containment Leak Paths Through Electrical Penetration Assemblies Under Sever Accident Conditions," NUREG/CR-3234, July 1983.

1.11-1 Dooley, W.T., Macek, R.W. and Sadik, S., "Ultimate Pressure Capacity Analysis of a Post-tensioned Reinforced Concrete Nuclear Reactor Containment Building," Work supported by U.S. DOE Contract No. DE-AC07-76ID01570 at EG&G Idaho, Inc., Idaho Falls, Idaho.

2.1-1 Atchison, R.J., Asmis, G.J.K. and Campbell, F.R., "Behavior of Concrete Containment Under Over-Pressure Conditions," Transactions of SMIRT 5, Paper No. J3/2, Berlin, Germany, August 1979.

2.1-2 Rizkalla, S., Simmonds, S.H. and Macgregor, J.G., "A Test of a Model of a Thin-Walled Prestressed Concrete Secondary Containment Structure," Transactions of SMIRT 5, Paper No. J4/2, Berlin, Germany, August 1979.

2.1-3 Murray, D.W., Chitnuyanondh, L. and Wong, C., "Modeling and Predicting Behavior of Prestressed Concrete Secondary Containment Structures Using BOSOR5," Transactions of SMIRT 5, Paper No. J3/5, Berlin, Germany, August 1979.

2.1-4 Chitnuyanondh, L., et al., "Effective Tensile Stiffening in Prestressed Concrete Wall Segments," Transactions of SMIRT 5, Paper No. J3/4, Berlin, Germany, August 1979.

2.1-5 Simmonds, S.H., Macgregor, J.C. and Rizkalla, S.H., "Response of Prestressed Concrete Model in Post-cracking Region," Transactions of SMIRT 6, Paper No. J4/11, Paris, France, August 1981.

2.2-1 Macgregor, J.G., Simmonds, S.H. and Rizkalla, S.H., "Cracking of Prestressed Concrete Containment Due to Internal Pressure," Transactions of SMIRT 6, Paper No. J4/10, Paris, France, August 1981.

3.1-1 Aoyagi, Y., et al., "Behavior of Reinforced Concrete Containment Models Under Thermal Gradient and Internal Pressure," Transactions of SMIRT 6, Paper No. J4/5, Berlin, Germany, August 1979.

3.2-1 Aoyagi, Y., Okada, K. and Tanka, N., "An Experimental and Analytical Study on Radial Shear of Reinforced Concrete Containment Under Pressure and Thermal Effects," Transactions of SMIRT 6, Paper No. J4/12, Paris, France, August 1981.

3.3-1 Aoyagi, Y., Isobata, O. and Tanka, N., "Design Method of Shell Wall End of Reinforced Concrete Containment Vessel (RCCV) Against Radial Shear," Transactions of SMIRT 6, Paper No. J4/6, Berlin, Germany, 1979.

4.1-1 Donten, K., et al., "Results of Strength Test on a 1:10 Model of Reactor Containment," Transactions of SMIRT 5, Paper No. J4/8, Berlin, Germany, August 1979.

5.1-1 Carmichal, G.D.T., Rajaraman, A. and Balakrishnan, S., "Nonlinear Analysis of Prestressed Concrete Containments," Transactions of SMIRT 6, Paper No. J3/3, Paris, France, August 1981.

6.1-1 Gulden, W., Goller, B. and Krieg, R., "Analysis of the Mechanical Behavior of LWR-Containments Under Accident Conditions," Proceedings of the Workshop on Containment Integrity, Vol. II of II, Prepared for the U.S. NRC, NUREG/CP-0033, SAND-82-1659, 319-336, October 1982.

7.1-1 Brochard, J., et al., "Study of the Behavior of Containment Buildings of PWR-Type Reactor, Until Complete Failure in Case of LOCA," Transactions of SMIRT 6, Paper No. J3/1, Paris, France, August 1981.

DISTRIBUTION:

US NRC Distribution Contractors (CDSI)
7300 Pearl St
Bethesda, MD 20014
515 copies to R1, RD and RG

US Nuclear Regulatory Commission (25)
Division of Risk Analysis
5650 Nicholson Lane
Rockville, MD 20852
Attn: Mark Cunningham

US Nuclear Regulatory Commission
Mechanical/Structural Engineering Branch
5650 Nicholson Lane
Rockville, MD 20852
Attn: J. F. Costello

US Nuclear Regulatory Commission
Office of Nuclear Regulatory Research
Division of Accident Evaluation
Washington, DC 20555
Attn: Mel Silberberg

Iowa State University (20)
Dept of Civil Engineering
420 Town Engineering Bldg
Ames, IA 50011
Attn: L. Greimann

TVA
400 Commerce Ave
Knoxville, TN 37902
Attn: D. Denton, W9A18

Los Alamos National Laboratories
PO Box 1663
Mail Stop N576
Los Alamos, NM 87545
Attn: C. Anderson

Nuclear Design Group
800 Jorie Blvd
Oak Brook, IL 60521

Southwest Research Institute (2)
Dept of Ballistics & Explosives Sciences
6220 Culebra
PO Drawer 28510
San Antonio, TX 78284
Attn: W. E. Baker
P. A. Cox

Bechtel Power Corporation
12400 East Imperial Highway
Norwalk, CA 90650
Attn: A. H. Hadjian

ANCO Engineers, Inc.
1701 Colorado Ave
Santa Monica, CA 90404
Attn: G. Howard

University of Illinois (3)
Dept of Civil Engineering
Urbana, IL 61801
Attn: M. A. Sozen
C. Siess
L. A. Lopez

Stevenson & Associates
9217 Midwest Ave
Cleveland, OH 44125
Attn: J. D. Stevenson

United Engineers & Constructors, Inc.
Structural Analysis Group
30 South 17th St
Philadelphia, PA 19101
Attn: J. J. Ucciferro

Cornell University
School of Civil & Env Engr
Hollister Hall
Ithaca, NY 14853
Attn: R. N. White

Electric Power Research Institute (2)
3412 Hillview Ave
PO Box 10412
Palo Alto, CA 94304
Attn: I. Wall
H. T. Tang

Battelle Columbus Laboratories (2)
505 King Ave
Columbus, OH 43201
Attn: R. Denning
P. Cybulskis

University of Alberta
Dept of Civil Engineering
Edmonton, Alberta, CANADA T6G 2G7
Attn: D. W. Murray

Technology for Energy Corporation
One Energy Center
Pellissippi Pkwy
Knoxville, TN 37922
Attn: E. P. Stroupe

EG&G Idaho
Willow Creek Bldg, W-3
PO Box 1625
Idaho Falls, ID 83415
Attn: S. Sadik

Fauske & Associates, Inc.
16W070 West 83rd St
Burr Ridge, IL 60521
Attn: H. K. Fauske

Sargent & Lundy Engineers
55 E Monroe St
Chicago, IL 60603
Attn: A. Walser

Offshore Power Systems, Inc.
PO Box 8000
Jacksonville, FL 32225
Attn: J. Tsai

General Electric Company (2)
175 Curtner Ave
San Jose, CA 95112
Attn: R. G. Fou
J. E. Love

R. F. Reedy, Inc.
236 N Santa Cruz Ave
Los Gatos, CA 95030

US Department of Energy
Office of Nuclear Energy
Mail Stop B-107
NE-540
Washington, DC 20545
Attn: A. Millunzi

NUTECH
6835 Via Del Oro
San Jose, CA 95229
Attn: N. W. Edwards

Quadrex Corporation
1700 Del Ave
Campbell, CA 95008
Attn: Quazi A. Hossain, Mgr.

Chiapetta, Welch & Associates, Ltd
9748 Roberts Rd
Palos Hills, IL 60465
Attn: R. L. Chiapetta

Merlin Technologies, Inc.
1717 Dell Ave
Campbell, CA 95008
Attn: P. Sharifi

Bechtel Power Corp
15740 Shady Grove Rd
Gaithersburg, MD 20760
Attn: K. Y. Lee

ANATECH International Corp
3344 N. Torrey Pines Court
Suite 320
LaJolla, CA 92037
Attn: Y. R. Rashid

EBASCO Servuces, Inc.
Two Worldl Trade Center
New York, NY 10048
Attn: J. J. Healdy, Consulting Engr

Kernforschungszentrum Karlsruhe GmbH
Postfach 3640
D-7500 Karlsruhe
FEDERAL REPUBLIC OF GERMANY
Attn: W. Gulden

HM Nuclear Installation Inspectorate (2)
Thames House Norlth
Millbank, London, SW1
UNITED KINGDOM
Attn: R. J. Stubbs
T. Currie

Structural Analysis
Advanced Energy Systems Division
Westinghouse Electric Corp
Waltz Mill Site
Box 158
Madison, PA 15663
Attn: V. K. Sazawal

Dr. William Bohl
Division Q7
Los Alamos National Laboratory
Los Alamos, NM 87545

Argonne National Laboratory (3)
9700 South Cass Ave
Argonne, IL 60439
Attn: D. Cho
R. Seidensticker
R. Kulak

Dr. Mike Corradini
University of Wisconsin
Nuclear Engineering Dept
Madison, WI 53706

Dr. Ted Ginsberg
Building 820M
Brookhaven National Laboratory
Upton, NY 11973

Dr. T. Theofanous
132 Halfway Ln
West Lafayette, IN 47905

Dr. A. Wooten
Westinghouse
Nuclear Technology Div
PO Box 355
Pittsburgh, PA 15230

Dr. D. Squarer
Nuclear Safety and Analysis Dept
3412 Hillview Ave
Palo Alto, CA 94304

Dr. Steve Hodge
Union Carbide Corp
Building 9108
PO Box Y
Oak Ridge, TN 37830

Dr. Trever Pratt
Building 130
Brookhaven National Laboratory
Upton, NY 11973

Dr. Raf Sehgal
Nuclear Safety & Analysis Dept
Electric Power Research Institute
3412 Hillview Ave
Palo Alto, CA 94304

MOTOR-COLUMBUS Consulting Engineers, Inc. (2)
Parkstrasse 27
CH-5401 Baden
Switzerland
Attn: K. Gahler
A. Schopfer

University of Tokyo
Institute of Industrial Science
22-1, Roppongi 7
Minatu-ku
Tokyo
Japan
Attn: H. Shibata

1520 D. J. McCloskey
1523 R. C. Reuter
1523 D. B. Clauss
1523 C. Conley
1833 G. A. Knorovsky
3141 C. M. Ostrander (5)
3151 W. L. Garner
3442 M. Carroll
3632 J. Bruneske
6400 A. W. Snyder
6410 J. W. Hickman
6411 A. S. Benjamin
6411 V. L. Behr
6411 F. E. Haskin
6411 J. H. Linebarger
6412 S. W. Hatch
6415 D. C. Aldrich
6417 D. D. Carlson
6427 M. Berman
6440 D. A. Dahlgren
6442 W. A. von Riesemann
6442 T. E. Blejwas
6442 D. S. Horschel
6442 J. Jung (15)
6442 L. N. Koenig
6442 C. V. Subramanian
6444 S. L. Thompson
6445 B. E. Bader
6447 D. L. Berry
6449 K. D. Bergeron
8424 M. A. Pound

NRC FORM 335 (6-83) U.S. NUCLEAR REGULATORY COMMISSION

BIBLIOGRAPHIC DATA SHEET

1 REPORT NUMBER (Assigned by TIDC add Vol. No., if any)
NUREG/CR-3653
SAND83-7463

2 Leave blank

3 TITLE AND SUBTITLE
Containment Analysis Techniques
A State-of-the-Art Summary

4 RECIPIENT'S ACCESSION NUMBER

5 DATE REPORT COMPLETED
MONTH: October YEAR: 1983

6 AUTHOR(S)
Lowell Greimann, Fouad Fanous and Delwyn Bluhm

7 DATE REPORT ISSUED
MONTH YEAR

9 PROJECT/TASK/WORK UNIT NUMBER

8 PERFORMING ORGANIZATION NAME AND MAILING ADDRESS (Include Zip Code)
Ames Laboratory - U.S. DOE
Ames, IA 50011
Under Subcontract to Sandia National Laboratories
Albuquerque, NM

10 FIN NUMBER
A1332

11 SPONSORING ORGANIZATION NAME AND MAILING ADDRESS (Include Zip Code)
Office of Nuclear Regulatory Research
Division of Risk Analysis
Washington, DC 20555

12a TYPE OF REPORT

12b PERIOD COVERED (Inclusive dates)

13 SUPPLEMENTARY NOTES

14 ABSTRACT (200 words or less)

The purpose of the work contained herein is to review the state-of-the-art for the analysis of LWR nuclear containments with uniform internal pressure. This includes:

(a) A review of calculated static failure pressure of various containments,
(b) A review of the different failure criteria used for predicting containment failure,
(c) Comments on possible uncertainties associated with analysis techniques, material and geometric models, and other analysis features.

A state-of-the-art containment analysis is a finite element solution of an axisymmetric model. Material and geometric nonlinearities are included. Nonsymmetric features may be analyzed on an individual basis but are omitted in the axisymmetric model. State-of-the-art models of the material constitutive relationships are used. Deformation predictions are generally regarded as reliable, assuming the containment configuration is accurately described, e.g., known geometry, material and loads. Predictions of leakage are much more uncertain. There is no general agreement on when and where leakage will occur.

15a KEY WORDS AND DOCUMENT ANALYSIS

15b DESCRIPTORS
Nuclear containment buildings, containment integrity, mechanical structural engineering, stress analysis, failure

16 AVAILABILITY STATEMENT
Unlimited

17 SECURITY CLASSIFICATION (This report)
Unclassified

18 NUMBER OF PAGES

19 SECURITY CLASSIFICATION (This page)
Unclassified

20 PRICE
$

☆U.S. GOVERNMENT PRINTING OFFICE: 1984—776-027 / 4298

120555078877 1 1AN1R11RD1RG
US NRC
ADM-DIV OF TIDC
POLICY & PUB MGT BR-POR NUREG
W-501
WASHINGTON DC 20555